**DOKUZ EYLÜL UNIVERSITY**
**GRADUATE SCHOOL OF NATURAL AND APPLIED SCIENCES**

# PRODUCTION OF BIODEGREDABLE AND BIOCOMPATIBLE POLYMERIC TISSUE SCAFFOLDS WITH DIFFERENT SURFACE CHARGES AND EVALUATION OF CELL - SCAFFOLD INTERACTIONS

**by**
**İrem ÜNALAN**

**October, 2015**
**İZMİR**

# PRODUCTION OF BIODEGREDABLE AND BIOCOMPATIBLE POLYMERIC TISSIUE SCAFFOLDS WITH DIFFERENT SURFACE CHARGES AND EVALUATION OF CELL - SCAFFOLD INTERACTIONS

**A Thesis Submitted to the**
**Graduate School of Natural and Applied Sciences of Dokuz Eylül University**
**In Partial Fulfillment of the Requirements for the Degree of Master of Science of Department of Biomedical Technologies Program**

**by**
**İrem ÜNALAN**

**October, 2015**
**İZMİR**

**M.Sc THESIS EXAMINATION RESULT FORM**

We have read the thesis entitled **"PRODUCTION OF BIODEGREDABLE AND BIOCOMPATIBLE POLYMERIC TISSUE SCAFFOLDS WITH DIFFERENT SURFACE CHARGES AND EVALUATION OF CELL-SCAFFOLD INTERACTIONS"** completed by **İREM ÜNALAN** under supervision of **ASSIST. PROF. DR. AYLİN ZİYLAN ALBAYRAK** and we certify that in our opinion it is fully adequate, in scope and in quality, as a thesis for the degree of Master of Science.

Assist. Prof. Dr. Aylin ZİYLAN ALBAYRAK

Supervisor

Assist. Prof. Dr. Aylin ŞENDEMİR ÜRKMEZ

(Jury Member)

Prof. Dr. Ahmet ÇAKIR

(Jury Member)

Prof. Dr. Ayşe OKUR
Director
Graduate School of Natural and Applied Sciences

## ACKNOWLEDGEMENTS

At first, I would like to express my deepest gratitude to my supervisor Assist. Prof Dr. Aylin ZİYLAN ALBAYRAK for her guidance, invaluable advice, supports and encouragements and useful critiques for this M. Sc. thesis. It was a pleasure to study with her and to have a chance of benefit from her scientific and personal experiences.

I would like to thank Assist. Prof Dr. Aylin ÜRKMEZ ŞENDEMİR for her guidance throughout all the cell culture experiments.

I would also like to thank Dr. Arda BÜYÜKSUDUR who provided us plasma surface device during our research.

I wish to give my special thanks to my friends Tülay KOÇ DELICE, and Bensu BAKIN for their valuable friendships and supports. I would like to thank Cansu GÖRGÜN who helped us cell culturing during our research. I also wish to thank my laboratory partner Research Assistants Oylum ÇOLPANKAN who helped me for the experimental part of this study.

Finally, I especially thank my parents and my sister for their support and encouragement throughout my thesis like always and every step of my life.

İrem ÜNALAN

**PRODUCTION OF BIODEGREDABLE AND BIOCOMPATIBLE POLYMERIC TISSUE SCAFFOLDS WITH DIFFERENT SURFACE CHARGES AND EVALUATION OF CELL-SCAFFOLD INTERACTIONS**

## ABSTRACT

The aim of this thesis study is to produce biodegradable and biocompatible poly(3-hydroxybutyrate-co-3-hydroxyvalerate) (PHBV) nanofiber mats with different surface charges for tissue engineering applications.

It is important for a scaffold to mimic fibrous form of the natural extracellular matrix (ECM). In the present study, nanofiber materials with morphologies similar to the native ECM were produced by electrospinning technique.

Most polymeric materials are hydrophobic in nature, therefore their surfaces are not favorable for cellular adhesion. In this sense, modification of the hydrophobic surfaces of polymers with plasma surface modification technique is proposed. In this study, hydrophobic PHBV polymer was used as the main matrix. In order to increase the surface hydrophilicity of the PHBV and also improve cell adhesion and proliferation, radio-frequency (RF) plasma surface modification technique was used. The nitrogen and oxygen gases were used as plasma atmosphere to create positive and negative surface charges, respectively. The hydrophilicity of the electrospun PHBV nanofiber mats was significantly increased by the plasma treatment, as confirmed by contact angle measurements. But, the sustainability of surface hydrophilicity of plasma treated polymeric mats is the main problem for the fabrication of tissue scaffold due to hydrophobic recovery. This problem was minimized by silk fibroin (SF) modification via preventing the reorientation of polar groups. Biominerilization results showed that incorporation of SF as well as oxygen plasma strongly activates the precipitation rate of the Ca-P minerals. Obtained nanofiber mats especially nitrogen plasma-treated and silk fibroin modified ($PS/N_2$) ones provide the most favorable environment for SaOS-2 osteoblastic cell attachment and growth. In addition, the mats showed no noticeable cytotoxic effect on SaOS-2 cell and L929 mouse fibroblast-like cells.

These results indicate that the plasma treated and silk fibroin modified PHBV nanofiber mats have great potential in the development of novel polymeric scaffolds for bone tissue engineering applications.

**Keywords:** Nanofiber, electrospinning, tissue scaffold, surface charge, PHBV, plasma surface modification, silk

# FARKLI YÜZEY YÜKLERİNE SAHİP BİYOBOZUNUR VE BİYOUYUMLU POLİMERİK DOKU İSKELELERİNİN ÜRETİMİ VE HÜCRE - İSKELE ETKİLEŞİMİNİN DEĞERLENDİRİLMESİ

## ÖZ


Bu tez çalışmasının amacı, doku mühendisliği uygulamaları için farklı yüzey yüklerine sahip biyobozunur, biyouyumlu poli (3-hidroksibutrat-ko-3-hidroksivalerat) (PHBV) nanofiber mat üretmektir.

Doku iskeleleri için doğal hücre dışı matris (ECM) yapısındaki fibröz yapıyı taklit etmek önemlidir. Bu çalışmada, doğal ECM morfolojisine benzer nanofiber malzemeler elektro-eğirme tekniği ile üretilmiştir.

Hidrofobik özellikli polimerik matris hücre tutunmasına uygun yapıya sahip değildir. Bu nedenle hidrofobik polimer yüzeylerinin plazma yüzey modifikasyon tekniği ile hidrofilik hale getirilmesi önerilmektedir. Tez çalışmasında matris malzemesi olarak, hidrofobik bir polimer olan PHBV kullanılmıştır. Matrisin hidrofilisitesinin arttırmak, ayrıca hücre tutunmasını ve çoğalmasını desteklemek amacıyla radyo frekanslı plazma yüzey modifikasyon tekniği uygulanmıştır. Plazma atmosferi olarak , azot ve oksijen gazları sırasıyla pozitif ve negatif yüzey yükleri oluşturmak için kullanılmıştır. Eğirilmiş PHBV nanofiber matlerin plazma işlemi ile hidrofilikliğinin önemli ölçüde arttığı temas açısı ölçümleri ile doğrulanmıştır. Ancak, plazma ile işlenmiş polimerik matlarin yüzey hidrofilikliğinin sürdürülebilirliği, hidrofobik geri dönüşten dolayı doku iskelesinin uygulanabilirliği açısından temel bir sorundur. Bu sorun, bu çalışmada polar grupların yeniden yönlendirilmesi, plazma işlenmiş PHBV nanofiber matlerin ipek lifi (SF) ile modifikasyonu sonucunda mimize edilmiştir. Biyominerilizasyon sonuçları SF'nin yanı sıra oksijen plazmanın da Ca-P minerallerinin çökme oranını arttırdığını göstermiştir. Elde edilen nanofiber matler arasından özellikle azot plazma işlenmiş ipek lifi ile modifiye ($PS/N_2$) edilmiş mat, SaOS-2 osteoblastik hücre tutunması ve büyümesi için en uygun ortamı sağlamıştır. Bunun yanı sıra, üretilen tüm matler, SaOS-2 hücreleri ve L929 fare fibroblast benzeri hücreleri üzerinde hiç bir sitotoksik etki göstermemiştir.

Bu sonuçlar, plazma işlemi ve ipek lifi modifikasyonu uygulanan PHBV nanofiber matlerin kemik doku mühendisliği uygulamaları için yeni polimerik iskeleleri geliştirilmesinde büyük bir potansiyele sahip olduğunu göstermektedir.

**Anahtar Kelimeler:** Nanofiber, elektro-eğirme, doku iskelesi, surface charge, PHBV, plazma yüzey modifikasyonu, ipek lifi

**CONTENTS**

**Page**

## LIST OF FIGURES

**Page**

## LIST OF TABLES

**Page**

# CHAPTER ONE
# INTRODUCTION

According to IUPAC Recommendations, Tissue engineering was defined as "applications that repair or replace portions of or whole tissues and use of a combination of cells, engineering and materials methods, and suitable biochemical and physiochemical factors to improve or replace biological functions"(Vert et al., 2012).

Disease, injury and trauma can lead to damage and degeneration of tissues in the human body, which necessitates treatments to facilitate their repair, replacement or regeneration. Treatment typically focuses on transplanting tissue from one site to another in the same patient (an autograft) or from one individual to another (a transplant or allograft). While these treatments have been revolutionary and lifesaving, major problems exist with both techniques. Harvesting autografts is expensive, painful, constrained by anatomical limitations and associated with donorsite morbidity due to infection and hematoma. Similarly, allografts and transplants also have serious constraints due to problems with accessing enough tissue for all of the patients who require them and the fact that there are risks of rejection by the patient's immune system and the possibility of introducing infection or disease from the donor to the patient. Alternatively, the field of tissue engineering aims to regenerate damaged tissues, instead of replacing them, by developing biological substitutes that restore, maintain or improve tissue function (O'Brien, 2011).

The best scaffold for an engineered tissue should be the extracellular matrix (ECM)of the target tissue in its native state. Nevertheless, the multiple functions, the complex composition and the dynamic nature of ECM in native tissues make it difficult to mimic exactly. Therefore, contemporary concept of scaffolding in tissue engineering is to mimic the functions of native ECM, at least partially (Chan & Leong, 2008).

ECM is consist of multiple components and tissue-specific composition. Also, the functions of ECM in tissues, they can be generally classified into five categories.

Firstly, ECM provides structural support and physical environment for cells residing in that tissue to attach, grow, migrate and respond to signals. Secondly, ECM gives the tissue its structural and therefore mechanical properties, such as rigidity and elasticity that is associated with the tissue functions. Thirdly, ECM may actively provide bioactive cues to the residing cells for regulation of their activities. Fourthly, ECM may act as reservoir of growth factors and potentiate their bioactivities. Fifthly, ECM provides a degradable physical environment so as to allow neovascularization and remodeling in response to developmental, physiological and pathological challenges during tissue dynamic processes namely morphogenesis, homeostasis and wound healing, respectively (Chan, & Leong, 2008).

Conventionally, regardless of the tissue type, a number of key considerations are important when designing a suitable of scaffold for use in tissue engineering applications, including scaffold morphologies (porosity, pore size, and inner pore connectivity), biocompatibility, mechanical properties and degradation. Recent researches, the natural ECM plays an important role in arrangement cellular behavior such as cell spreading, migration and differentiation (O'Brien, 2011; Smith, Liu & Ma, 2008).

### 1.1 Scaffold Requirement for Tissue Engineering

The design of the scaffold for tissue engineering should meet several requirements. An ideal scaffold should have;

a- Adequate porosity to support cell seeding, proliferation, differentiation and to a diffusion of nutrient to and metabolites out from the cell scaffold structure.

b- Sufficient mechanical stability to provide a suitable environment for new tissue formation.

c- The degradation rate must be compatible to permit cell growing.

d-The surface chemistry must be appropriate for cell adhesion and function.

### *1.1.1 Porosity and Pore Size*

The fabrication of a porous scaffold is very important in tissue engineering. Porosity is defined as the percentage of void space in a solid and it is a morphological property independent of the material. Pores are necessary for tissue formation because they allow migration and proliferation of cells, as well as vascularization. (Karageorgious & Kaplan, 2005; Singh, Kasper, & Mikos,).

In order to promote tissue growth, the scaffold must have large a large surface area to allow cell attachment. This is usually done by creating a highly porous polymer foam. In these foams, the pore size should be large enough so that cells penetrate the pores, and the pores must be interconnected to facilitate nutrient and waste exchange by cells deep within the construct. These characteristics (porosity and pore size) are often dependent on the method of scaffold fabrication (Mikos, & Temenoff, 2000).

The most common techniques used to create porosity in a biomaterial are salt leaching, gas foaming, phase separation, freeze-drying and sintering depending on the material used to fabricate the scaffold (Karageorgious, & Kaplan, 2005).

The authors of more recent studies have proposed that ideal pore size vary for a type of cells. For instance, fibroblasts cell culture results showed that pores smaller than 160 μm are suitable for human skin fibroblast cell growth (Yang et al.; 2002). Another example, osteoblasts cell culture results showed that pore size of 325 mm were optimal for successful cell attachment and facilitating bone growth in scaffolds (Murphy, Haugh, & O'Brien; 2010).

### *1.1.2 Mechanical Properties*

Mechanical properties are crucial to the achievement of the implant as a biomaterial to be used in tissue engineering application. Scaffold must be strong to enable surgical utilization during implantation. Scaffold's low strength and rigidity restrict their use in soft tissue applications.

Scaffolds provide mechanical and shape stability to the tissue defect. Also, it grants rigidity and stiffness to tissue. For bone tissues, the implanted scaffold must have sufficient mechanical integrity to function from the time of implantation to the completion of the remodeling process. So, the intrinsic mechanical properties (such as tensile strength, elasticity, material interface adsorption and chemical degradation) of the biomaterials used for scaffolding property should match that of the host tissue (Dhandayuthapani et al. 2011; O'Brien, 2011; Mitra et al., 2013).

Recent studies have highlighted the importance of mechanical properties of a scaffold for cell adhesive and morphology. Exerting traction forces on a substrate, many mature cell types, such as epithelial cells, fibroblasts, muscle cells, and neurons, sense the stiffness of the substrate and show dissimilar morphology and adhesive characteristics (Chan, & Leong, 2008). For instance, The hMSCs (human mesenchymal stem cells) were differentiate along the neuronal, muscle, or bone lineages according to stiffness that approximate those of the brain, muscle, and bone tissues, respectively ( Engler et al., 2006).

### *1.1.3 Biocompatibility and Biodegradation*

Biocompatibility is the main criteria to limiting the use of biomaterial for tissue engineering applications. According to IUPAC Recommendations, biocompatibility was defined as “the ability to be in contact with a living system without producing an adverse effect and ability of a material to perform with an appropriate host response in specific application” (Vert et al., 2012).

Biocompatibility is also directly related with material’s biodegradability. The tissue response to an implant depends on a myriad of factors ranging from the chemical, physical and biological properties of the materials to the shape and structure of the implant. In the case of biodegradable biomaterials, their active biocompatibility must be demonstrated over time. The chemical, physical, mechanical and biological properties of a biodegradable material will vary with time and degradation products

can be produced that have different levels of tissue compatibility compared to the starting parent material (Burg, Porter, & Kellam, 2000; Nair, & Laurencin, 2007).

Polylactide, (PLA), polyglycolide, (PGA), poly(lactic-co-glycolic acid) (PLGA), polycaprolactone, (PCL), and poly(3-hydroxybutyrate-co-3-hydroxyvalerate) (PHBV), which are biodegradable polymers, were shown to be biocompatible (Panchence, Bohrer & Kohn; 2007). Therefore, they are used or tested for medical applications. Scaffolds and constructs, are not intended as permanent implants. The scaffold must therefore be biodegradable so as to allow cells to produce their own extracellular matrix. The by-products of this degradation should also be non-toxic and able to exit the body without interference with other organs (O'Brien, 2011; Wang et al., 2004).

### *1.1.4 Surface Properties*

The scaffold properties influence cellular adhesion, migration, and proliferation. Besides, the surface properties develop the biocompatibility and "bio-recognition" of biomaterial. Important material surface properties including hydrophobicity, charge, roughness, stiffness/softness and chemical composition are covered in chapter three. (Chang, & Wang, 2011; Ma, Mao and Gao, 2007; Wang et al., 2004).

## 1.2 Materials Developed for Scaffold Applications

Material selection plays a key factor in cell adhesion, proliferation and differentiation, nutrient transport and the excretion of waste while the cell secrete their own ECM. Many material types such as polymers, ceramics and composites are convenient for tissue engineering applications. Within the scope of this thesis, polymers were used as a scaffolding material.

### *1.2.1 Biodegrable Polymer*

Scholars have argued that the use of biodegradable materials to repair and replace damaged tissue gives promising results and especially biodegradable polymers have contributed significantly to the need of the temporary therapeutic applications. The main reason of choosing biodegradable polymers is their long-term biocompatibility features. Other features of biodegradable polymeric biomaterials are; appropriate degradation time and mechanical properties. Natural and synthetic polymers are used in order to fabricate scaffolds for transient implants, drug delivery vehicles and tissue engineering scaffolds (Langer, & Vacanti, 1993; Nair, & Laurencin, 2007; Vert, 2007).

Biodegradation of polymeric biomaterials involves cleavage of hydrolytically or enzymatically sensitive bonds in the polymer leading to polymer erosion. Depending on the mode of degradation, polymeric biomaterials can be further classified into hydrolytically degradable polymers and enzymatically degradable polymers. Most of the naturally occurring polymers undergo enzymatic degradation. The rate of in vivo degradation of enzymatically degradable polymers varies significantly with the site of implantation depending on the availability and concentration of the enzymes. The inherent bioactivity of these natural polymers has its own downsides. These include a strong immunogenic response associated with most of the polymers, the complexities associated with their purification and the possibility of disease transmission (Nair, & Laurencin, 2007).

Hydrolytically degradable polymers are polymers that have hydrolytically labile chemical bonds in their back bone. The functional groups susceptible to hydrolysis include esters, carbonates, amides, urethanes etc. Hydrolytically degradable polymers are generally preferred as implants due to their minimal site-to-site and patient-to-patient variations compared to enzymatically degradable polymers. Two general routes are used to develop hydrolytically sensitive polymers for biomedical applications. They are step (condensation) polymerization and addition (chain) polymerization including ringopening polymerization. Step process is used to prepare a variety of hydrolytically sensitive polymer classes, such as polyanhydrides, poly(ortho esters) and polyurethanes. Ring opening polymerization (ROP) is an

extensively investigated polymerization route to develop hydrolytically sensitive polymers, including the poly(a-esters) and polyphosphazenes. Radical polymerization mostly results in the formation of non-degradable polymers; however, recent studies have demonstrated the feasibility of developing synthetic degradable polymers or cross-linked gels by radical polymerization processes ( Nair, & Laurencin, 2007).

*1.2.1.1 Natural Polymers*

Natural polymers are used clinically as biodegradable biomaterials and are qualified by their biocompatibility, biodegradation, minimal antigenicity and minimal inflammatory responses. However, the disadvantages of natural polymers are the risk of microbial contamination and uncontrolled rate of biodegradation. Natural polymers consist of three main groups as proteins (collagen, silk, gelatin, fibrinogen, elastin, keratin, actin and myosin), polysaccharides (chitosan, cellulose, amylose, dextran and glycosaminoglycan), and polynucleotides (DNA and RNA) (Dhandayuthapani et al., 2011; Mitra et al., 2013).

Collagen is the most abundant protein in the extracellular matrix. Therefore, collagen is stated as an ideal scaffold material for cell adhesion, proliferation, and differentiation. For example, in a review by Silver and Pins in1992, collagen was used as a substrate for the growth of cell transformed from skin tissue. According to the experimental results, the matrix surface mimic in vivo cell activity and fibroblasts spreading and differentiation is enhanced. Also, fibroblasts presented almost the same morphology and metabolism. On the other hand, poor mechanical properties, uncontrolled rate of degradation and microbial contamination effects of the collagen-based biomaterials limited their use for tissue engineering applications (Langer, & Vacanti, 1993; Nair, & Laurenci, 2007; Pharm, Sharma & Mikos, 2006).

Silk fibroin (SF) protein is a natural polymer that is acquired from silkworm cocoons for use in tissue engineering applications such as 3D porous fibroin scaffold for cartilage tissue regeneration, silk film for skin tissue regeneration and SF nanofiber

for bone regeneration. SF has a good biocompatibility, high mechanical property and biodegradability (Karageorgious, & Kaplan, 2005; Kundu,2013).

Another group of natural polymers are polysaccharides. Most known polysaccharide is chitosan. Chitosan is the deacetylated derivative of chitin. Chitin is a naturally abundant polysaccharide, and it is extracted from crustaceous, inserts, etc. (Kumar, 2000). Chitosan is often used in cosmetics, photograph and medical applications such as sutures, wound dressings and drug delivery systems. Apart from chitosan other polysaccharides such as cellulose, hyaluronate, and alginate are used in many tissue engineering applications (Langer, & Vacanti, 1993).

#### *1.2.1.2 Synthetic Polymers*

Synthetic polymers comprise the most important part of biodegradable polymers. They enable biomaterials to repair the structure and function of the damage tissue. Due to the fact that synthetic polymers have controlled structure, higher degree of processing flexibility, no immunological concern, and long shelf time, they are advantageous to use as biodegradable materials compared to natural polymers. Besides, mechanical and physical properties such as tensile strength, elastic modulus, and degradation rate can be changed according to specific applications (Baolin, & Ma, 2014; Sabir, Xu, & Li, 2009).

The most commonly used synthetic biodegradable polymers include poly(α-ester)s, poly(carbonate)s, poly(urethanes), poly(fumarate)s, poly(anhydride)s, poly(orthoester)s, poly(phosphazene)s, poly(hydroxy alkanoate)s etc. (Nair & Laurencin, 2007). Poly (α-ester) s are the most investigated synthetic biodegradable polymers in tissue engineering applications. PLA, PGA, and PCL are the most widely used poly (α-ester) s (Figure 1.1).

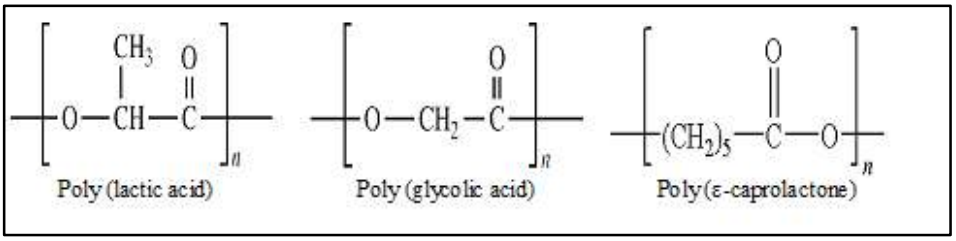


Figure 1.1 Chemical structures of the most widely used poly (α-ester) s (Gunatillake, & Adhikari, 2003).

Poly (glycolic acid), (PGA), is a rigid thermoplastic material with high crystallinity (45-55%). It has a melting point greater than 200°c and a glass transition temperature about 35-40°c. PGA is not soluble in most organic solvents on account of its high crystallinity (Nair, & Laurenci, 2007). PGA is an acids and more hydrophilic than poly (lactic acid), (PLA). It can only be dissolved in highly fluorinated solvents such as hexafluoroisopropanol. When the compare to PLA, PGA degrades at a faster rate (4-72 months for PGA and up to 2 years for PLA and also has a higher tensile strength and modulus. PGA was developed into the first synthetic absorbable suture; one of the most widely used scaffolds in tissue engineering today. A major cause of widespread use of PGA in medical applications is its degradation product, glycolic acid, is a natural metabolite. ın human body, glycolic acid can be extracted from urine (Gunatilake, & Adhikari, 2003; BaoLin, & Ma, 2014).

PLA has an extra methyl group, thus this makes it more amorphous and hydrophobic than PGA. Furthermore, PLA is soluble in various organic solvents such as chloroform, methylene chloride, methanol, ethanol, benzene, acetone, DMF and etc. It has a melting point around 175°C and a glass transition temperature about 60-65°C. PLA is a slow-degrading polymer compared to PGA, has good tensile strength and low extension and high modulus and hence, has been considered an ideal biomaterial for load bearing applications such as orthopaedic fixation devices and sutures (Sabir, Xu, & Liu, 2009). In addition, PLA has three isomeric forms L-PLA (PLLA), D-PLA (PLDA) and blend of D, L-PLA (PDLLA) and degradation product lactic acid is a natural metabolite, like PGA (Nair, & Laurencin, 2007).

Poly (ε-caprolactone), (PCL), is a semicrystalline polymer with a glass transition temperature of about -60ºC. The polymer has a low melting temprature(59 to 64 ºC)

and is compatible with a range of other polymers (Kramschuster, & Turng, 2013). PCL degrades at a much lower rate that PLA and PGA, which makes PCL less attractive for general tissue regeneration applications but more attractive for long term implants and drug delivery systems (Gunatillake, & Adhikari, 2003; Langer, & Vacanti, 1993).

Recently that, as a microbial polyester group, Polyhydroxyalkonoates, (PHA), began to attract interest for tissue engineering. PHA family comprises both homopolymers of hydroxy alkanoic acid and copolymers of two or more hydroxy alkanoic acid. These are some copolymers of polyhydroxy alkanotes (PHA), containing PHB, PHBV (poly (3-hydroxybutyrate-co-3-hydroxyvalerate)), P4HB copolymer of 3-hydroxy-butrate, 3-hydroxyhexanonoate (PHBHHX) and poly-3-hydroxyhaxanoate (PHO). This situation of polymers allows different chemical structure, degradation rate, and mechanical properties. PHA forms have become widespread use in wound healing, orthopedics and drug delivery systems. But, the most important limiting factor is attainability for PHA group polymers. Because, only poly-3-hydroxybutratevalerate can be produced commercially (Nair, & Laurencin, 2007; Sabir, Xu, & Liu, 2009).

Chemical structures of PHBV (poly (3-hydroxybutyrate-co-3-hydroxyvalerate)) are shows in Figure 1.2. PHB and PHBV polymers have a longer degradation rate than PLA and PGA polymers. This feature of a polymer provides adequate tissue formation on the scaffold. PHBV is a less brittle than PHB. When the PHBV degrades, revealed hydroxybutyric acid. In addition, it is a natural component found in human blood. Therefore, PHBV doesn't exist inflammation problem in implants. PHBV is a promising material for tissue engineering due to the economic and superior features (Sultana, & Wang, 2008; Chang, & Wang, 2011).

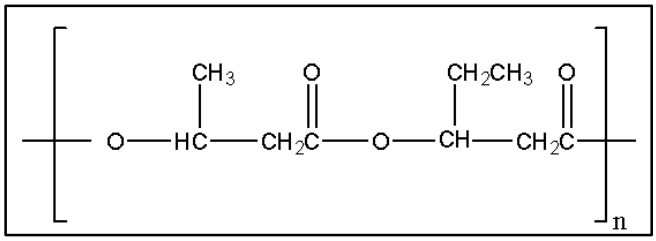

Figure 1.2 Chemical structures of PHBV (poly (3-hydroxybutyrate-co-3-hydroxyvalerate)) (Gunatillake, & Adhikari, 2003).

Some essential properties of commonly used synthetic polymers in tissue engineering are given in Table 1.1.This material mechanical strengths are inadequate for hard tissue repair application. Synthetic polymers combined with inorganic materials, produced composite materials, using to increase mechanical strength (Gunatillake, & Adhikari, 2003).

Table 1.1 Some essential properties of commonly used synthetic polymers in tissue engineering (Gunatillake, & Adhikari, 2003)

| PROPERTY | PGA | PLLA | PLGA | PDLLA | PCL | P3HB |
|---|---|---|---|---|---|---|
| $T_{Melting}$ (°C) | 225- 230 | 173-178 | - | - | 58 | 170-175 |
| $T_{Glass\ Transition}$ (°C) | 35-40 | 60-65 | 45-55 | 55-60 | -72 | -4-10 |
| Young's Modulus, E(GPa) | 7- 10 | 1.2 - 3.0 | 1.4 - 2.8 | 1.9 - 2.4 | 0.4 | 1.1 - 3.5 |
| (%) Elongation | 15-20 | 5 - 10 | 3 - 10 | 3 - 10 | >70 | 3 - 6 |
| Crystallinity (%) | 55-56 | 37 | 0 | 0 | - | 55-80 |
| Degradation rate (Month) | 6 - 18 | >24 | 1 - 12 | 12 - 16 | >24 | >18 |

### *1.2.2 Bioceramics*

Ceramics are polycrystalline materials. The main characteristics of ceramic materials are hardness and brittleness, great strength and stiffness, resistance to corrosion and wear, and low density. Ceramics are typically electrical and thermal insulators. They are used in several different fields such as dentistry, orthopedics, and

as medical sensors. Ceramics have become a diverse class of biomaterials presently including three basic types: bioinert, bioactive, bioresorbable ceramics. Alumina ($Al_2O_3$), Zirconia ($ZrO_2$) and Pyrolytic carbon are termed bioinert. Bioglass and glass ceramics are bioactive. Calcium phosphate ceramics are categorized as bioresorbable (Pate, & Gohil, 2012; Siraparapu, Bassa, & Sanasi, 2013). In this group hydroxyapatite (HAp) has a dominant place, being used for oral and maxillofacial surgery as bone substitute and as coating for metal and carbon implants. HAp is found in different parts of the body as a constituent of various types of calcified tissues. The mineral phase of the bone is mainly made up of calcium phosphate micro-crystals, among them hydroxyapatite is the most important, its chemical formula reads $Ca_{10}(PO_4)_6(OH)_2$ (Pattanayak, Rao, & Mohan, 2001).

### *1.2.3 Biocomposites*

Biocomposites are composite materials composed of biodegradable matrix and biodegradable natural fibres as reinforcement. The development of biocomposites has attracted great interest due to their environmental benefit and improved performance. Biocomposites materials most commonly used in drug/gene delivery, cosmetic orthodontics and tissue engineering applications comprises a polymeric matrix and bioactive ceramics. Biocomposites the used in bone tissue engineering, it should have high strength and modulus of elasticity near the bone (Tanner, 2010).

## 1.3 Scaffold Fabrication Techniques

Fabrication technologies are important for tissue engineering to facilitate the cell adhesion and their growth into scaffold. Therefore, many different methods are used for highly porous scaffolds, including gas foaming, solvent casting/particulate leaching and emulsion freeze-drying manufacturing (Ma, & Choi, 2001). While a large number of scaffolding fabrication methods have been developed, the techniques for controlling the architecture of the scaffold at nano-scale level are still limited. Only three techniques have been developed in the fabrication of nano-fibrous scaffolds for

use in tissue engineering: thermal induced phase separation, self-assembly and electrospinning (Smith, Liu, & Ma, 2008).

This thesis will study that method in terms of electrospinning, fiber morphology, efficacy of promoting tissue growth and ease of use in a clinical setting.

### *1.3.1 Thermal Induced Phase Separation*

Thermal induced phase separation technique with the thermal effect of is a simple method for production porous tissue scaffold and this method was firstly developed by Lo et al (1995) (Kramschuster, & Turng, 2013).

This method essentially consists of five steps. This steps respectively, dissolving of polymer, phase separation and gelation, remove from the solvent, freezing and drying. To sum up, the polymer is first dissolved in solvent that has a high temperature and then a polymer-rich phase and polymer-lean phase separation is induced by reducing the solution temperature. Next, the solvent is removed by solvent extraction or freeze-drying. Thus, the polymer-rich phase is solidified and the porous polymer is obtained (Figure 1.3).

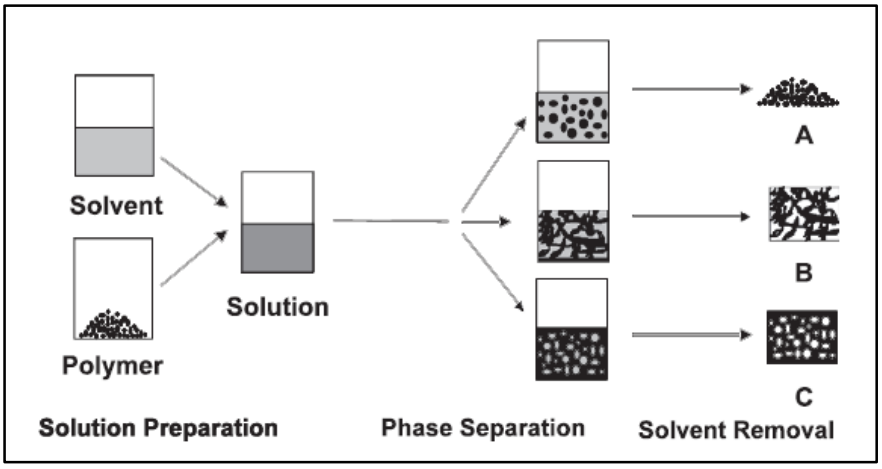


Figure 1.3 Diagram of thermally induced phase separation technique (Kramschuster, & Turng, 2013).

More recently, thermal induced phase separation has also been utilized to fabricate nano-fibrous matrices. For instance; Ma, & Zhang (1999) were fabricated nanofibrous

matrices by using poly-L-lactide (PLLA) to mimic the fibrous structure of natural type I collagen. A solution poly-L-lactide (PLLA) of is dissolved in tetrahydrofuran (THF) is thermally induced following a series of processes to phase separate. The solvent is exchanged with water and then freeze-dried to yield nanofibrous PLLA matrices. The fibers formed in this manner have diameters ranging from 50 to 500 nm, and a porosity almost 98 % ( Smith, Liu, & Ma, 2008).

### *1.3.2 Self-Assembly*

Molecular self-assembly is a useful research area for producing to nano-scale scaffold. The self-assembly method is provided to be stable with non-covalent bonding such as, hydrogen bonds, Van der Walls interaction, electrostatic interaction and hydrophobic interaction. Self-assembly molecules often are occurred spontaneously in nature. Biomolecules such as peptides and proteins are interacted with each other mutually and produced properly and functional structure (Ma, & Choi, 2001; Liu, & Ma, 2004).

The nano-size fibers are produced under suitable conditions by self-assembly methods. For example, Collagen molecules to collagen fibrils are collected side by side in parallel bundles to create collagen fiber with a diameter range of 50 to 500 nm (Smith, Liu, & Ma, 2004). Moreover, Self-assembly method produces very thinner diameter nanofibers than the electrospinning method. But, Lack of important macropores, for cell growth and delivery of nutrient, limits the use of this method (Subia, Kundu, & Kundu, 2010).

### *1.3.3 Electrospinning*

Electrospinning process can produce ultrafine fibers with special orientation, have control over pore geometry and have a solid and hallow inter structure to fabricate of nonwoven nanofiber matrices. When the electrospinning technology combines with sol-gel method, polymer or ceramic solution can be performed continuous nanofiber and nanotubes production under an electrical field. In recent years, produced

nanofibers by electrospinning are very important for nanotechnology applications due to unique features and ease of manufacturing. Typically nanofiber matrices have more than 90 % porosity and diameters range from 200 nm to 5 μm (Kramschuster, & Turng, 2013). In this thesis, Electrospinning method used for the production of tissue scaffold will be examined a detail in Chapter 2.

# CHAPTER TWO
# ELECTROSPINNING

## 2.1 Introduction

Electrospinning is an old process to fabricate fiber with electrostatic forces and it was first reported in 1897 by Rayleigh. He was reported the electrical charge of liquid droplet necessary to eject the droplet to for smaller droplets. Formhals patented in 1934 was the first to file patents about the process and the apparatus, which it based on a needless set up equipped with a rotating collector, for producing synthetic fibers using electrostatic force and it was the first development milestones about electrospinning. Thus, Formhals was able to create cellulose acetate fiber by this apparatus. In 1969, Taylor developed the charged jet forming process. In his studies, he observed conical shape of the jet and now called the 'Taylor Cone' (Goh, Shakir, & Hussain, 2013; Martins, Reis, & Neves, 2008).

Baumgartner in 1971 invented a simple apparatus to electrospinning acrylic fiber with diameter ranging between 0.05-1.1 μm and to begin research effect of solution and processing parameters on the structural properties of electrospinning fibers. In 1978, Annis and Barnat developed polyurethane mats for use as vascular prosthesis by electrospinning technique. Fisher and Annis began to investigate the long-term in vivo biocompatibility of an electrospinning arterial prosthesis, until 1985.In 1995,Reneker et al. finally reinvented electrospinning for usage of nanoscale nature and this method still used today (Bhardwaj, & Kundu, 2010; Still, & Recum,2008; Persano et al.,2013).

## 2.2 Electrospinning Process

The process of electrospinning is a method in which using electrostatic forces to produce polymer fibers thus formed into nano- and micro- sized continuous fiber. The electrospinning process allowing formation of different nanofibrous structures (Bhardwaj, & Kundu, 2010; Liu, Ding, & Zhou, 2013; Still, & Recum, 2007).

A typical electrospinning system basically consists of three component; a high voltage power supply, a spinneret and grounded collector (Figure 2.1. (A)). In an electrospinning process, initially the polymer are dissolved in some solvent and is loaded into the syringe having an attached needle. An electrode from the high voltage source can be attracted to the metal needle tip. Afterward, the high voltage source is turned on and is created on electrically charged jet of polymer solution. When the electric field applied reaches a critical value, the repulsive electrical forces overcome the surface tension force and a 'Taylor Cone' is formed, which is further elongated into a fluid jet (Figure 2.1. (B)). Later, if the applied high voltage is increased, the charged fluid jet is collected on the grounded collector which leads to evaporation of the solvent, leaving polymer behind. Thus, the collection of the polymer fiber mesh on the collection plate (Huang et al., 2003; Lee, & Arinzeh, 2011; Still, & Recum, 2007).

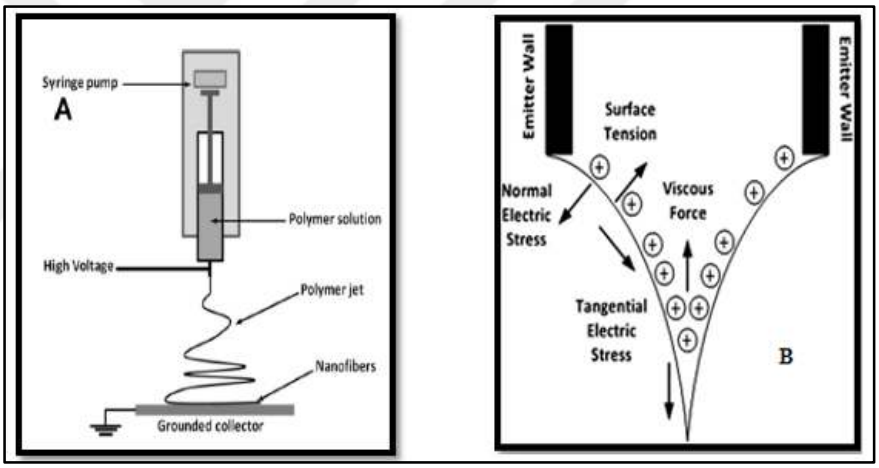


Figure 2.1 A) Electrospinning apparatus B) Taylor cone (Wu, Oleschuk, & Cann, 2012)

## 2.3 Effect of Various Parameters on Electrospinning

The ideal electro spinning fibers are consist of uniform, consistent, without bead formation and controllable fiber diameter. But, many parameters that can greatly influence electrospun fiber morphology and size. These parameters classified into solution parameters, process parameter and ambient parameters. The parameters of electrospinning are given in Table 2.1 (Martins, Reis, & Neves, 2008).

Table 2.1 The parameters of electrospinning

| Solution Parameters | Processing Parameter | Ambient Parameters |
|---|---|---|
| Viscosity/Concentration | Applied Voltage | Temperature |
| Surface Tension | Flow Rate | Humidity |
| Solution Conductivity | Type of Collector | |
| Dipole Moment and Dielectric Constant | Diameter of Needle | |
| | Distance between Tip and Collector | |

### *2.3.1 Solution Parameters*

Solution parameters include the viscosity, conductivity, surface tension and dipole momentum and dielectric constant.

#### *2.3.1.1 Viscosity/Concentration*

In the electrospinning process, solution viscosity which it can controlled by changing the polymer concentration plays on important role in determining of fiber size and morphology when spinning fibers. The solution should be an optimum polymer concentration for the electrospinning process. Used solution viscosity during production are very important parameter to determining the range of polymer concentration to obtain continuous fibers. If the solution is low concentration, there is no continuous fiber formation. Because the polymer fiber will break up into droplets before reaching the collector owing to the influence of surface tension. But, if the solution high concentration, again there is no continuous fiber formation. Because, controlling of polymer solution flow rate is difficult due to the high viscosity. Therefore, there is a requirement of an optimum range of a polymer concentrations for electrospinning (Bhardwaj, & Kundu, 2010; Still, & Recum, 2008).

Further problem of electrospinning method is the presence of defect in the form of beading. Also, the polymer concentration affects the formation of the beads. In the low solution concentration and low viscosity, is obtained a mixture of beads and fibers. However, in high solution concentration and high viscosity is formed uniform fiber with bead forming changes from spherical to spindle like (Huang et al., 2003; Pharm, Sharma, & Mikos, 2006).

Fong, & Reneker (1999), in their experiment were used different polyethyleneoxide (PEO) concentration to observing effects of viscosity and polymer concentration. Different fiber morphologies were captured in which the lowest viscosity 13 centipoise (1 wt. %PEO concentration) while the highest viscosity 1250 centipoise (4 wt. % PEO concentration) as shown in Figure 2.2. In this experiment showed that the beads were not reported in the 4wt. % PEO concentration and were observed the forming of a beads altered spherical to spindle like when the polymer concentrations diverse from lower to higher level (Huang et al., 2003).

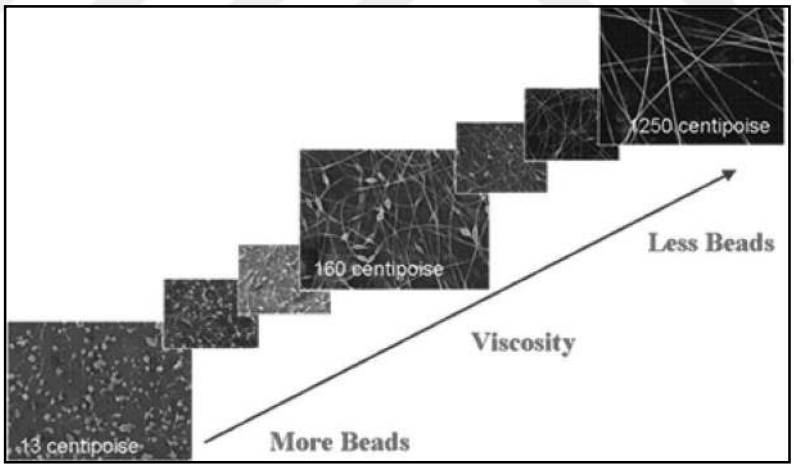


Figure 2.2 SEM photographs of electrospun nanofibers from different polymer concentration solutions (Huang et al., 2003).

*2.3.1.2 Surface Tension*

Surface tension plays a crucial role on the morphology and size of electrospun fibers. When the decreasing the surface tension of nanofiber solution, fiber can be obtained without beads. However, due to the instability of the jet and generating of

sprayed droplets, the high surface tension of solution obstructs the electrospinning process. Different solvent may contribute different surface tension. For example, when the triethylbenzyl ammonium chloride using with PHBV solution was obtained different surface tension and similar conductivity (Bhardwaj, & Kundu, 2010; Pharm, Sharma, & Mikos, 2006).

*2.3.1.3 Solution Conductivity*

Solution conductivity or charge density is another important parameter to produce more uniform fiber and it's depend on polymer type, solvent used and the availability of ionisable salts. When the increase of electrical conductivity of the solution, can be obtained smallest fiber diameter and greater charge carrying capacity than solution with low conductivity. Therefore, the fiber jet of highly conductive solution will be subjected to higher tensile force with the applied electric field than will a fiber jet from a solution with a low conductivity (Bhardwaj, & Kundu, 2010; Still, & Recum, 2008).

One approach to increase solution conductivity has been through the addition of ionic solution, such as $KH_2PO_4$, $NaH_2PO_4$, NaCl and BTEAC. Zhang et al. (2005) investigated the effect of adding NaCl to poly(vinyl alcohol) (PVA) /water solution on the diameter of electrospun fibers. They found that with 0.05 to 0.2 wt. % NaCl addition, the resulting nanofibers were able to decrease the mean fiber diameter. They argued that the addition of salts, resulted increased net charge density on the surface of the solution jet during the electrospinning which increased the electric force exerted on the jet. Thus, they were obtained thinner diameter due to increasing amount of salts (Still, & Recum, 2008).

Another approach to increasing solution conductivity has been through the addition of surfactants. Dayong et al. (2009), used neutral, cationic and anonionic surfactant (Tween 80, CTAB and SDS) with polycarbonate (PC) /chloroform solution to investigate effect of solution conductivity. They found that anonionic surfactant, SDS, did not dissolved into PC /chloroform solvent and did not completely prevent the formation of beads However, the use of cationic surfactant, CTAB, and neutral

surfactant, Tween 80,dissolved in PC / chloroform solution and prevented bead formation. So, charged surfactant increased the solution conductivity and net charge density, causing an increase in the instability yielded more uniform fibers (DaYong et al., 2009).

*2.3.1.4 Dipole Moment and Dielectric Constant*

Dipole moment and dielectric constant of solvent has an influence on electrospinning. Also, some studies have examined dipole moment and dielectric constant to investigate effects of bead formation and the diameter of resultant electrospun fiber. If the higher dielectric constant, the beading instability of electrospinning jet increase. Thus, the deposition area of the fibers increase. As a result of that the fiber diameter decrease due to the increased jet path (Pharm, Sharma, & Mikos, 2006; Ramakrishra et al., 2005).

### *2.3.2 Processing Parameter*

Processing parameters can significantly affect the fiber morphology. This parameters include the applied voltage, flow rate, type of collector, diameter of needle and distance between the needle tip and collector.

*2.3.2.1 Applied Voltage*

One of the most studied parameters amount the processing parameter is the applied voltage and it controls fiber formation diameter ranging from several microns to tens of nanometers. Researchers have suggested that when the lower voltages are applied, a drop is suspended at the needle tip and jet will originate from the Taylor cone producing bead-free spinning. However, at the higher applied voltage, the volume of the pendant decreases until Taylor cone is formed at the tip of the capillary. When the voltage is increased further, the fiber jet being moved from within the capillary, with no visible Taylor cone. As a result of this, many bead defects can be formed (Figure 2.3) (Bhardwaj, & Kundu, 2010; Pharm, Sharma, & Mikos, 2006).

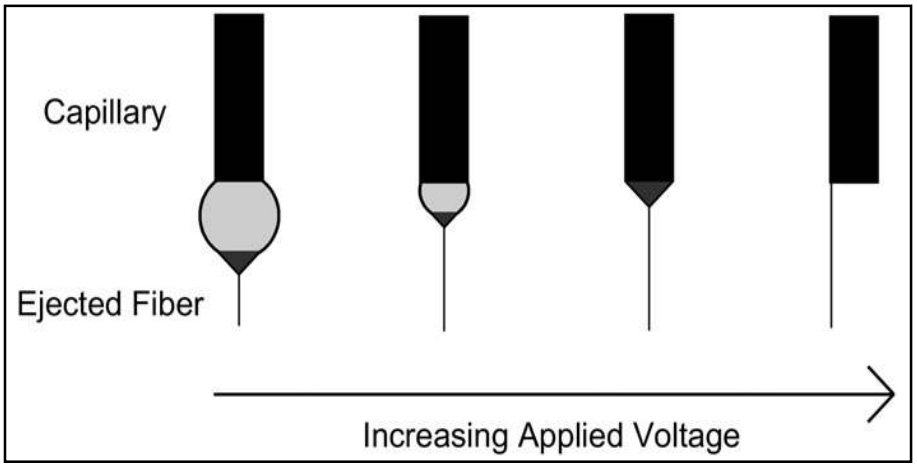


Figure 2.3 The applied voltage on the formation of the Taylor Cone (Still, & Recum, 2008).

Meechaisue et al., (2006) examined the effect of applied voltage for electrospinning, on the morphology of poly (desaminotyrosys-tryrosine ethyl ester carbonate) (poly (DTE carbonate)) nanofibers. They investigated that the applied voltage is too weak or too strong, polymer/solvent system will lead to the formation of beaded fibers. Other study examined by Dietzel et al., (2001) they observed that PEO nanofibers morphological change with applied voltage and they demonstrated that nanofibers become rougher when the increase of applied voltage. Their result are shown in Figure 2.4 (Huang et al, 2003; Still, & Recum, 2008).

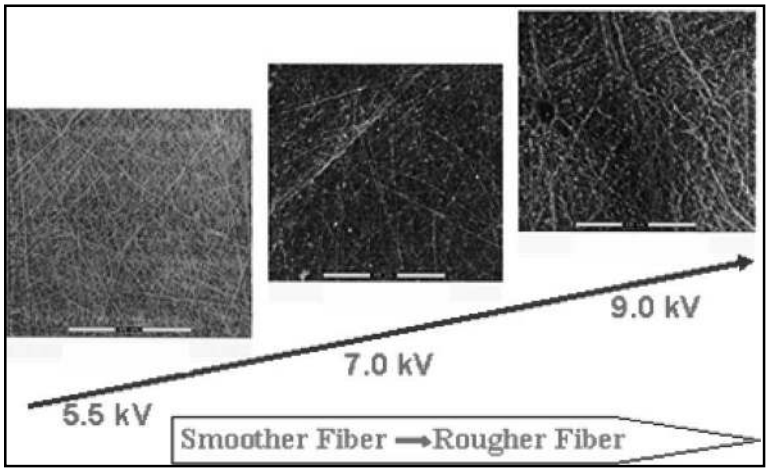


Figure 2.4 SEM photographs of PEO nanofibers electrospun under different electrical potentials (Huang et al., 2003).

*2.3.2.2 Flow Rate*

Polymer flow rate is a crucial process parameters as it influence the fiber size and fiber porosity. Many studies showed that lower flow rates yielded fibers with smaller diameters. When the flow rate is increased, there is increase in the fiber diameter and pore size due to the fact that increased volume of solution drawn away from the needle tip and the jet will take a longer time to dry. Therefore, fibers will not get enough time for evaporation (Ramakrishna et al., 2005; Pharm, Sharma, & Mikos, 2006).

Megelski et al.(2002) investigated the effect of the flow rate on the fiber morphology and size of electrospun fibers from a polystyrene (PS) / THF solution. They reported that fiber diameter and pore size increase with increasing flow rate. Furthermore, amount of bead defects were observed at high flow rates, because of the fiber has inadequate drying time before reaching the collector (Bhardwaj and Kundu, 2010; Still, & Recum, 2008).

*2.3.2.3 Type of Collector*

The collector plate as a conductive material such as aluminum foil which is electrically grounded so there is a stable potential difference between the source and the collector to usage the nanofiber collection (Bhardwaj, & Kundu, 2010; Ramakrishna et al., 2005).

*2.3.2.4 Diameter of Needle*

The internal diameter of the needle has an influence on the electrospinning process. When the decreasing in the internal diameter of needle, the electrospun fibers diameters decreases. Besides, a smaller internal diameter reduces the amount of beads on the electrospun fibers (Ramakrishna et al., 2005).

*2.3.2.5 Distance between Tip and Collector*

The distance between the tip and the collector has been inspected as another parameter to control the fiber diameter and morphology. When the distance between the tip and the collector is decreased the fiber may have enough time to dry before reaching the collector. Also, beads have been observed when the distance that are either too close or too far (Bhardwaj, & Kundu, 2010; Pharm, Sharma, & Mikos, 2006).

### *2.3.3 Ambient Parameters*

Aside from solution and processing parameters, there is also ambient parameter include temperature, humidity etc. Studies have been conducted to examine the effect of ambient parameters on the electrospinning process.

*2.3.3.1 Temperature*

The temperature of the electrospinning environment is important parameter to forming electrospun fibers. Mit-Uppatham, Nithitanakul, & Supaphol (2004) have found that the influence of temperature on electrospun fiber from polyamide-6 solution and ranging from 25 to 60 °***C***. They invented that with increase is temperature, yielded fiber with a decreased fiber diameter (Bhardwaj, & Kundu, 2010).

*2.3.3.2 Humidity*

The humidity of the electrospinning environment may have on effect in the polymer solution during electrospinning. Casper et al. (2004) spun polystyrene solution at various humidity condition. Their study showed that increasing the humidity resulted in the appearance of small circular pores to form on the fiber surface. Furthermore, the humidity of the environment will also decide the rate of evaporation of the solvent in the solution. (Ramakrishna et al., 2005; Pharm, Sharma, & Mikos, 2006).

## 2.5 Potential Application of Electrospun Nanofibers

Electrospun nanofibers application areas have been extended especially in recent years. These fibers are broadly applied in filtration, in cosmetics, as a biosensor, defense and security, energy storage and generation, and in biomedical applications. A schematic diagram illustrating these more extended application areas are shown in Figure 3.5.

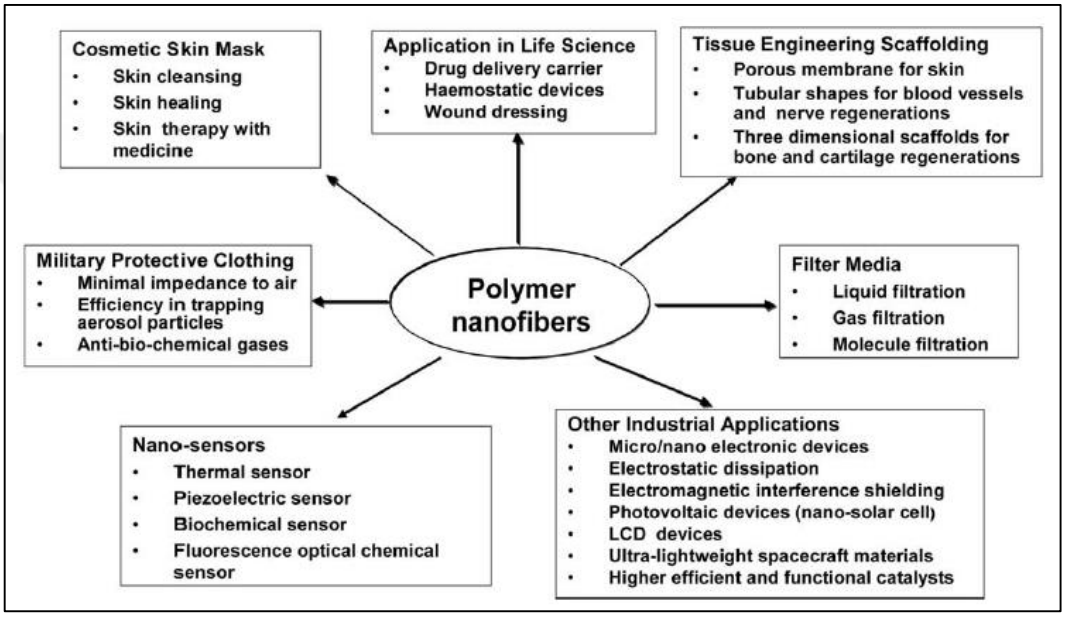


Figure 2.5 Potential applications of electrospun polymer nanofibers (Huang et al., 2003).

### *2.5.1 Biomedical Applications*

From a biological aspect, almost all human tissue and organs are deposited in nanofibrous forms or structures such as bone, cartilage, dentin, collagen and skin. These structures are characterized by well-organized hierarchical fibrous structure realigning in nanometer scale. Indeed recently research in electrospun polymer nanofibers has focused extensively on biomedical areas. Examples include; drug delivery system, wound dressing and scaffold of tissue engineering (Huang et al., 2003; Martins, Reis, & Neves, 2008).

*2.5.6.1 Drug Delivery System*

Electrospun fiber mats have been applied as drug carries in the drug delivery system due to the high functional characteristics such as nanofiber morphology, large surface area and fiber net porosity (Bhardwaj, & Kundu, 2010; Martins, Reis, & Neves, 2008). Many researchers have successfully encapsulated drugs within electrospun nanofibers by mixing the drug in the polymer solution to be electrospun. Kenawy et al.(2002) were investigated the delivery of the tetraryline hydrochloride based on fibrous delivery matrices of poly (ethylene-co-vinylacetate) (PEVA), PLA, and their blend. They found that poorly water soluble drugs loaded in water soluble and water insoluble nanofibers polymer carries have potential for use in drug administration (Huang et al., 2003; Khadka, & Haynie, 2012).

*2.5.6.2 Dressing or Wound Healing*

Polymer nanofibrous membranes have a potential to use for the treatment of wounds or burns of a human skin due to the microfibrous and nanofibrous structure and cytocompatibility. Several electrospun fiber review articles include wound dressing. For example, Rho et al. (2006) were investigated open-wound test with collagen nanofiber membranes. They found that early-stage healing was faster with the electrospun nanofibers than with normal cotton gauze (Khandka, & Haynie, 2012).

*2.5.6.3 Scaffold for Tissue Engineering*

A variety of electrospun scaffolds have been examined in a number of different tissue applications such as vascular, neural, skin, and bone (Bhardwaj, & Kundu, 2010; Liu, Ding, & Zhou, 2013). For instance, Stitzel et al. fabricated a prototypic vascular graft with the use of electrospun PLA fibrous meshes and collagen type I fibers. They found that vascular graft prototype was able to support the growth of human aortic smooth muscle cells (SMCs). In another study, Anuradha et al. was evaluated the effect of fiber alignment on the morphology and proliferation of schwann cells into PLGA.They invented that aligned PLGA fibers were able to guide

the Schwann cells along their length and illustrated a better rate of cell proliferation than oriented randomly (Goh, Shakir, & Hussain, 2013; Liu, Ding, & Zhou, 2013). Furthermore, Li et al. (2013) was examined silk fibroin nanofiber scaffold containing human recombinant bone morphogenetic protein 2 (BMP-2) and/or nanoparticles of hydroxyapatite (nHAP) scaffolds. They observed that electrospun SF-based scaffold supported human bone- marrow-derived mesenchymal stem cells (hMSCs) growth and differentiation toward osteogenic outcomes.

Consequently, recent technological advances has improved the generation of a variety of scaffolds with a pore and nano-structure. It is generally agreed today that electrospun nanofibers scaffolds for tissue engineering applications (Goh, Shakir, & Hussain, 2013; Jang, Castano, & Kim, 2009; Liu, Ding, & Zhou, 2013; Xie, Li, & Xia, 2008).

# CHAPTER THREE
# SURFACE PROPERTY OF BIOMATERIAL

## 3.1 Introduction

Cell adhension and cell spreading is an important parameter for tissue engineering. But, biomaterials, especially tissue engineering scaffolds don't have the necessary specific bioactivity to accelerate ECM secretion and regeneration of cultured cells. Therefore, biomaterials exibit low performance. As a consequence, the researchers have been focused on surface engineering for the development of biomaterials' surface promote cell adhesion, proliferation and to maintain cell normal phenotype function. These material surface properties comprise the hydrophobicity, charge, roughness, softness&stiffness and pore size of the material (Ponsonnet et al., 2003; Wang, 2003).

## 3.2 Surface Modification of Polymers

Many diverse application of polymers, in "every-day" uses, in industrial uses, and in medical uses, depend upon physical, chemical and biological interaction of molecules or microorganisms with their surface. Polymeric surfaces are usually modified to increase or reduce:

- Surface Wettability
- Surface Topography and Roughness
- Surface Softness and Stiffness
- Surface Pore size and Porosity
- Surface Charge

### *3.2.1 Surface Wettability*

Surface modification is an important parameter in order to control of material characteristics for regulating biocompatibility. Surface wettability (generally referred to as hydrophobicity/hydrophilicity) is one of the most important parameters that could regulate the protein adsorption and cell behavior (Chang, & Wang, 2011; Xu, & Siedlecki, 2007). Generally hydrophobic surfaces are considered to be more protein-adsorbent than the hydrophilic surfaces, but may induce strongly irreversible adsorption and denature the protein's native conformation and bioactivity. On the other hand, hydrophilic surfaces have a higher rate of cell attachment. But, most synthetic biodegrable polymers are hydrophobic. For that reason, surface engineers have developed some methods for the improvement of hydrophilicity of the surfaces (Hoffman, 1995; Xu, & Siedlecki, 2007).

One convenient method is plasma treatment. Plasma surface modification is an effective and economical way to modify the surface physicochemical properties including surface wettability of materials. This method can easily introduce polarized groups such as hydroxyl, carboxyl, amino and sulfate on polymer surfaces using different reaction gases such as air, $NH_3$, $SO_2$, $CO_2$ or other organic compounds (Ma, Mao, & Gao, 2007; Wei et al., 2009).

Several research reports have claimed changes in surface biocompatibility in terms of cell attachment and protein adsorption upon plasma treatment. It was explained by Park et al. (2007) that the effect of surface wettability on the cells has an important role for cell adhesion and proliferation. The researcher investigated mouse fibroblasts attachment and proliferation on plasma treatment electrospun Poly(lactic-co-glycolic acid) (PLGA) nanofibers. They found that the contact angle of non-treated PLGA nanofibers was 134º and decreased to 115º and 45º after treatment with oxygen plasma and ammonia plasma, respectively. They reported that the adhesion and proliferation of mouse fibroblasts on the plasma-treated nanofibers significantly enhanced and cellular adhesion to PLGA nanofiber was significantly improved by plasma treated, especially by ammonia plasma treatment (Park et al., 2007).

The surface wettability can be assessed by measuring contact angle. When measuring contact angle, a drop of a desired wetting liquid is placed on the surface of the specimen, and the angle between the tangent of the drop at the solid/liquid/gas three-phase boundary and the horizontal baseline of the solid surface is measured as shown in Figure 3.1.

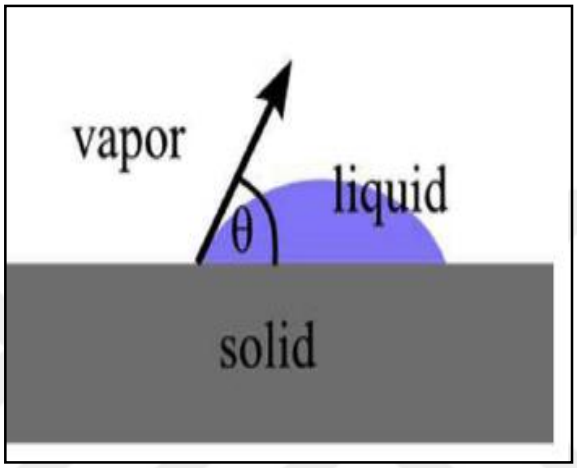


Figure 3.1 The surface wettability measured by contact angle (Rupp et al., 2014).

This angle, the so-called contact angle (CA or θ) and can be calculated from equation 1;

$$\mathrm{Tan}(\theta_s\backslash 2) = h\backslash x \qquad (3.1)$$

in which $\theta_s$ is the static contact angle, h is the droplet height, and x is half of the droplet width (Goddard, & Hotchkiss, 2007).

The contact angle characterizes the surface wettability when water is used as the wetting agent. In principle, contact angle can range from 0 to 180 °, indicating that the wetting liquid is being drawn toward the surface or is being repelled by the surface. The water contact angles lower than 90° designate surfaces as hydrophilic with a high wettability, and contact angles very close to 0° ascribe surfaces as super hydrophilic. While the water contact angles higher than 90 ° designate surfaces as hydrophobic

with a low wettability and the contact angle above 150 °, are termed as super hydrophobic surface (Figure 3.2) (Rupp et al., 2014).

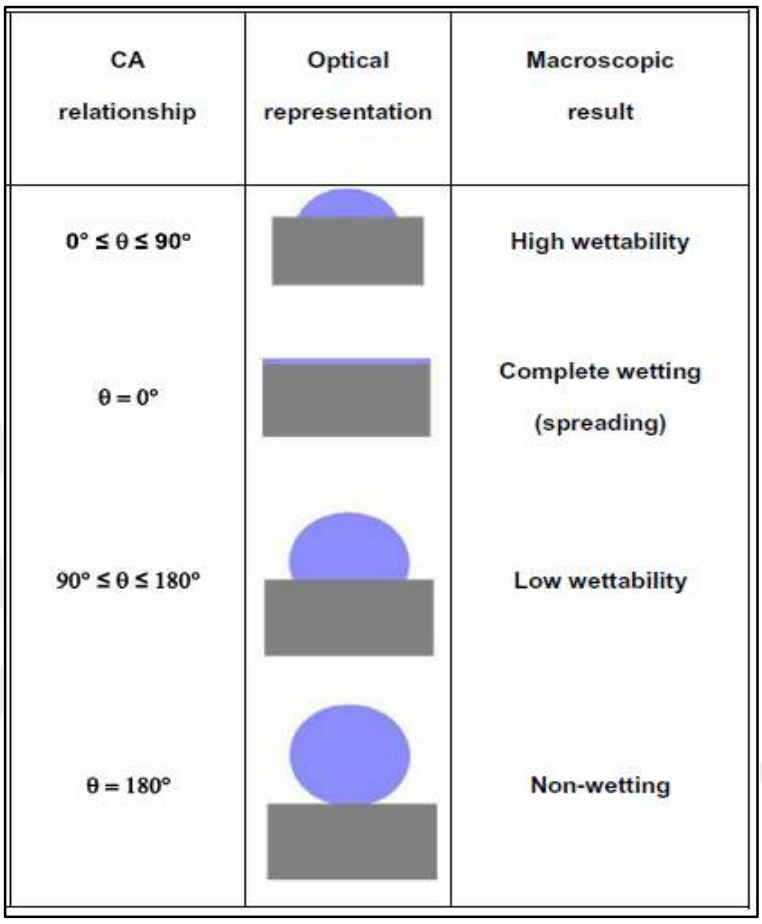


Figure 3.2 Interrelations between contact angle and the wetting of a solid (Rupp et al., 2014).

Wei et al. (2009) studies showed the more hydrophilic surface of material films is the much more cell adhesion on the surface. Osteoblast adhesion was reported decrease when the contact angle of hexamethyldisiloxane (HMDSO) coated thin-film surface increased from 0° to 106°.

### *3.2.2 Surface Topography and Roughness*

Material surface topography and roughness are another important factors influencing the formation of fibrous capsule around implants, inflammatory response at tissue implant interface, angiogenesis and cell adhesion. For instance, Chung et al. (2003) investigated that a nanometer scale of surface roughness could improve the

adhesion and growth human endothelial cells on polyurethanes (PU) surface and grafted cell adhesion peptide Gly-Arg-Gly-Asp (GRGD) on a modified PU surface. They argued that the adhesion and growth of human endothelial cells for the roughness surfaces was better than that of smooth surface for both GRGD grafted and ungrafted surfaces, respectively (Chung et al., 2003; Chang, & Wang, 2011; Lee et al., 2004; Wang et al., 2004).

The response of cells to roughness differs depending on the cell type. For example, a macroscopic scale of surface roughness could improve for osteoblasts and neurons. Surface roughness is an important criteria to osteointegration. Rough surfaces produce better bone fixation than smooth ones, in vivo. In the research by Lee et al. (2004), they investigated the ability of the MG63 osteoblast-like cells to be cultured on polycarbonate (PC) membrane surfaces, it was found that a higher amount of cells attached to rougher surface. In another study by Bartolo et al. (2008), they examined how the membranes surface roughness affect the behaviour of neurol cells. They used neurons isolated from hippocampus which is the important area of brain. These neurons were cultured onto different polymeric membranes such as polyester(PE), modified polyetheretherketone (PEEK-WC), flurocarbon (FC), and polyethersulfane (PES) in order to investigate the effect of surface roughness. As a result, they found that the axonal length increased and neuritis becomes highly branched on the nanoscale rough surfaces (6.26-49.38 nm). In case of microscale rough membranes (87.2-200 nm), the neurons were less developed as demonstrated by round-shape soma and poorly branched structure was observed. Therefore, the nanoscale rough membranes seem to be more supportive for the development of the neurons (Lee et al., 2004; Bartolo et al., 2008).

### *3.2.3 Surface Softness & Stiffness*

The surface mechanical properties of biomaterials are emerging as a crucial factor in the adhesion and biological response of cells that are in contact with these materials. Surface stiffness is measure of how soft (as silk) or stiff (as rock) a material surface. Many researches have reported that cell attachment, proliferation and differentiation

are all modulated by substrate rigidity to a degree dependent upon the substrate stiffness in relation to the stiffness of the native tissue (Chang, & Wang, 2011; Jiang et al., 2008).

In addition, specific cellular properties can actively modify the surface of the implants, changing the stiffness of microenviroment of their own or other cells. For instance, aortic smooth muscle cells have been found to spread and organize their cytoskeletons and focal adhesions to greater extent on stiff gels than on soft gels. Kim et al. (2009) used AFM to measure the surface elasticity and they observed the effect of these parameter on endothelial cell attachment was demonstrated by seeding 2-hydroxyethyl methacrylate (HEMA) and 2-methancryloxyethyl trimethyl ammonium chloride (MAETAC) copolymer hydrogels with porcine pulmunary artery endothelial cells (PPAECs). They found that stiffer hydrogels promote cellular attachment and growth more than softer hydrogels. In another study, the tissue level matrix stiffness effect on human mesenchymal stem cells (hMSCs) seeded on a polyacrylamide hydrogel was examined (Engler et al., 2006).They observed that the cells commit to the lineage specified by matrix elasticity, consistent with the elasticity-insensitive commitment of differentiated cell types. Such as soft matrices that mimic brain are neurogenic, stiffer matrices that mimic muscles are myogenic and comparatively rigid matrices that mimic collagenous bone are osteogenic. Further, morphotype and the expression of the focal adhesion plaque proteins of endothelial cells are also modulated by substrate elastisity (Deroanne et al., 2001; Engler et al., 2006; Jiang et al., 2008; Kim, English, & Kihm, 2009).

### *3.2.4 Surface Pore Size and Porosity*

Transport issues are very important for tissue engineering scaffolds and include delivery, waste removal, exclusion of materials or cells, protein transport and cell migration, which, in turn, are governed by the scaffold's porous structure. Pore size, total porosity and the overall continuity of the pores are generally used to characterize the pore structure. Porosity is defined as the percentage of void volume in the material and it is a morphogical property independent of the material. Pores are necessary for

tissue formation because they allow migration and proliferation of cells, as well as vascularization. Besides, a porous surface improves mechanical interlocking between the implant biomaterial and the surrounding native tissue, providing greater mechanical stability at this critical interface. However, cell seeding in the center of the scaffold and feeding the inner surface scaffold are limitted when the pores are too small, whereas larger pores effect the stability of the scaffold and its ability to provide physical support for seeded cells (Yang et al., 2002; Karageorgious, & Kaplan, 2005).

There are several methods have been used to evaluate scaffold porosity and pore size including theoretical assessment, scanning electron microscopy, gravimetry (for total porosity measurment), mercury porosimetry, gas phyconometry and adsorption. SEM analysis complements the theoretical calculation of porosity and allows direct measurements of pore size and wall thickness and cell morphology. However, SEM cannot examine the scaffold interior without sample sectioning (Karageorgious, & Kaplan, 2005). Total porosity (P) is measured by gravimetry according to the equation;

$$\Pi = 1 - p_{scaffold} / p_{material}, \quad (4.2)$$

where $p_{material}$ is the density of the material of which the scaffold is fabricated and $p_{scaffold}$ is the apparent density of the scaffold measured by dividing the weight by the volume of the scaffold.

Mercury porosimetry is a well known and established method, but it neither measures small mesopores (2-50 nm pores) due to lack of mercury penetration nor measures very large pores (500µm pores) as the mercury penetrates the structure before measurement can be made (Giesche, 2006). The gas adsorption method is relevant to the study of porosity in nano-featured and nano-modified scaffolds and is based on the electrical forces of attraction that bind atoms in solids. Surface atoms bind surrounding gas molecules via Van der Waals and electric forces to counter the net inward attractive forces (Chang, & Wang, 2011).

Specific cells require different pore size for optimal attachment, growth and mobility. For example, in porous silicon nitride scaffolds, endothelial cells bind preferentially to scaffolds with pores smaller than 80 μm, while fibroblasts preferentially bind to larger pores ( > 90 μm). In PLLA scaffolds, vascular smooth muscle cells prefentially bind to one range of pore size (63-150 μm) while fibroblasts bind to a wider range (38-150 μm) (O'Brien et al., 2005; Chang, & Wang, 2011).

Researchers are focused on the design of the scaffold to ensure appropriate porosity and porous structure for cell penetration and ingrowth. Higher porosity did not affect cell attachment but resulted in increased cell proliferation, since pore space increased with porosity and facilitated transport of oxygen and nutrients. Besides, higher porosity is expected to enhance osteogenesis. Also, the minimum requirement for pore size is considered to be ~100 mm due to cell size, migration requirements and transport. However, pore sizes > 300 mm are recommended, due to enhanced new bone formation and the formation of capillaries (Karageorgious, & Kaplan, 2005). Hulbert et al. (1970), where calcium aluminate cylindrical pellets with 46% porosity were implanted in dog femoral. Large pores (100–150 and 150–200 mm) were showed substantial bone ingrowth. Smaller pores (75–100 mm) resulted in ingrowth of un-mineralized osteoid tissue (Hulbert et al., 1970). In another study, Lee et al. (2004) examined the behavior of MG63 osteoblast-like cells cultured on polycarbonate (PC) membrane surfaces with different micropore size (0.2-0.8μm in diameter). The purpose of the their study was to examine the MG63 osteoblast-like cells were cultured on a range of porous (PC) membranes with well-defined surface topography as an attempt to investigate the effect of surface micropore on the interaction of cells onto polymeric materials. They reported that the MG63 cells were protruded fillodopia and lamellapodia resulting in being less spread and flattened on larger micropore sizes (3.0, 5.0, and 8.0 mm of diameter) than smaller ones (0.2, 0.4, and 1.0 mm). It seems that the cell adhesion and proliferation were progressively inhibited as the PC membrane surfaces had micropores with increasing size, due to surface discontinuities produced by track-etched micropores. However, on the large micropore membrane with 3.0–8.0 mm in diameter, the cells appeared spherical shape morphologies with phenotype of osteoblasts. Figure 3.3 revealed that the MG63 cells on smaller micropore sizes (0.2–

1.0 mm of diameter) were tested adhered and spread well and were showed spindle-shape in cellular morphology.

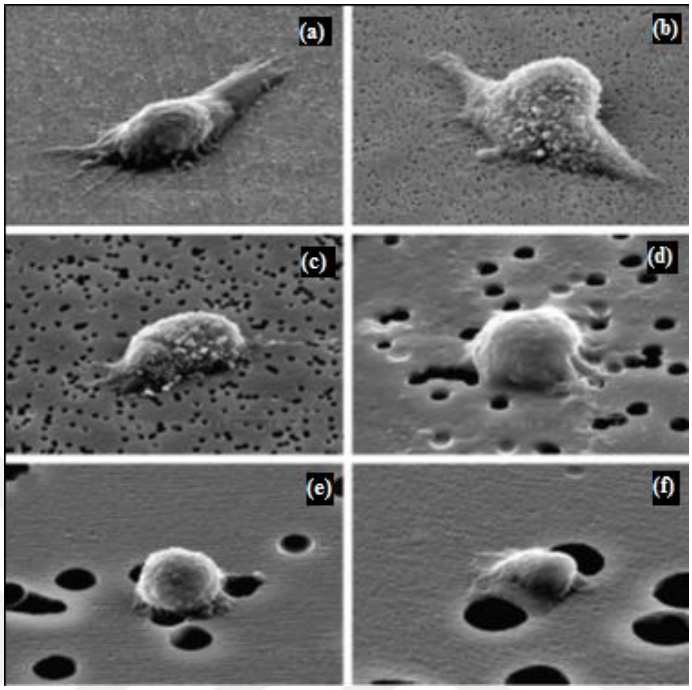


Figure 3.3 SEM pictures of the MG63 cells attached on the PC membrane surfaces with different micropore sizes, (a) 0.2, (b) 0.4, (c) 1.0, (d) 3.0, (e) 5.0, and (f) 8.0 μm in diameter of micropore sizes. (Lee et al., 2004).

### *3.2.5 Surface Charge*

Surface charge is the electrical potential diffrence between the inner and the outer surface of the different aggregate state: liquid and gas, liquid and solid or gas and liquid. Besides, the surface-charge of biomedical implant is known to be a key factor to guild cells adhesion. Thus, surface-charge modification seems to be a promising new direction for improving the cell behaviour of a biomaterial. Although surface-charge modification is a relatively new methodology, it has been rapidly gaining research attention in recent years (Butt, Karlheinz, & Micheal, 2006).

After surface wettability, surface charge has been recently described a lot in the cell attachment phenomenon. Firstly, the amount of surface charges can influence cell behavior (Ishikawa et al., 2007). For example, Jung et al. (2008) observed that as the degree of charge density of poly (styrene-co-acrylic acid) increased, fibroblasts cells

adhesion and proliferation increased. In another study, Kim, English, & Kihm (2009) examined the positive charge density effect on 2-hydroxyethyl methacrylate (HEMA) and 2-methacryloxyethyl trimethyl ammonium chloride (MAETAC) copolymer hydrogel. They observed that the viability of endothelial cells increase on hydrogels with the increase of the concentration of MAETAC which acted as the positive charge functional group (Figure 3.4).

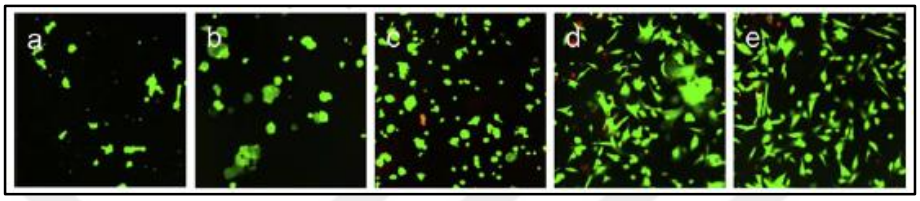


Figure 3.4 Chondrocyte viability on hydrogels with different concentrations of maetac in their formulation on day 1: (a) 0%; (b) 5%; (c) 10%; (d) 20%; (e) 30% (Kim, & Kihm, 2009).

Secondly, many researchers reported improved-biocompatibility, cell afinity and cell differentiation on the implanted surface by using positive ions and negative ions. For instance, Schneider's group also investigated the positive, negative or neutral charge density effect on the attachment, spreading and proliferation of osteoblast and fibroblasts cells on HEMA hydrogel. Their results show that positively charged HEMA hydrogel supported the greatest cell attachment than negatively and neutral charge densities (Schneider et al., 2004). In another study by Dadseta et al. (2011), were compared the effects of negative and positive fixed charges on chondrocyte behavior. Small negatively charged molecules of sodium methacrylate (SMA) were co-polymerized with the oligo(poly(ethylene glycol)fumarate) (OPF) hydrogel to produce a negatively charged hydrogel. [2-(Methacryloyloxy) ethyl]-trimethylammonium chloride (MAETAC), which is a positively charged monomer, was co-polymerized with the OPF hydrogel for comparison of the charge effects. They found that negatively charged OPF hydrogel increased the extent of chondrocyte differentiation rather than positively charged OPF hydrogel scaffold. On the other hand, Makohliso et al. (1993) mentioned that positively charged coating material such as polylysine improved neural attachment in vivo.

Finally, the surface charges can be used to modify cell behvaior through the chemical functionalities of the polymer materials (Table 3.1).

Table 3.1 The effect of material surface functional groups on proteins and cells (Schmidt et al., 2009).

| Functional group | Properties | Effect on cells |
|---|---|---|
| $-CH_3$ | Neutral, hydrophobic | Promotes increased leukocyte adhesion and phagocyte migration |
| -OH | Neutral, hydrophilic | Increases osteoblast differentiation |
| -COOH | Negative, hydrophilic | Increase osteoblast attachment |
| $-NH_2$ | Positive, hydrophilic | Promotes myoblast and endothelial proliferation and osteoblast differentiation |
| $–CH_2NH_2$ | Neutral, hydrophilic | Enhance CHO attachment of Chinese hamster ovary cells |

Lee et al. (1994) prepared polyethylene (PE) surfaces with differently chargeable functional groups (-COOH,$-CH_2OH$, $-CONH_2$ and $–CH_2NH_2$ groups) by corona discharge treatment, graft copolymerization and substitution reaction to study the effect on Chinese hamster ovary (CHO) cells behavior (Lee et al., 1994). Results indicated that the best cell adhesion, growth and spreading rate were recorded on polar and positively charged surfaces (amine group grafted PE) while the negatively charged surface (carboxylic acid group-grafted PE) had poor growth. Moreover, the surfaces grafted with neutral amide and hydroxyl groups showed a similar number of cell attachments; however; the morphology of cells attached on the surfaces was quite distinct. The cells were spread much more on the hydroxyl group grafted surface than the amide group-grafted one. The arguments given above prove that surface charge plays an important role in the application of cell biology and tissue engineering.

# CHAPTER FOUR
# MATERIALS AND METHODS

Stages of the study, parameters that are encountered and characterizations performed within the scope of this thesis are summarized in Figure 4.1.

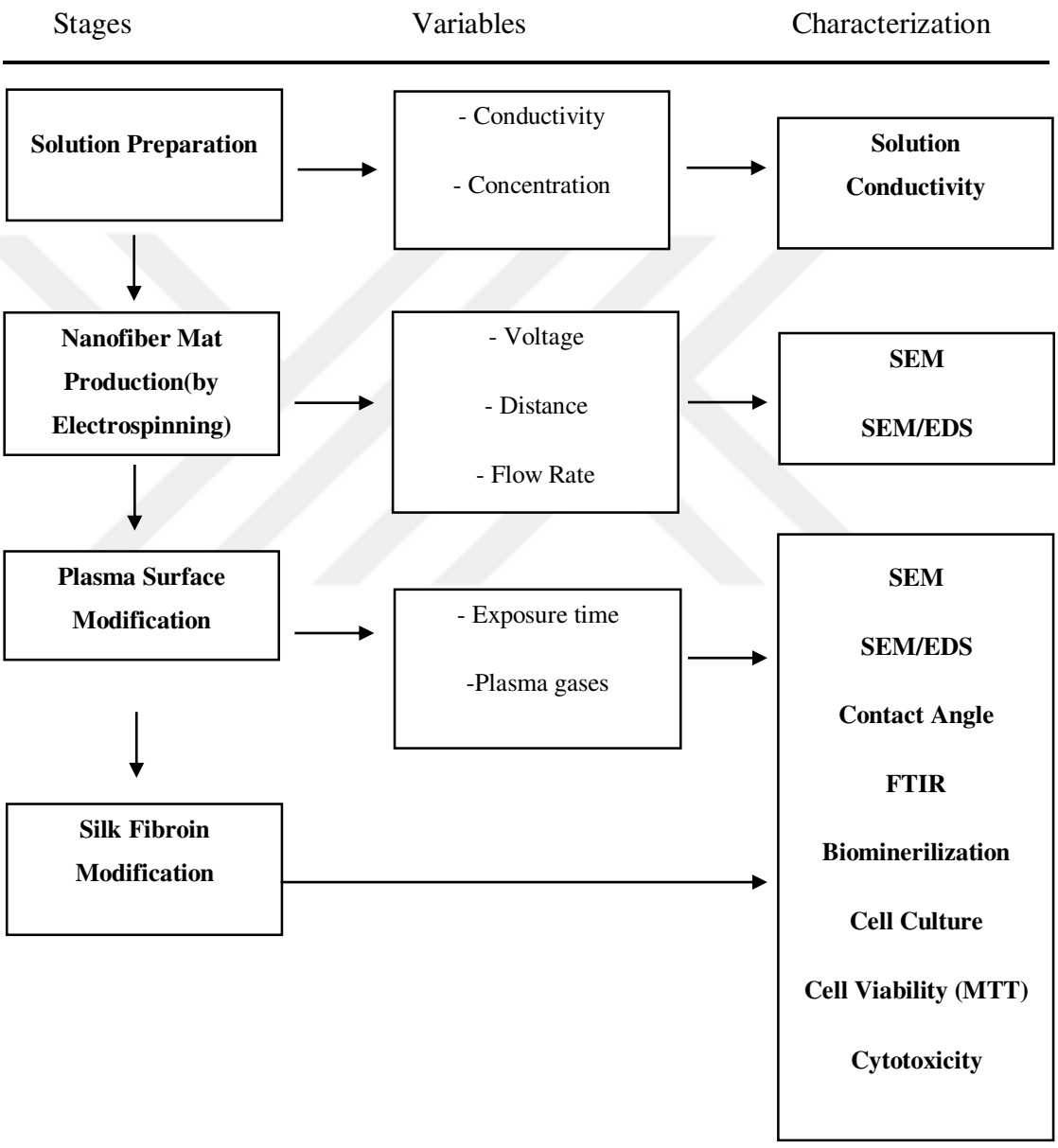


Figure 4.1 Summary of parameter and characterization.

## 4.1 Materials

PHBV of Tianan Enmat with a molecular weight of 310,000 Da containing about 3% mol of 3-hydroxyvalerate was purchased from Helian Polymers, Netherlands. The organosoluble salt, benzyl triethylammonium chloride (BTEAC), chloroform and dialysis tubing cellulose membrane (D9777) which was used in the purification of silk fibroin solution were obtained from Sigma-Aldrich. Cocoons of *Bombyx mori* silkworm silk were supplied from North Cyprus. Sodium carbonate ($Na_2CO_3$), calcium chloride ($CaCl_2$) and methanol were purchased from Merck. All the chemicals were used as received without further purification.

## 4.2 Methods

### *4.2.1 Preparation of PHBV Solution*

PHBV solution was prepared for the electrospinning process. First, PHBV (3, 5, 10, or 15 % wt/v) including an organosoluble salt BTEAC (0.1 or 0.2 % wt/v) was dissolved in chloroform by gentle stirring using a hotplate with a magnetic stirrer (Heidolph MR Hei-Standard, USA) for 2 hours in a water bath of 50˚C. Then it was left to stir for 24 h at room temperature. Preparation of the optimazed PHBV solution %3 (wt/v) is given in Figure 4.2.

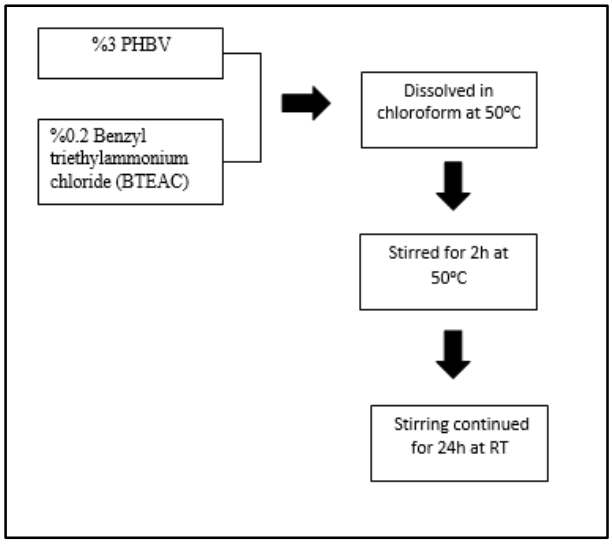


Figure 4.2 Preparation of %3 PHBV solution

### *4.2.2 Production of Fiber Mats*

Nanofiber mats were obtained by the electrospinning process. First, PHBV solution (3 wt%) including an organosoluble salt BTEAC (0.2 wt%) was prepared for spinning (Figure 4.2). Then it was loaded into a 10 mL plastic syringe equipped with a 22-gauge stainless steel needle. During electrospinning, the PHBV solution was pushed from a syringe to a stainless steel needle by a syringe pump (NE-1000,New ERA Pump System, Inc., USA) at different solution feeding rates (1 or 3 ml/h). Different electrospinning voltages (15 or 20 kV) were applied by a power supply (ES30P-5W; Gamma High Voltage Research, USA) which was connected to the needle. Nanofibers were collected on a grounded fiber collecting plate covered with an aluminum foil that was placed at different working distances ( 15 or 20 cm). After the electrospining process, the fiber mats were kept in a desiccator. The electrospinning setup is shown in Figure 4.3. The optimized electrospinning parameters were as follows: (1) working distance = 15 cm, (2) solution feeding rate = 1 ml/h, and (3) applied voltage = 20 kV.

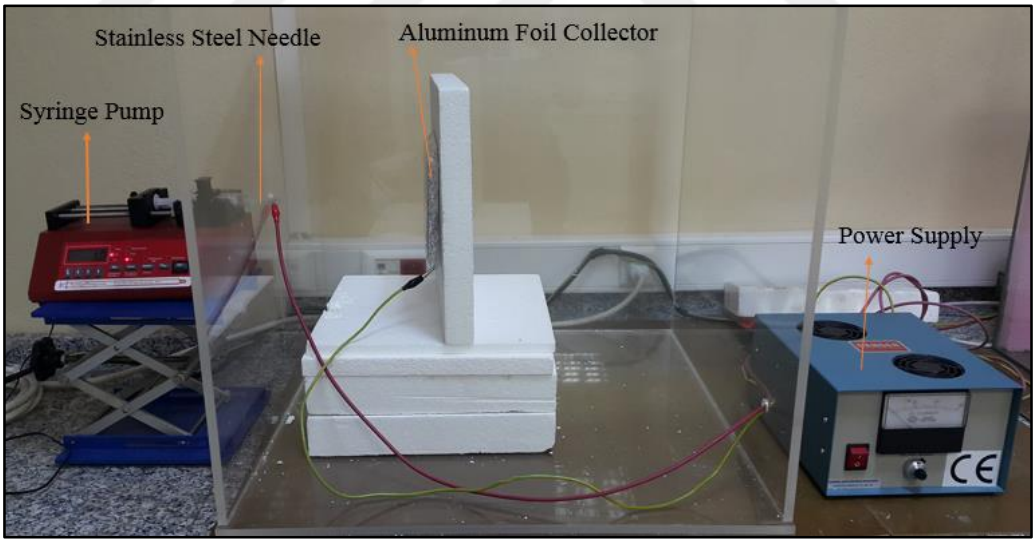


Figure 4.3 The electrospinning setup for the formation of PHBV nanofibers.

### *4.2.3 Surface Modification of Fiber Mats*

Electrospun PHBV nanofibers were treated with plasma using low pressure radio frequency (RF) plasma system ( Diener Electronic/Pico, North USA) under either oxygen and nitrogen gases. First, PHBV mats were placed in the plasma reactor

chamber in a petri dish and the chamber was evacuated. Then the chamber was filled with either oxygen or nitrogen and the pressure inside the plasma chamber was kept at $3x10^{-1}$ mbar. The plasma power was set to be 25 W and the mats were subjected to different exposure periods (2, 5, and 10 minutes) in order to determine an optimal exposure time which was evaluated by SEM analysis and contact angle values of the mats.

### *4.2.4 Silk Fibroin Immobilization*

#### *4.2.4.1 Formation of Silk Fibroin Solution*

Silk fibroin was prepared by the degumming and dissolving of Bomboxy mori silkworms. Raw silk fibers were degummed three times with 0.01 M $Na_2CO_3$ solution at 50ºC for 3 hour and then rinsed throughly with distilled water to extract the glue-like sericin proteins. The degummed silk (silk fibroin, SF) was dissolved in a ternary solvent system of $CaCl_2/CH_3CH_2OH/H_2O$ in molar ratio of 1/2/8 at 70ºC for 6h. After filtration, the filtrate was dialysed with tubular cellulose membrane in distilled water for 3 days. The aqueous silk fibroin solution with a concentration of ~2% (w/v) was collected and stored at 4ºC.

#### *4.2.4.2 Silk Fibroin Modification*

The plasma-treated PHBV nanofiber mats were immediately immersed into 2% (w/v) SF solution for 24 hour after plasma treatment, and then dried overnight at room temprature. Also, PHBV nanofiber mats without plasma-treatment was immersed into same solution under the same conditions and used as the control group. Thereafter, in methanol-annealing process, the SF modified mats were immersed in 90% methanol solution for about an hour to change the SF conformation from soluble random coil to insoluble β-sheet form. Finally, SF immobilized nanofiber mats were rinsed with distilled water three times and vacuum dried overnight at room temperature.

### *4.2.5 Characterization of the Scaffolds*

#### *4.2.5.1 Solution Conductivity Measurement*

The conductivity of the PHBV solution prepared for electrospinning was measured by conductivity meter (WTW Cond 3110).

#### 4.2.5.2 *Scanning Electron Microscope (SEM)*

All electrospun PHBV fibrous scaffolds were sputter-coated with a thin layer of gold (Quorum Technologies Polaron range, SC7620 sputter coater). The coated samples were characterized using a scanning electron microscope (SEM, JEOL JSM-6060) at an accelerating voltage of 5-10 kV. The average diameter of electrospun fibers was estimated from the SEM micrographs with 1000 fold magnifications by the Image J program (National Institutes of Health, USA). The diameters of at least 100 fibers were measured for each SEM image and the average fiber diameter was calculated. Also, the cell morphology of SaOS-2 cells on the nanofiber mats were observed by SEM.

#### *4.2.5.3 Energy Dispersive X-ray Spectroscopy (EDS)*

Disperison and presence of Hap on the fiber surface after minerilization were investigated by EDS/mapping analyses (EDS, JEOL JSM-6060).

#### *4.2.5.4 Contact Angle*

The wettability of the PHBV nanofiber mats was measured using a contact angle meter (Attension Theta Live) with the sessile drop method. The mat was first attached onto the holder of the contact angle meter. Then, 6 µl of distilled water was dropped onto the mat's surface. Then, images of the water droplets were recorded using a video camera system. From the measured angle between the droplet baseline and the tangent at the water/air boundary, a contact angle was calculated as the average of the measured left and right contact angles. Three measurements were taken at different

locations of the same mat and the average value was obtained. All measurments were conducted at room temprature.

*4.2.5.5 Fourier Transform Infrared Spectroscopy (FTIR)*

The chemical structure of the nanofiber mats was analyzed by Attenuated Total Reflectance Fourier Transform Infrared Spectroscopy (ATR-FTIR) (Perkin Elmer Spectrum BX) in the wavanumber range of 4000-650 $cm^{-1}$ with the resolution of 4 $cm^{-1}$ and 25 scans per sample. ATR-FTIR analysis is also used to determine the presence and conformation of silk fibroin on the surface of silk fibroin-modified/plasma-treated PHBV nanofiber mats by investigating the amide I and amide II bands in IR spectrum.

### *4.2.6 In Vitro Biological Evaluation*

*4.2.6.1 Biomineralization Tests*

For the observation of apatite like mineral formation on the plasma treated/untreated or silk modified/non-modified PHBV nanofiber mats, SBF solution was prepared according to Kokuba and Takadama (2006).PHBV nanofiber mats were placed into 50 mL falcon conical tubes and the SBF solution was poured into each conical tube up to 20 mL. Then, the tubes were incubated at 36.5±5ºC for 5 weeks and SBF solutions were changed every 48 h. After biomineralization, the nanofiber mats were washed three times with distilled water to remove residual salts and dried at room temperature before further analysis.

*4.2.6.2 Cell Culture*

The SaOS-2 osteoblast-like human osteosarcoma cancer cells and L929 fibroblast cells were cultured in McCoy's 5A (Hyclone) expansion medium supplemented with 15% FBS (fetal bovine serum)(Hyclone), 1% L-glutamine, 0.1% gentamicin and L929 mouse fibroblast cells were cultured DMEM F12 medium with 10% FBS (fetal bovine serum)(Hyclone), 1% L-glutamine, and 0.1% gentamicin at 37°C in a 5% $CO_2$ humidified incubator, in 75 $cm^2$ cell culture flasks. After a subconfluent monolayer

was achieved, cells were harvested by gentle digestion with 0.25% trypsin/EDTA, counted with a hemocytometer and suspended in fresh media before seeding onto nanofiber mats. The mats were put into a petri dish and sterilized by ultraviolet (UV) light for 45 minutes for each side of the mats. The sterilized nanofiber mats were placed in a 96-well plate for the cell viability and in a 6-well plate for the cytotoxicity tests. Then, SaOS-2 cells were seeded onto mats 12 µl and 120 µl of the cell suspension at a density of $8.25 \times 10^5$ cells/ml was applied dropwise to the top surface of the mats for MTT assay and cytotoxicity test, respectively. Also, L929 fibroblasts cells were seeded onto mats at a concentration of $1.5 \times 10^6$ cells/ml by adding 60 µl of the cell suspension for cytotoxicity test. After cell seeding, the culture media were added and the cells on the mats were cultured for up to 7 days in a 5% humidified atmosphere at 37°C. The media were changed every two days. All experiments were performed in triplicate (n=3).

*4.2.6.3 MTT Assay*

Cell proliferation and viability of SaOS-2 cells on the nanofiber mats was determined by MTT assay. The assay is dependent on the cellular reduction of MTT [3-(4, 5-dimethylthialzol-2-yl)-2, 5-diphenyltetrazolium bromide], by the mitochondrial dehydrogenase enzymes of viable cells, to a blue formazan product, which can be measured by a spectrophotometer. The amount of purple formazan crystals formed is proportional to the number of viable cells. In 1, 3, and 7 days after cell seeding, culture medium from each well was aspirated and replaced with 100 µl per well of MTT solution for each scaffold in 96-well culture plates. The plate was incubated for 3 hour at 37°C with 5% $CO_2$.The media were aspirated and the cells were then lysed using 100µL per well of dimethylsulfoxide (DMSO) to release and solubilize formazan crystals. After 10 min of rotary agitation, the absorbance of the dissolved formazan crystals was measured using a UV-visible spectrophotometer (MDS Molecular Devices, Versa Max, USA) at a wavelength of 570 (690 nm ref.).

*4.2.6.4 Cell Morphology*

The cell morphology of the SaOS-2 cells on nanofiber mats surfaces after cell culture for 7 days was observed using scanning electron microscopy (SEM, JEOL JSM-6060). The media were aspirated from culture wells, the mats were washed with 0.1 M sodium cacodylate buffer (C-0250, Sigma, USA) and fixed in 5% glutaraldehyde (8.20603.1000, Merck, Germany) in 0.1 M sodiumcacodylate for 30 min. Later, the mats were washed with 0,1 M sodium cacodylate in the buffer B ( 0,1 M sodium cacodylate buffer and fixed in 7% sucrose (1.07651.1000, Merck, Germany) for 30 min and post fixed in 2% osmium tetroxide in 0.1 M cacodylate for 30 min in the dark. Following a buffer rinse, the samples underwent gradual dehydration in an ethanol series (35%, 50%, 70%, 85%, 95%, and 100%, respectively). Finally, samples were placed in hexamethyldisilazane solution (HMDS) for 5 min, allowed to dry overnight, and stored in a desiccator. Samples were sputter-coated with thin layer gold prior to imaging.

*4.2.6.5 Cytotoxicity*

Indirect contact test was conducted in accordance with ISO 10993-5 (2009) standards. The L929 fibroblasts and SaOS-2 cells were passaged and seeded to a 6-well plate until confluent monolayers were re-obtained. These cells were incubated in a humidified incubator at 37 °C with 5% $CO_2$, to obtain a monolayer cell growth. After incubation, the nanofiber mats were placed in contact with the solidified agar surface in 6-well cell culture plates and incubated at 37°C in 5% $CO_2$ humidified incubator for 72 h. At the end of 72 hours, material and fixation agent in agar were aspirated and the cells were stained with crystal violet dye. The effect of cytotoxity on the stained cells was examined under a microscope.

# CHAPTER FIVE
# RESULTS AND DISCUSSION

The engineering of nanoscale surfaces allows tailoring the material surface characteristics, which can lead to significant effects upon the cellular behavior. The main advantage of this engineering approach is the ability to design the material surfaces to provide microenvironments closer to the native ECM and thus facilitate cell activity. Theoretically, an optimal substrate for cells should emulate as near as possible the topographical and biochemical nature of the native tissue (Martins et al., 2009). In the present study, nanostructured materials with morphologies similar to the native ECM were produced by electrospinning. Electrospun-processed materials have the potential to generate scaffolds capable of providing ECM-like surfaces, facilitating cell–matrix and cell–cell interactions, and therefore being very useful for tissue engineering strategies. However, cells recognize not only topographical clues on the surfaces, but also the surface chemistry, which can significantly influence their behavior. Surface functionalization of biodegradable synthetic polymers has been successfully achieved by plasma treatments, thus decreasing their intrinsic hydrophobicity.

Artificial polymer scaffolds that are typically used in tissue engineering applications may not be well suited for optimal cellular adhesion and may need to be chemically or physically enhanced. In this study, PHBV nanofiber mats that can be potentially used in tissue engineering applications were prepared by the electrospinning method. The surfaces of these PHBV nanofiber mats were modified to be hydrophilic by plasma treatment using oxygen or nitrogen gases. Then the PHBV nanofiber mats were interacted with SF solution to improve the biocompatibility of the PHBV nanofiber mats. The surface characterization, hydrophilicity, biominerilization ability and biocompatibility of the mats were also investigated.

## 5.1 Optimization of PHBV Concentration

At the first stage of the thesis, PHBV nanofiber production with uniform diameter distribution without bead formation was targeted. PHBV solution was prepared in chloroform at various concentrations (15, 10, 5, and 3 % w/v) in order to determine the optimal PHBV concentration for electrospinning.

Solution viscosity in electrospinnng is very important parameter to obtain continuous fibers. If the solution concentration is low, there is no continuous fiber formation. Because the polymer fiber will break up into droplets before reaching the collector owing to the influence of surface tension. On the other hand, if the solution concentration is high, due to the high viscosity it will be hard to have continuous fiber formation. Therefore, there is a requirement of optimum polymer concentration for electrospinning (Bhardwaj, & Kundu, 2010; Still, & Recum, 2008). Also, polymer concentration affects the formation of the beads. In the literature, the bead structure formation within the produced nanofibres are depended on three main reasons; low solution viscosity, insufficient charge density, and high surface tension (Fong, & Reneker, 1999).

In this study, solutions with higher concentrations (such as 15 wt%) were very difficult to electrospun most probably because the surface tension prevented the solution from being ejected. Therefore, solution with low concentrations (such as 3 wt % ) were virtually easy to electrospun. Besides, it was found that the diameter of the nanofibers decreased with decreasing the concentration of the polymer solution (from 15% to 3% w/v) (Table 5.1).

The charge density or solution conductivity is also important to produce continous and bead-free nanofibers. When the electrical conductivity of the solution increases, the fiber jet will be subjected to a higher tensile force with the applied electric field than will a fiber jet from a solution with a low conductivity leading to smaller fiber diameters (Bhardwaj, & Kundu, 2010; Still, & Recum, 2008). For this purpose,

BTEAC which is an organosoluble salt was added into PHVB solution at different concentrations (0.2 and 0.1 % w/v) (Table 5.1).

Table 5.1 Sample parameter

| Sample Code | PHBV (% w/v) | BTEAC (% w/v) | Flow Rate (ml/h) | Voltage (kV) | Distance (cm) | Electrical Conductivity (µS/cm) | Fiber Diameter (nm) |
|---|---|---|---|---|---|---|---|
| 1.5PHBV/0,02BTEAC | 15 | 0.2 | 3 | 15 | 15 | 2,8 | 2508 ±595 |
| 1.0PHBV/0.02BTEAC | 10 | 0.2 | 1 | 20 | 15 | 1,8 | 1987 ±568 |
| 0.5PHBV/0.01BTEAC | 5 | 0.1 | 1 | 20 | 15 | 0,9 | 1263 ±261 |
| | 5 | 0.1 | 1 | 20 | 20 | | 1209 ±277 |
| 0.3PHBV/0,01BTEAC | 3 | 0.1 | 1 | 20 | 15 | 0,7 | 876 ± 224 |
| | 3 | 0.1 | 1 | 20 | 20 | | 829 ± 200 |
| 0.3PHBV/0.02BTEAC | 3 | 0.2 | 1 | 20 | 15 | 1,4 | 637 ± 95 |
| | 3 | 0.2 | 1 | 20 | 20 | | 636 ± 149 |

The structural characteristics of PHBV fibers were analyzed by using SEM and the average diameters of the fibers were determined by J-image analysis. Uniform fibers with the diameter of 2508 ± 595nm were obtained from PHBV solution with the concentration of 15% (w/v) at a voltage of 15 kV (Figure 5.1). Due to high viscosity of the solution, the flow rate was increased from 1 ml/h to 3 ml/h.

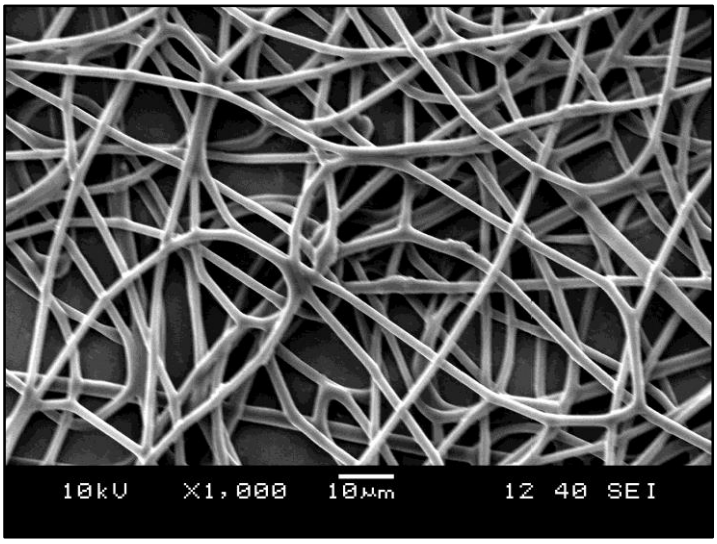


Figure 5.1 SEM images (magnification = 1000 x, scale bar = 10 µm )of 15 % (w/v) PHBV solution produced at a voltage of 15kV at a flow rate of 3 ml/h and at a distance of 15cm.

The morphology of 10 % (w/v) PHBV fiber mat obtained at voltage of 20 kV, was similar to that of 15% (w/v). However, the average fiber diameter was decreased to 1987 ± 568 nm due to the lowering of the concentration of the solution from 15 % (w/v) to 10 % (w/v) (Figure 5.2). 15% (w/v) and 10% (w/v). PHBV solution conductivity were 2.8 and 1.8 µS/cm, respectively.

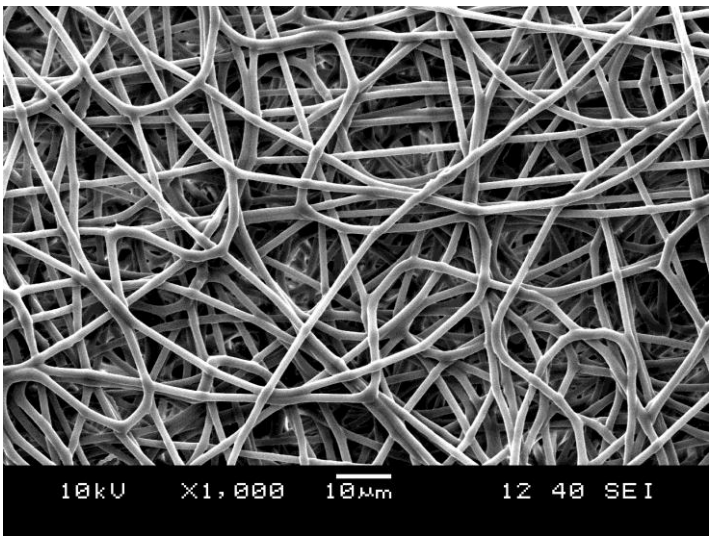


Figure 5.2 SEM images (magnification = 1000 x, scale bar = 10 µm ) of 10% (w/v) PHBV and 0.2% (w/v) BTEAC solution produced at a voltage of 20kV, at a flow rate of 1 ml/h and at a distance of 15cm.

Figure 5.3 (a) and 5.3 (b) illustrate the morphology of 5 % (w/v) PHBV fiber mats. When the concentration of the PHBV solution was halved to 5 % (w/v), the average fiber diameter was reduced as expected. The average fiber diameters of these mats at a distance of 15 cm and 20 cm were measured as 1263 ± 261nm, and 1209 ± 277 nm, respectively. 5 % (w/v) PHBV solution conductivity was 0.9 µS/cm.

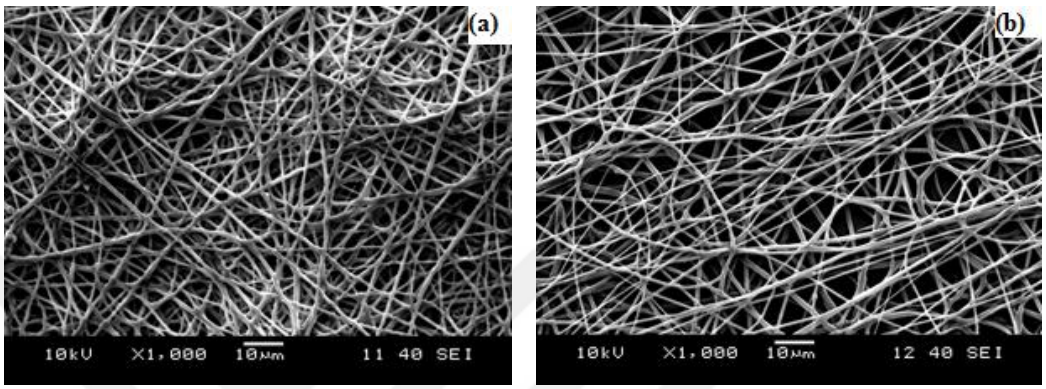


Figure 5.3 SEM images (magnification = 1000 x, scale bar = 10 µm )of 5 %(w/v) PHBV and 0.1% (w/v) BTEAC solution produced:(A) at a voltage of 20kV, at a flow rate of 1 ml/h and at a distance of 15cm. (B) at a voltage of 20kv,at a flow rate of 1 ml/h and at a distance of 20cm.

To decrease the fiber diameter in nano scale, 5 % (w/v) PHBV solution concentration was reduced to 3 % (w/v). The average fiber diameters of these mats at a distance of 15 cm and 20 cm were measured as 876 ± 224 nm and 829 ± 200 nm, respectively. 3 % (w/v) PHBV solution conductivity was 0,7 µS/cm. Unfortunately, bead formation was observed due to decreased polymer solution concentration and solution conductivity. Bead structures are given in Figure 5.4 (a) and Figure 5.4 (b).

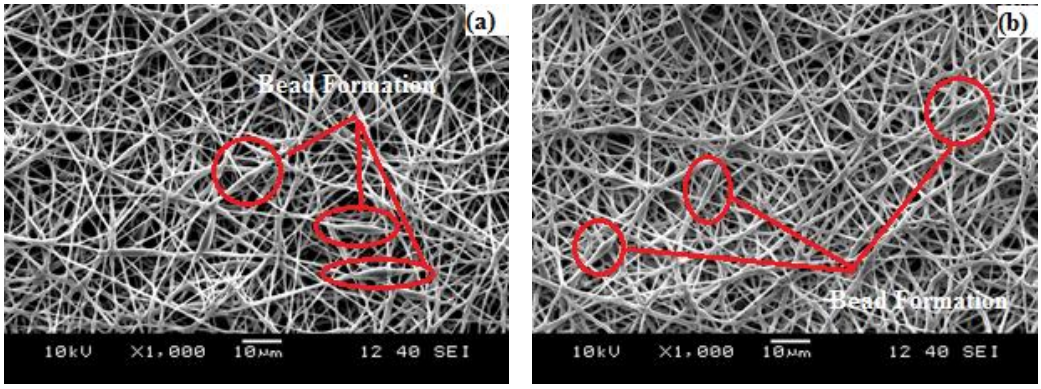


Figure 5.4 SEM images (magnification = 1000 x, scale bar = 10 µm )of 3 % (w/v) PHBV and 0.1% (w/v) BTEAC solution produced:(a) at a voltage of 20kV, at a flow rate of 1 ml/h and at a distance of 15cm. (b) at a voltage of 20kV,at a flow rate of 1 ml/h and at a distance of 20cm.

Beaded fibers are not desirable for tissue engineering scaffold applications because the formation of beads greatly reduces the surface area-to-volume ratio of electrospun fibrous mat and the morphology of beaded fibers significantly deviates from that of the native fibrous ECM (Tong, & Wang, 2011). To avoid the formation of beads, BTEAC amount was increased from 0.1 to 0.2 % to increase the conductivity of the PHBV solution. Solution conductivity was increased from 0.7 to 1.4 µs/cm. sem images of the nanofibers produced from 3% phbv solution, at a distance of 15 cm and 20 cm, without bead and with average diameters of 637±95 nm and 636±149 nm are shown in figure 5.5 (a) and figure 5.5 (b), respectively.

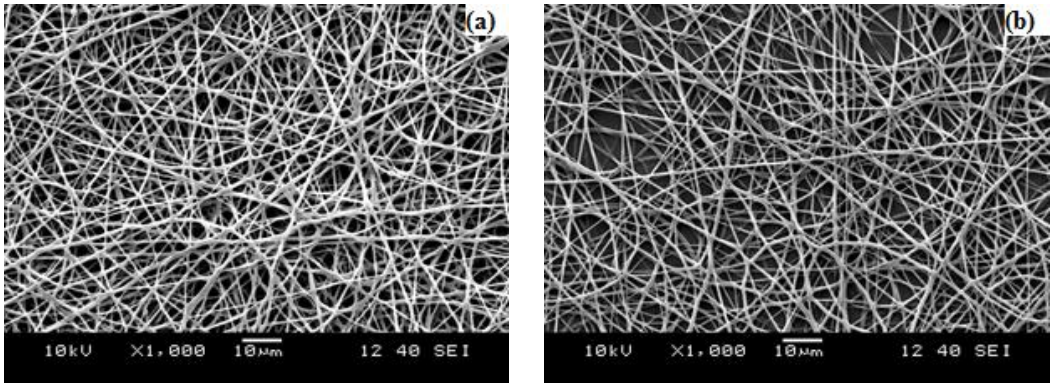


Figure 5.5 SEM images (magnification = 1000 x, scale bar = 10 µm )of 3 %(w/v) PHBV and 0.2% (w/v) BTEAC solution produced:(a) at a voltage of 20kV, at a flow rate of 1 ml/h and at a distance of 15cm. (b) at a voltage of 20kV, at a flow rate of 1 ml/h and at a distance of 20cm.

The best results in terms of fiber uniformity and nanoscale diameter were achieved with the 3 % (w/v) of PHBV solution with the flow rate of 1 ml/h, at a voltage of 20

kV and at a distance of 15 cm (Figure 5.6). Further experiments were carried out using these electrospinning parameters.

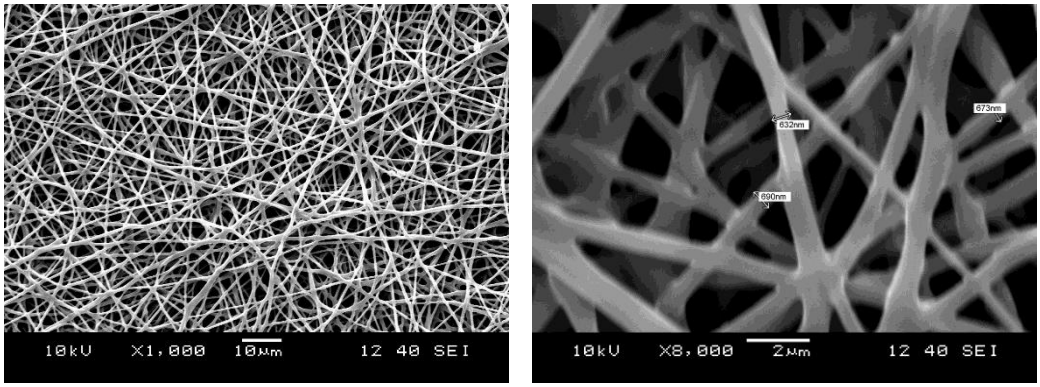


Figure 5.6 SEM images (magnification = 1000 x, scale bar = 10 µm ) of optimum PHBV fiber mat.

## 5.2 Plasma Surface Modification of The Fiber Mats

Plasma treatment is a versatile and effective method for modifying the surface properties or introducing desired chemical groups at the surface of a material without affecting its bulk properties. The most apparent effects of plasma treatment are surface cleaning, microetching and surface activation (attachment of chemical groups, modification of surface charge, increase of the surface free energy). A common application of this technique is to improve the surface hydrophilicity by forming oxygen containing groups at the surface of the materials. In recent years, plasma surface modifications have been used very intensively in the field of biomedical materials research For medical applications, plasma treatment has been used to improve the biocompatibility of surfaces and to create functional groups for the attachment of other molecules such as drugs, peptides, or natural polymers (Matins et al., 2009; Valence, Tille, & Gurny, 2013).

In this thesis, PHBV nanofiber mats obtained from optimized electrospinning parameters were treated with radio-frequency (RF) plasma in the presence of either oxygen or nitrogen gases. The plasma power was 25 W and exposure time was 2, 5, or 10 min. The results of fiber diameter measurments on untreated PHBV (P) nanofiber mats, $O_2$ plasma-treated PHBV (P/$O_2$) nanofiber mats, $N_2$ plasma-treated PHBV (P/

$N_2$) nanofiber mats are given in Table 5.2. Changes in the surface characteristics of the plasma-treated PHBV nanofibers including morphological changes, and surface hydrophilicity were investigated using scanning electron microscopy, and contact angle meters respectively. The cellular responses to plasma-treated PHBV nanofiber matrices were also investigated to test their potential utility in bone tissue engineering application.

Table 5.2 Optimum PHBV fiber mats treated with plasma surface modification

| **Material** | **Power (W)** | **Exposure Time (min)** | **Plasma treated gas** | **Fiber Diameter (nm)** |
|---|---|---|---|---|
| P | - | - | **-** | 637 ± 95 |
| P/$N_2$ | 25 | 2 | $N_2$ | 563±227 |
| P/$O_2$ | 25 | 2 | $O_2$ | 495±177 |
| P/$N_2$ | 25 | 5 | $N_2$ | 540±186 |
| P/$O_2$ | 25 | 5 | $O_2$ | 503±142 |
| P/$N_2$ | 25 | 10 | $N_2$ | 537±189 |
| P/$O_2$ | 25 | 10 | $O_2$ | 512±191 |

### *5.2.1 Morphology of Plasma-Treated PHBV Fiber Mats*

In order to evaluate the effect of plasma treatment on the morphology of the PHBV nanofibers, SEM tehnique was used and untreated PHBV nanofibers were used as the control group.

The SEM image of the electrospun PHBV nanofiber mats exposed to nitrogen and oxygen plasma for 2 minutes are shown in Figure 6.7 (a) and Figure 6.7 (b), respectively. Both of the mats did'nt show any discernible structural changes as a result of plasma treatment. However, $N_2$ and $O_2$ plasma treatments revealed that 2 minutes

exposure reduced the average fiber diameters to 563±277 nm and 495±177 nm, respectively (Tablo 5.2). Therefore, it can be stated that the etching power of $O_2$ as the plasma gas was more compared to $N_2$.

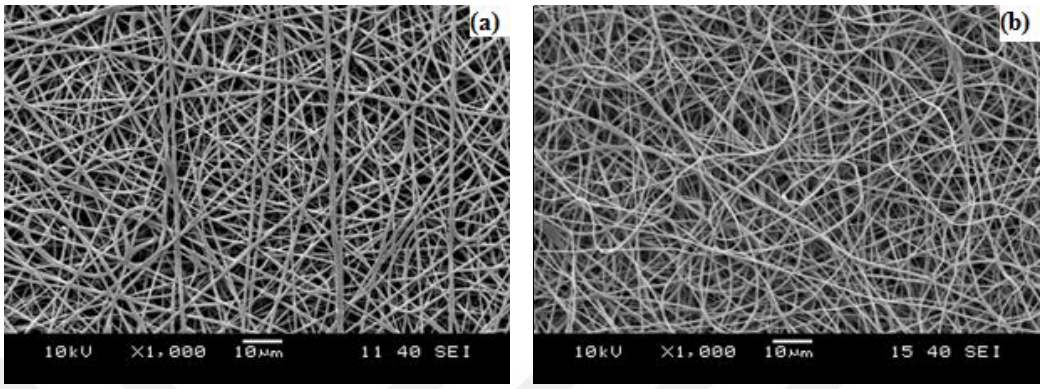


Figure 5.7 3% PHBV, 0.2 % BTEAC; 2 min, (a) $N_2$ plasma, (b) $O_2$ plasma.

Fiber morphologies of PHBV mats treated with $N_2$ and $O_2$ plasma for 5 minutes are illustrated in Figure 5.8 (a) and Figure 5.8 (b). No significant physical changes were observed in the morphology of plasma-treated PHBV nanofibers. The average diameters of PHBV nanofibers exposed to $N_2$ and $O_2$ plasma were 540±186 and 503±142 nm, respectively (Tablo 5.2). In the literature, Ko et al. (2015) were reported that the polycaprolactone (PCL) nanofibers surfaces were modified by plasma treatment using acrylic acid or oxygen gas. The average fiber diameter for the PCL, acrylic acid and oxygen plasma treated PCL were found 2.34 µm, 1.76 µm and 2.16 µm, respectively. This result suggested that plasma treatment is reduced average fiber diameter.

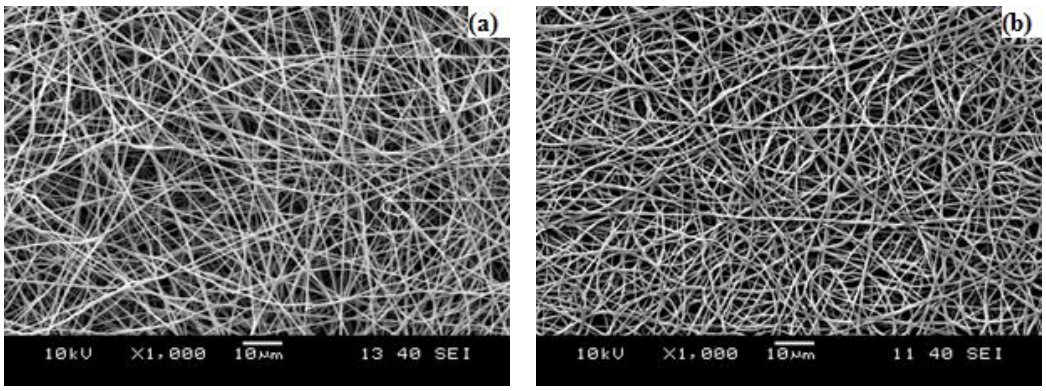


Figure 5.8 3% PHBV, 0.2 % BTEAC; 5 min, (a) $N_2$ plasma, (b) $O_2$ plasma

Figure 5.9 (a) and (b) illustrate SEM photographs of the 10 minutes $N_2$ plasma and $O_2$ plasma-treated PHBV nanofiber mats. Uniform fibrous structures with no morphological changes were observed. The average fiber diameters for $N_2$ and $O_2$ plasma treated PHBV nanofiber mats were found to be 537±189 and 512±191 nm, respectively.

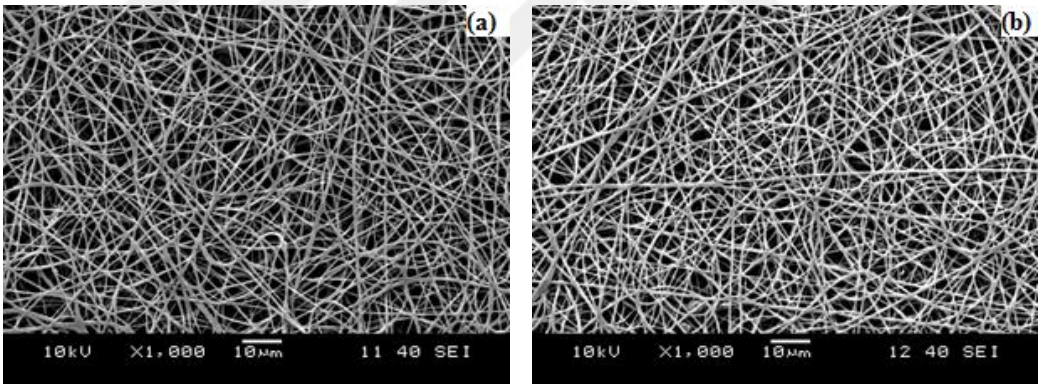


Figure 5.9 3% PHBV, 0.2 % BTEAC; 10 min, (a) $N_2$ plasma,(b) $O_2$ plasma

The PHBV nanofiber mats treated with the $N_2$ and $O_2$ plasma yielded fibers with no morphology change even the exposure time was increased up to 10 min. It is noteworthy that fibers with diameters in the range of five hundreds of nanometers were obtained from a plasma-treated PHBV mats, while fiber diameters of approximately six hundreds nanometers were obtained from untreated PHBV. Lastly, when $O_2$ plasma was compared the with $N_2$ plasma, $O_2$ plasma was better in turns of etching power.

### *5.2.2 Hydrophilicity of Plasma-Treated PHBV Fiber Mats*

Plasma process has been used to increase the hydrophilicity of the polymeric materials and to improve their surface properties (Gogolewski et al., 1996). PHBV nanofiber mats have a hydrophobic property. Therefore, it is required to improve the surface afinity towards cells by a plasma treatment.

Contact angle measurements for the untreated and plasma-treated electrospun PHBV nanofiber mats were performed to determine the degree of surface hydrophilicity. In this thesis, the nanofiber mat surface hydrophilicity was measured by a contact angle meters and three measurements were taken at different locations of the same nanofiber mat and the average value was obtained. The measurements were done using ultrapure water. The results of the contact angle measurements on unmodified and plasma-modified PHBV samples are given in Tablo 5.3.

Table 5.3 Untreated and plasma-treated PHBV mats contact angle measurements results.

| **Modification type** | **Conctact Angle (deg)** | | |
|---|---|---|---|
| | **Ultra pure water** | | |
| | **1. week** | **2. week** | **3.week** |
| Untreated PHBV | 123 | 123 | 123 |
| Plasma PHBV/$N_2$/2 | 59 | 78 | 112 |
| Plasma PHBV/$N_2$/5 | 50 | 65 | 105 |
| Plasma PHBV/$N_2$/10 | 33 | 64 | 82 |
| Plasma PHBV/$O_2$/2 | 63 | 77 | 94 |
| Plasma PHBV/$O_2$/5 | 54 | 71 | 86 |
| Plasma PHBV/$O_2$/10 | 45 | 69 | 79 |

To investigate the changes in surface hydrophilicity after plasma treatment, we measured the contact angles of plasma treated PHBV nanofibers for three weeks.

Hydrophilic characteristic of PHBV nanofiber mats was substantially increased after plasma treatment in the presence of both oxygen and nitrogen gases (Tablo 5.3).

In the literature, Tong, & Wang (2011) were reported that the water contact angle of PHBV microfibrous scaffolds were measured 104.2±3.1°. In my thesis, the contact angle of water droplets contacting untreated PHBV nanofibers was 123°, indicating hydrophobic characteristics with a low wettability, as expected. This value decreased after treatment with $O_2$ and $N_2$ plasma. This reduction in water contact angle clearly indicates increased surface hydrophilicity, which may be caused by the introduction of new polar nitrogen and oxygen containing functional groups on the surface. However, the deterioration of the surface properties as indicated by an increase in the water drop contact angle at the second and third weeks, is due to the reorientation of polar groups towards the bulk of the material. This condition is called hydrophobic recovery (Khorasani, & Irani, 2008).

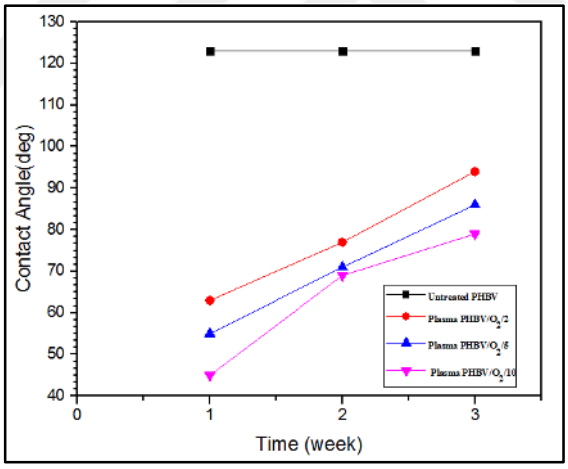


Figure 5.10 Water contact angle over time on PHBV nanofiber mats(■)Untreated PHBV,(●) Plasma PHBV/$O_2$/2,(▲) Plasma PHBV/ $O_2$/5 ,(▼) Plasma PHBV/ $O_2$/10.

Figure 5.10 shows water contact angles over time on untreated PHBV and $O_2$ plasma-treated PHBV nanofiber mats. The contact angle of untreated PHBV is about 123º. After 2 minutes of $O_2$ plasma treatment, at the end of the first week, contact angle decreased to 63º. The contact angles changed to 77 º at the second week and 94º at the third week. After 5 minutes of $O_2$ plasma treatment, PHBV nanofiber mats reached 54º, and at the end of second and third weeks, contact angle changed to 71º and 86º,

respectively. When 10 minutes of $O_2$ plasma was applied onto the surface of PHBV nanofiber mats, water contact angles was measured as 45º for the first week. After second and third weeks, contact angle changed to 69 º and 79º, respectively. The contact angle images are given in Tablo 5.4.

Table 5.4 The contact angle images of $O_2$ plasma-treated PHBV nanofiber mats.

| **Contact Angle (deg)** | | | |
|---|---|---|---|
| | 1 week | 2 week | 3 week |
| **Untreated PHBV** | 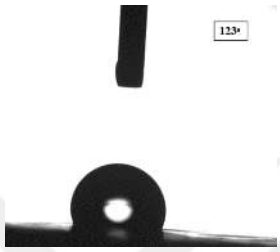 | 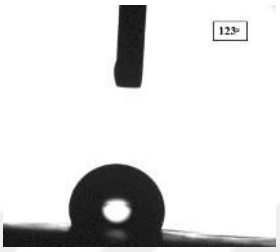 | 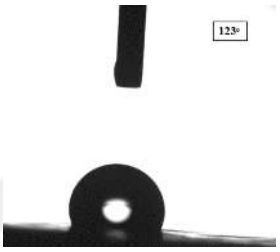 |
| **Plasma PHBV/$O_2$/2** | 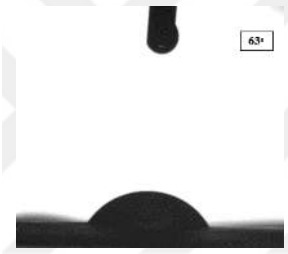 |  | 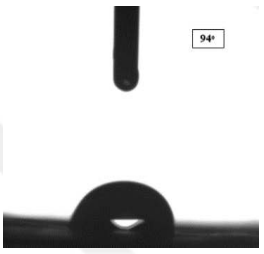 |
| **Plasma PHBV/$O_2$/5** |  | 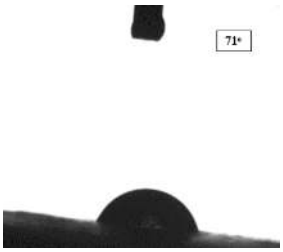 | 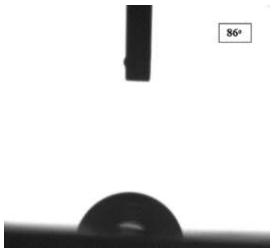 |
| **Plasma PHBV/$O_2$/10** | 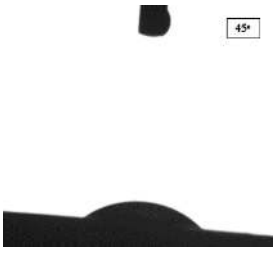 | 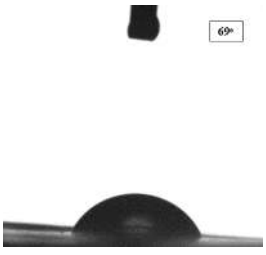 | 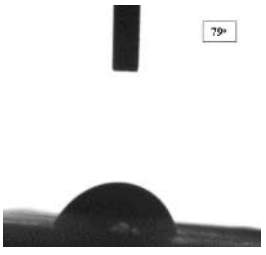 |

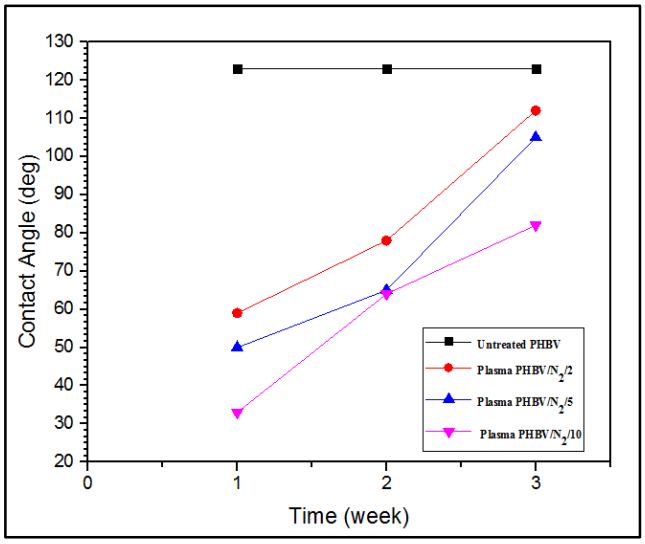


Figure 5.11 Water contact angle over time on PHBV nanofiber mats (—■—) Untreated PHBV, (—●—) Plasma PHBV/$N_2$/2, (—▲—) Plasma PHBV/ $N_2$/5 , (—▼—) Plasma PHBV/ $N_2$ /10

Figure 5.11 shows water contact angles over time on untreated PHBV and $N_2$ plasma-treated PHBV nanofiber mats. Before plasma treatment, contact angles measured on PHBV nanofiber mats were much higher than that of a $N_2$ plasma-treated PHBV nanofibers. While the non-treated PHBV nanofibers was 123°, this value decreased to 59° after 2 minutes treatment with $N_2$ plasma at the end of the first week. After second and third weeks, contact angle increased to 78º and 112º, respectively. The contact angle measurement of the mats exposed to 5 minutes $N_2$ plasma was measured as 50º after a week. This contact angle increased to 65° and 105° after second and third weeks. When 10 minutes of $N_2$ plasma was applied onto the surface of PHBV nanofiber mats, water contact angles was measured as 33º for the first week. After second and third weeks, contact angle changed to 64º and 82º, respectively. The contact angle images are given in Tablo 5.5.

Table 5.5 The contact angle images of $N_2$ plasma-treated PHBV nanofiber mats.

| | 1 week | 2 week | 3 week |
|---|---|---|---|
| **Untreated PHBV** | 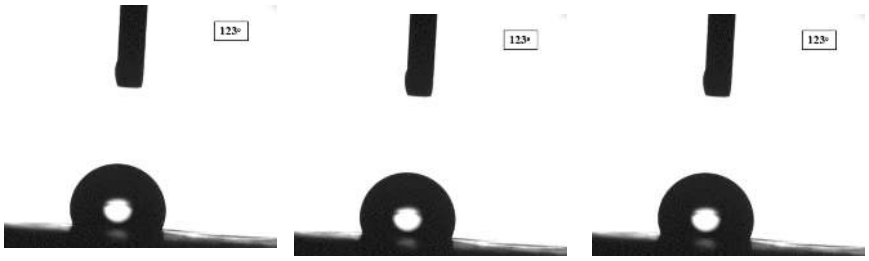 | | |
| **Plasma PHBV/$N_2$/2** | 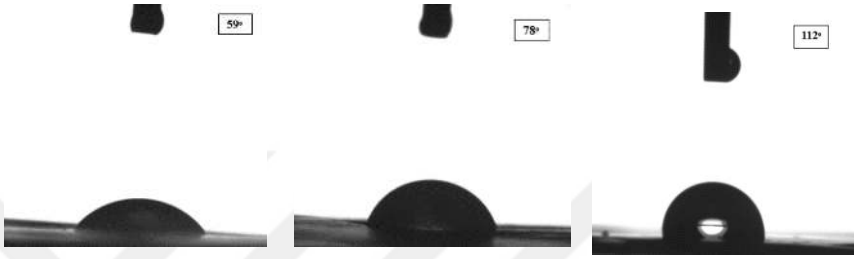 | | |
| **Plasma PHBV/$N_2$/5** | 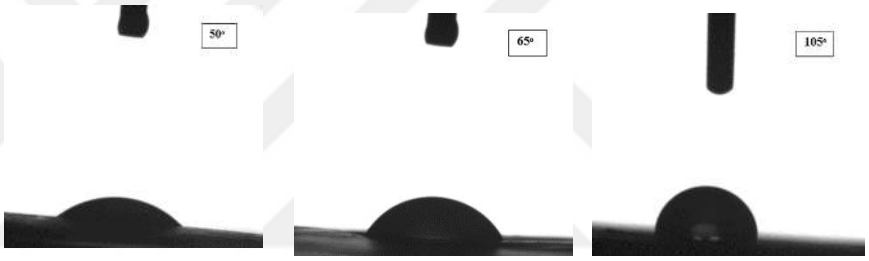 | | |
| **Plasma PHBV/$N_2$/10** | 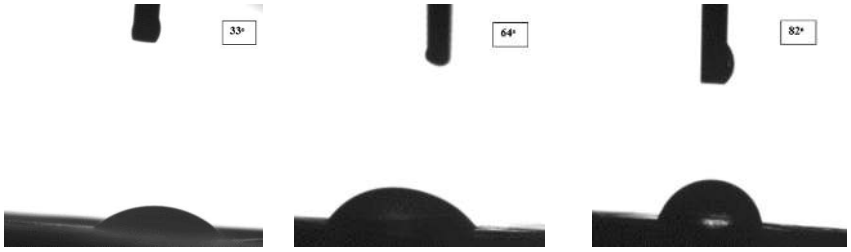 | | |

These results demonstrated that plasma treatment is an effective method to increase the surface hydrophilicity of PHBV nanofiber mats which was proven by the decrease of the contact angles of the mats after $O_2$ and $N_2$ plasma treatments. But, the surface contact angles were increased after second and third weeks due to hydrophobic recovery. The nitrogen gas plasma seems to be more effective to enhance the surface hydrophilicity of the PHBV nanofiber mats compared to $O_2$ plasma. In the literature, Espesito et al. (2012) were modified poly(lactide-co-glycolide) (PLGA) membranes by oxygen and nitrogen plasma to improve polymer hydrophilicity. They reported that the contact angle of oxygen and nitrogen plasma treated PLGA membranes were

measured approximately 62ºand 54.6º, respectively. These results s prove that nitrogen plasma treatment is an efficient method to improve the surface hydrophilicity of the material. However, over time hydrophobic recovery was faster on $N_2$ plasma modifed surfaces. Moreover, for all the mats hydrophilicity increases with the increase of plasma gas exposure time from 2 minutes to 10 minutes.

The optimal plasma exposure time was evaluated by considering both water contact angle measurments and morphological analysis. 10 minutes of exposure time was selected as an optimal time in our experiment as we obtained the highest hydrophicity with no morphology change.

## 5.3 Silk Fibroin Modified Plasma-Treated PHBV Fiber Mats

In bone tissues engineering, SF matrices have been shown to be non-immunogenic, biocompatible and capable of supporting the attachment, spreading, growth and differentiation of cells as well as eliciting a negligible response. In this study, plasma-treated PHBV nanofiber mats surfaces were modified by SF immobilization for its potential application in bone tissue engineering. Various techniques such as SEM, contact angle meters, and FTIR were used to characterize the modified surfaces. The capabilities of SaOS-2 cells attachment and growth onto these surfaces were also analyzed to evaluate the biocompatibility of SF modified plasma-treated PHBV nanofiber mats.

### *5.3.1 Morphology of Silk Fibroin Modified Plasma-Treated PHBV Fiber Mats*

The SF were firmly adsorbed on the plasma-treated PHBV nanofiber mats due to the hydrophilic chemical groups newly grafted on mats' surfaces. Then, they were immobilizated by methanol treatment.

The results of fiber diameter measurments on untreated PHBV (P) nanofiber mats, silk fibroin modified PHBV (PS) nanofiber mats, $O_2$ plasma-treated PHBV (P/$O_2$) nanofiber mats, $N_2$ plasma-treated PHBV (P/ $N_2$) nanofiber mats, $O_2$ plasma-treated PHBV modified by silk fibroin (PS/$O_2$) nanofiber mats, and $N_2$ plasma-treated PHBV

modified by silk fibroin (PS/ $N_2$) nanofiber mats are given in Table 5.6. According to the results, SF impregnation increased the diameter of the fibers. Moreover, the increase in fiber diameter was more for plasma-treated mats.Therefore, it can stated that SF was immobilized better on the plasma-treated surfaces than on the surfaces without plasma treatment.

Table 5.6 The average fiber diameter with a untreated/treated SF modification.

| **Material** | **Fiber Diameter without Silk Modification(nm)** | **Material** | **Fiber Diameter with Silk Modification (nm)** |
|---|---|---|---|
| P | 637 ± 95 | PS | 706 ± 213 |
| $P/N_2$ | 537±189 | $PS/N_2$ | 659±196 |
| $P/O_2$ | 512±191 | $PS/O_2$ | 620±172 |

The morphologies of the six types of fibrous scaffolds are shown in Figure 5.12-5.14. Figure 5.12 shows SEM images of P and PS nanofiber mats with a magnification of 1000x. As can be seen from Table 5.6 after silk fibroin modification, fiber diameter of the P mat changed from 637±95 nm to 706±213 nm. The PS mats exhibited a SF film formation on the fiber surfaces that might be due to hyrophobicity of the P mat that did not allow silk impregnation.

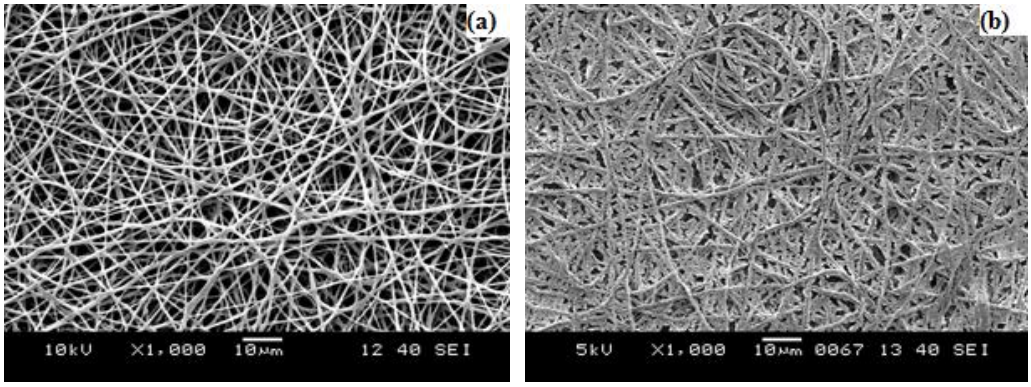


Figure 5.12 SEM images (magnification = 1000 x, scale bar = 10 µm) (a) Untreated PHBV (P) nanofiber mats (b) Silk fibroin modified PHBV (PS) nanofiber mats.

Figure 5.13 shows the SEM images of P/$N_2$ and PS/$N_2$ nanofiber mats. The average fiber diameters were measured as 537±189 nm and 659±196 nm, respectively (Table 5.6). The results are shown that silk modified PHBV carried out film formation between the fiber morphologies and after silk fibroin coating, fiber diameter is increased.

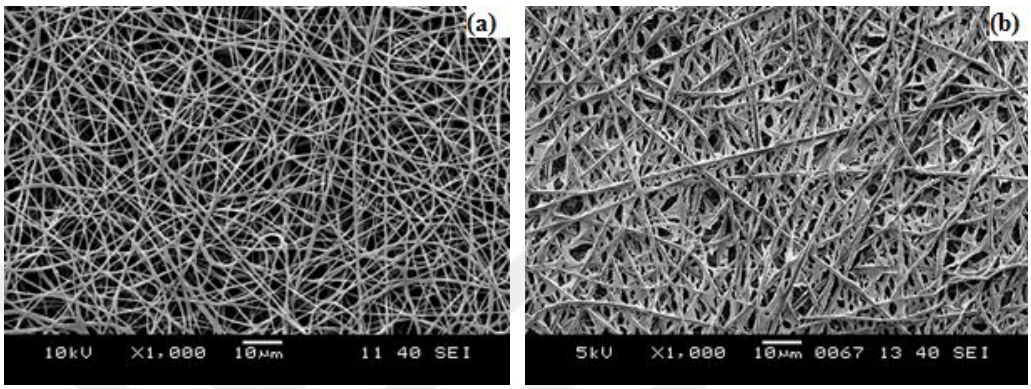


Figure 5.13 SEM images (magnification = 1000 x, scale bar = 10 μm ) (a) $N_2$ plasma-treated PHBV (P/$N_2$ )nanofiber mats, (b) $N_2$ plasma-treated PHBV modified by silk fibroin (PS/$N_2$) nanofiber mats.

Figure 5.14 illustrates the morphology of P/$O_2$ and PS/$O_2$ nanofiber mats. The average fiber diameters of P/$O_2$ and PS/$O_2$ were 512±191 nm to 620±172 nm, respectively.

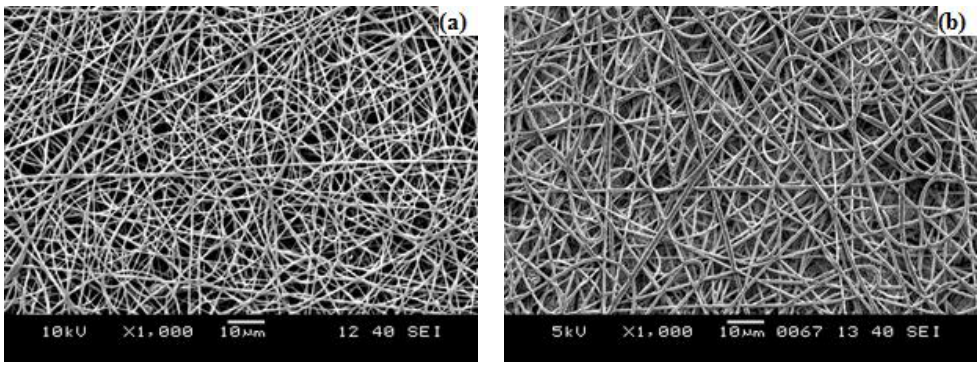


Figure 5.14 SEM images (magnification = 1000 x, scale bar = 10 μm ) (a) $O_2$ plasma-treated PHBV (P/$O_2$) nanofiber mats (b) $O_2$ plasma-treated PHBV modified by silk fibroin (PS/$O_2$) nanofiber mats.

### *5.3.2 Hydrophilicity of Silk Fibroin Modified Plasma-Treated PHBV Fiber Mats*

Plasma surface modification technique was used to improve the surface hydrophilicity of PHBV nanofiber mats by forming oxygen or nitrogen containing

groups. The decrease in the water contact angles was contributed to the hydrophilic groups that were formed on the surface of PHBV nanofiber mats after plasma treatment. But, within three weeks, hydrophobic recovery was observed on the surface of PHBV nanofiber mats (Tablo 5.3). So, plasma treated PHBV nanofiber mats were modified by SF in order to prevent hydrophobic recovery by minimizing the migration of polar groups and surface conformation.

The results of contact angle measurments on PS, PS/$N_2$ and PS/$O_2$ nanofiber mats are given in Table 5.7.

Table 5.7 PS, PS/$N_2$ and PS/$O_2$ nanofiber mats contact angle measurments results

| Modification type | Conctact Angle (deg) | | |
|---|---|---|---|
| | 1. week | 2. week | 3.week |
| PS | 78 | 78 | 78 |
| PS/$N_2$/10 | 69.7 | 72.5 | 70.2 |
| PS/$O_2$/10 | 69.8 | 73.3 | 91.4 |

The results from Table 5.3 and Table 5.7 indicated that the contact angles decreased from 123° to 78° when the P nanofiber mats were modificated by silk fibroin and no hydropboic recovery was observed as expected. This implies that intorduction of SF enhances efficiently the hydrophilicity of P nanofiber mats. At the first week all the silk modified mats had similar contact angle values. However, hydrophobic recovery was more dominant on PS/$O_2$ nanofiber mats at the end of the third week. This was probably due to the repulsion of negatively charged SF (Wang et al., 2007) with the negatively charged oxygen-containing groups on the mat surface. Therefore, reorientation and mobility of oxygen-containing groups could not be prevented. On the other hand, contact angle of PS/$N_2$ nanofiber mats was stabilized to 74$^o$ after the SF modification process. This was attributed to the interaction of nitrogen-containing groups with the SF that slowed down the hydrophobic recovery and minimized the reorientation of polar groups.

### *5.3.3 FTIR Measurements of Silk Fibroins Modified Plasma-Treated PHBV Fiber Mats*

ATR-FTIR analysis was performed to examine the presence of silk fibroin on the surface of PS/$N_2$ and PS/$O_2$ nanofiber mats as well as the behavior of silk fibroin conformation. The bands of amide I and amide II in IR spectrum are very useful for the conformational analysis of silk fibroin protein. In general, the IR spectral region within 1700–1500 $cm^{-1}$ is assigned to the peptide backbone of amide I (1700–1600 $cm^{-1}$) and amide II (1600–1500 $cm^{-1}$) absorption, which have been commonly used for the analysis of different secondary structures of silk fibroin.The absorption bands observed for SF at 1655±10 $cm^{-1}$ (amide I) and 1540±10 $cm^{-1}$ (amide II) are assigned to random coil structure.The absorption bands for SF treated with methanol have frequencies of 1625±10 $cm^{-1}$ (amide I) and 1525±10 $cm^{-1}$ (amide II),the characteristics of β-sheet structure (Pan, Chen, & Chen, 2006).

Figure 5.15 (a,b,c) shows the ATIR–FTIR spectra of P nanofiber mat (a), PS/$O_2$ nanofiber mat (b), and PS/$N_2$ nanofiber mat (c). Compared with the peaks in the spectrum of untreated PHBV nanofiber mat (Figure 5.15.a), the peaks at 1628 $cm^{-1}$ and 1528 $cm^{-1}$ from silk fibroin are found in the spectra of silk fibroin-modified/plasma treated PHBV nanofiber mats (Figure 5.15.a).It demonstrates that silk fibroin was successfully absorbed on the nanofiber mats even the mats were washed distilled water with three times. The peak at ~1772 $cm^{-1}$ was due to C=O streching band of PHBV.

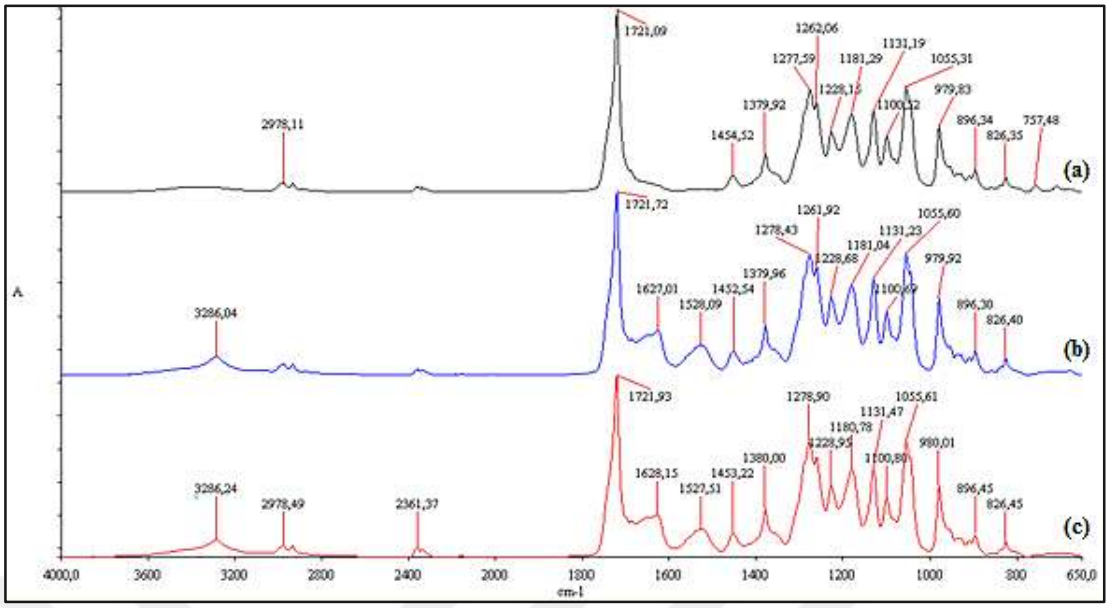


Figure 5.15 The ATIR–FTIR spectra of P nanofiber mat (a), PS/$O_2$ nanofiber mat (b), and PS/$N_2$ nanofiber mat (c).

## 5.4 In Vitro Biological Evaluation

A key step to develop a nanofibrous scaffold for tissue engineering is to evaluate the biocompatibility of the materials. In current study, MTT colorimetric assay, SEM analysis and cytotoxcity test were used to evaluate the biocompatibility of various PHBV nanofiber mats by considering the cell viability and cell morphology.

### *5.4.1 Biominerilization Test*

Apatite formation tendency on the surface of the electrospun mats in SBF solution containing ion concentrations nearly equal to human blood plasma revealed information on bone-bonding ability of the samples. In this study, Ca-P precipitations on the nanofiber mats at the end of 1, 3 and 5 weeks were investigated by SEM and EDS mapping analysis.

For the SBF incubation of P, P/$N_2$ and P/$O_2$ nanofiber mats, non-homogenously distributed Ca-P clusters which also got bigger in time were observed on the surface of mats (Figure 5.16). The dispersions of the Ca and P ions on P, P/$N_2$ and P/$O_2$ nanofiber mats were given in Figure 5.17.

Formation of apatite-like minerals on the SF modifed nanofiber mats were also given in Figure 5.16. Ca-P clusters were detected on the PS/$N_2$ nanofiber mats similar to P, P/$N_2$ and P/$O_2$ nanofiber mats. However, plenty of spherical apatite-like minerals nucleated on the surface of both PS and PS/$O_2$ mats at the end of three weeks of biominerilization. As shown in Figure 5.18, spherical apatite-like minerals were distributed homogenously on the entire PS and PS/$O_2$ mats surfaces. Also, at the end of the fifth week in incubation, the PS/$O_2$ nanofiber mat surface was virtually covered with these minerals. As can be seen in Figure 5.18, PS/$O_2$ nanofiber mats triggered more apatite-like mineral formation compared to PS mats. Unfortunately, neither spherical apatite-mineral formation nor surface coverage with these minerals were observed on PS/$N_2$ mats. Accordingly, SF modification as well as oxygen plasma promoted the nucleation of apatite-like minerals due to the creation of negatively charge surfaces.

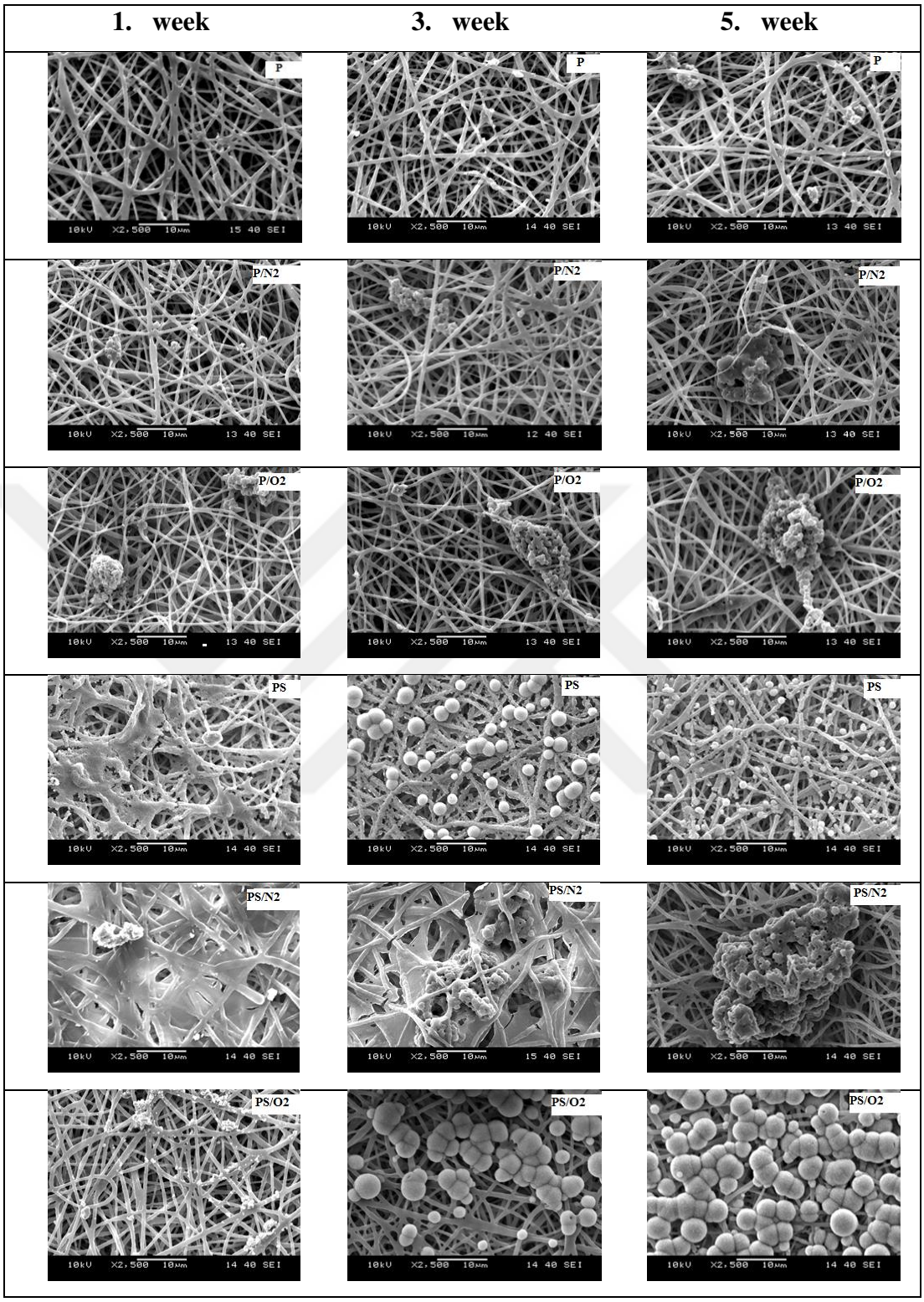


Figure 5.16 SEM images of biominerilization at the end of 1, 3 and 5 weeks.

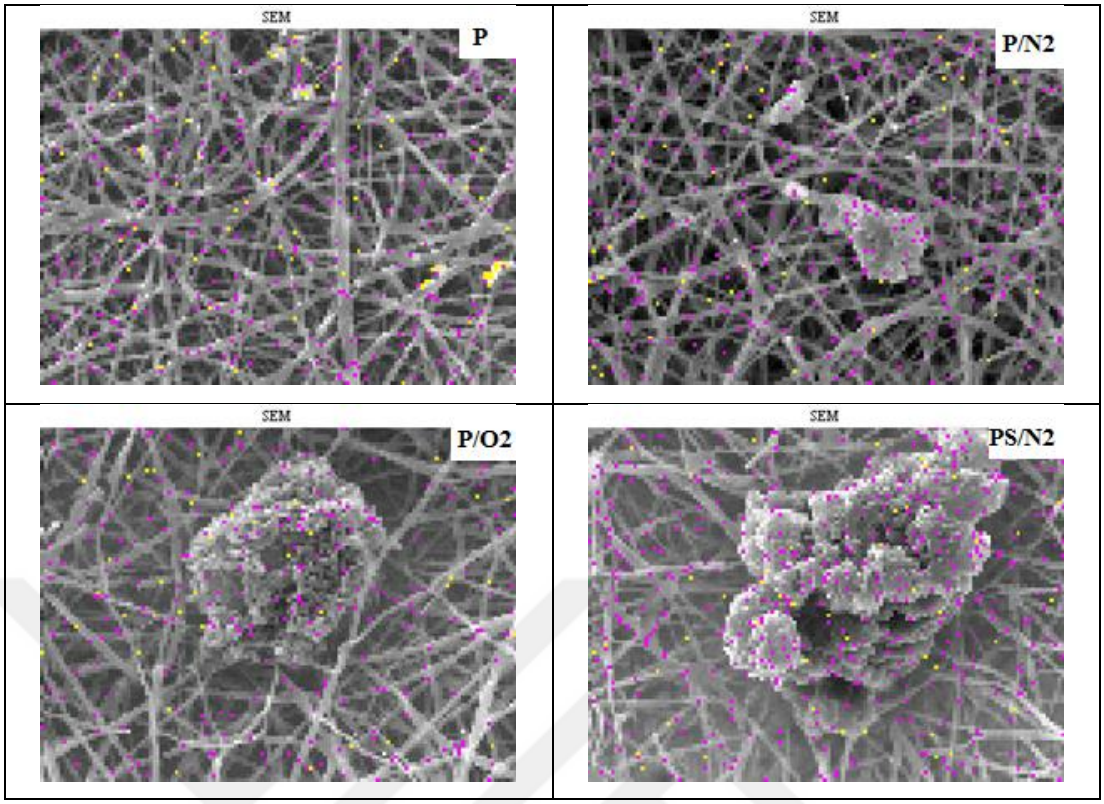


Figure 5.17 EDS mapping analysis of biominerilization at the end of 5 week.

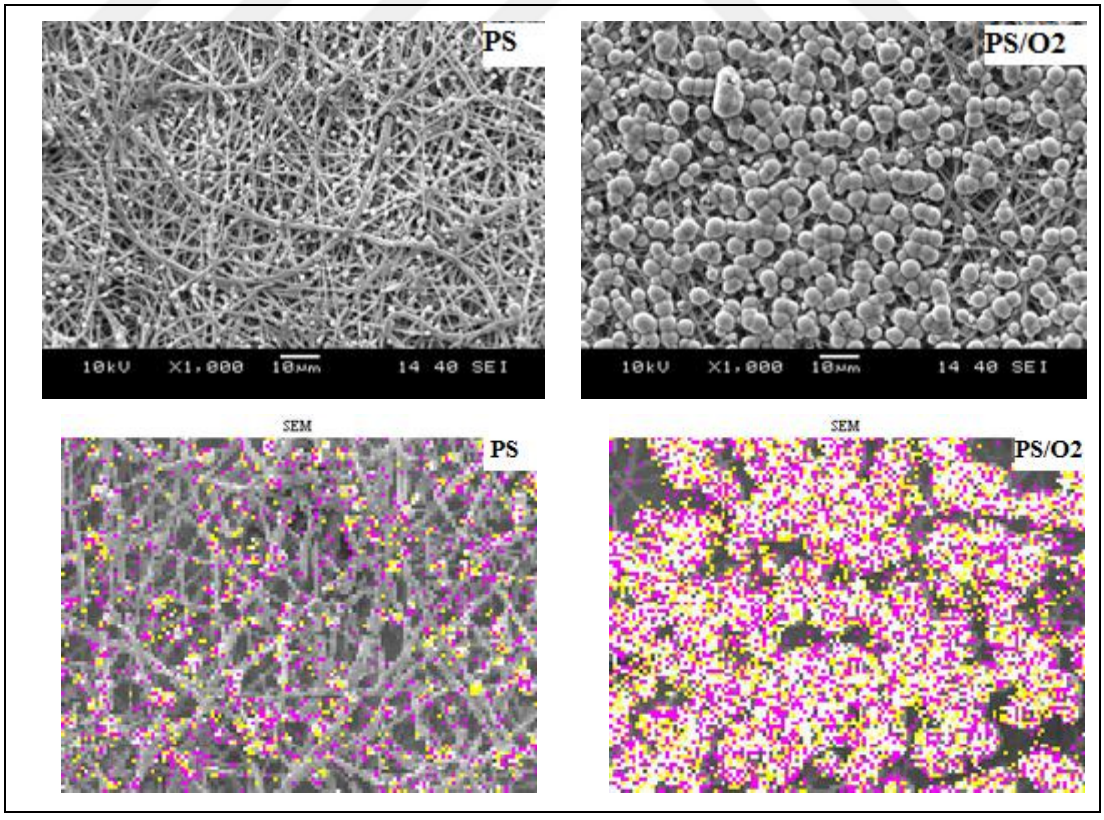


Figure 5.18 SEM images and EDS mapping analysis of biominerilization on PS and PS/$O_2$ nanofiber mats at the end of 5 week.

In recent years, various researchers have stated that the negatively charged surfaces are always favorable for the nucleation of Ca-P minerals in SBF solution whereas the nucleation is inhibited on positive surfaces. The accepted explanation is that the accumulation of $Ca^{2+}$ ions near the negative surfaces as a result of the electrostatic attraction increases, and as a result, the initial nucleation of Ca-P minerals is preferentially triggered. In the literature, Zhu, Masuda and Koumoto (2003) investigated the deposition of HAp onto positively charged surfaces (i.e., self-assembled monolayers (SAMs) terminated with $NH_2$ head groups) and negatively charged surfaces (i.e., OH SAMs (weak) and COOH-SAMs (strong)) in 1.5 SBF, pH < 7.4 solutions. The results revealed that the negative surfaces had a more powerful induction capability for the nucleation of HAp (COOH > OH), whereas nucleation was obviously prohibited on a positive surface ($NH_2$-SAM).

### *5.4.2 Cell Growth and Proliferation on the Studied Fiber Mats*

In the present study, growth and proliferation of SaOS-2 cells cultured on the PHBV nanofiber mats were evaluated up to 7 days by MTT assay. The MTT assay results are shown in Figure 5.18-5.20 which demonstrates the cell viability on the nanofiber mats (P, PS, P/$O_2$, P/$N_2$, PS/$O_2$ and PS/$N_2$) at different culture times (1, 3 and 7 days).

SaOS-2 cells seeded on the PS/$N_2$ nanofiber mats have better cell viability compare to P/$N_2$, after cultured for 1 day (Figure 5.19). Furthermore, PS/N2 nanofiber mats supports the growth and proliferation of the cells better than the PS/$O_2$ mat.. However, MTT assay results on the P, PS, P/$O_2$ and PS/$N_2$ mats did not reveal any statistically significant variation in term of cell viability after cell culture for 1 day.

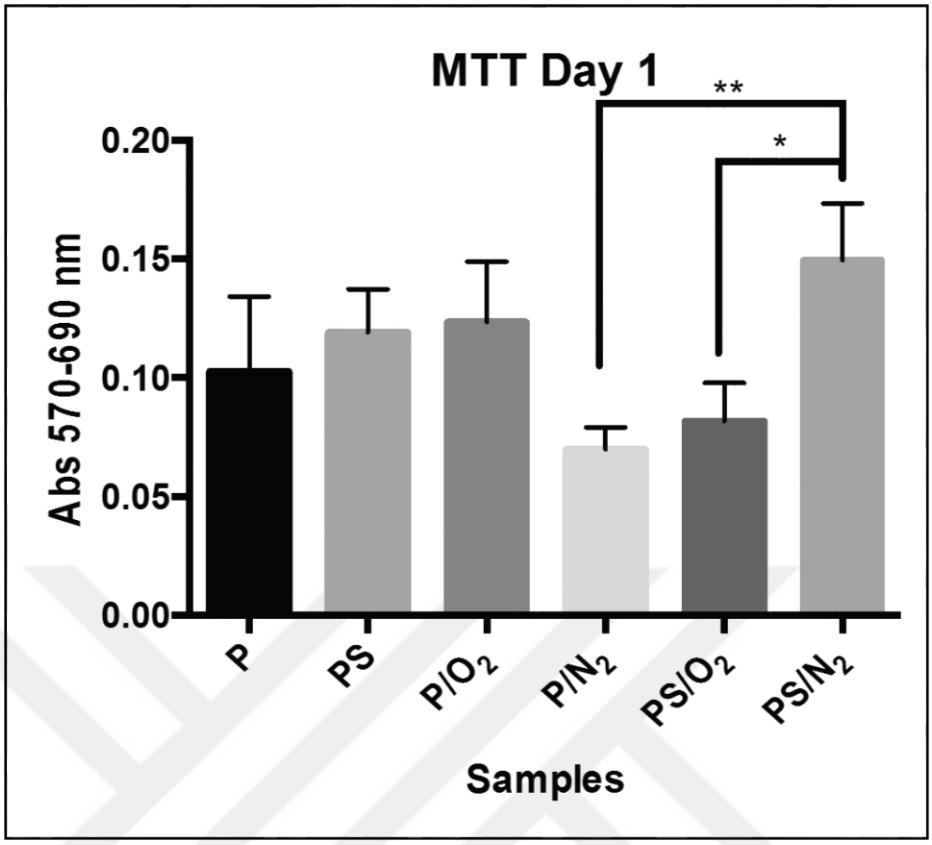


Figure 5.19 SAOS-2 cells seeded on the PHBV nanofiber mats after cultured for 1 day.

After cultured for 3 days, SaOS-2 cells seeded on the PS/$N_2$ nanofiber mats have better cell viability than PS, as shown in Figure 5.20. Also, the PS/$N_2$ nanofiber mats showed better cell viability compared to P/$N_2$, suggesting that SF modification promoted the cell proliferation. Moreover, SaOS-2 cells showed higher cell density on the PS/$N_2$ nanofiber mats than that on the PS/$O_2$ nanofiber mats. Accordingly, nitrogen plasma treatment as well as SF modification have an important contribution on the biocompatibility of the mats.

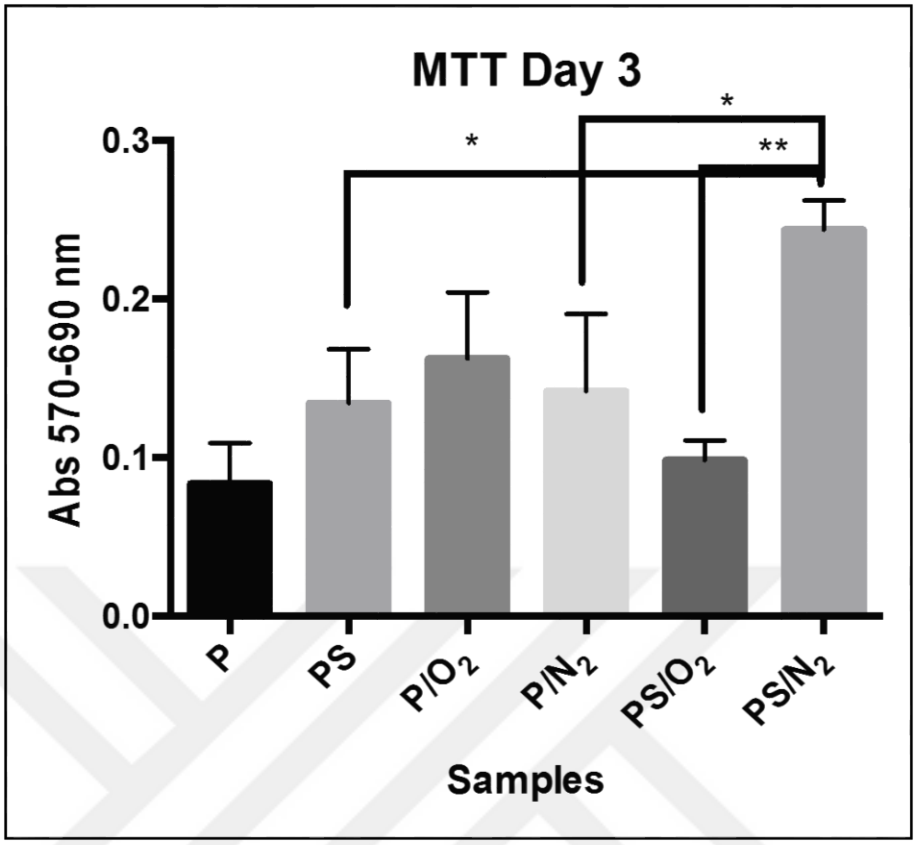


Figure 5.20 SAOS-2 cells seeded on the PHBV nanofiber mats after cultured for 3 day

From the Figure 5.21 on day 7, the cell density measured on the PS/$N_2$ nanofiber mats exhibited the highest proliferation of SaOS-2 cells. Moreover, cell proliferation on the PS/$N_2$ and P/$N_2$ nanofiber mats was more than that on the PS/$O_2$ and P/$O_2$ nanofiber mats which was probably due to the negatively charged surface created by oxygen plasma. Besides, better cell proliferation onto P nanofiber mats than P/$O_2$ mats and was observed. In the litarature, Kumar et al. (2010) investigated the effect of developing a surface charge on HA discs with respect to osteoblast activity in vitro. The HA discs were then electrically polarized (positive and negative surfaces) or non-polarized (controls) and seeded with MC3T3-E1 osteoblast-like cells. At 7 days, the picogreen data were showed a significant increase in cell number on the positively charged HA sample in comparison to non-charged control HA samples. These results clearly suggested us that nitrogen plasma treatment compared to oxygen triggered better cell proliferation as the SaOS-2 cells did not like to proliferate on negatively charged surfaces.

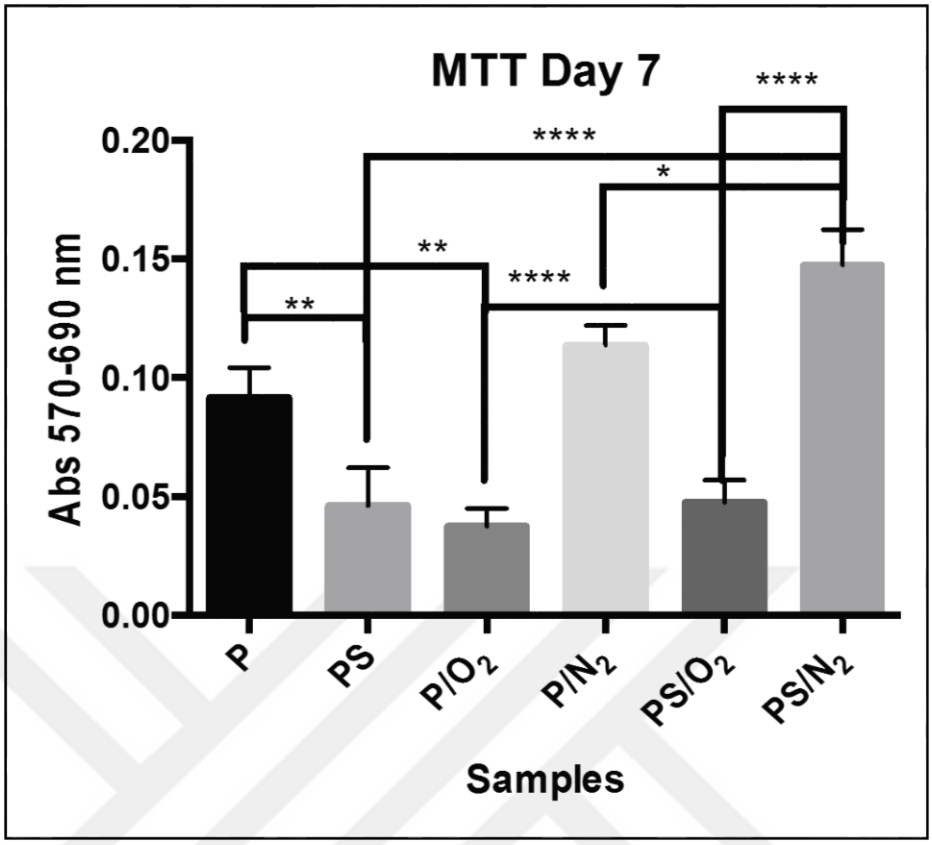


Figure 5.21 SAOS-2 cells seeded on the PHBV nanofiber mats after cultured for 7 day.

In the literature, , Khorasani, & Irani (2008) reported that the oxygen-based plasma treated poly (L-lactic acid) (PLLA) film could improve the B65 nervous tissue cells adhesion and growth. Similarly, Park et al. (2007), showed that the oxygen or ammonia plasma treated poly(lactic-co-glycolic acid) (PLGA) nanofibers significantly decreased the hydrophobicity and increased the number of polar groups on the nanofiber surface. Thus, adhesion and growth of mouse fibroblasts on PLGA nanofibers were also substantially improved by plasma treatment in the presence of oxygen or ammonia gas. In another study, Martins et al. (2009),found that the oxygen and argon plasma treated polycaprolactone (PCL) nanofibers could enhance the SaOS-2 cells adhesion and growth. These results substantially prove that plasma treatment for the material is an efficient method to improve the biocompatibility of the material. On the other hand, Zhou et al., in 2006 and 2009, also found out that the cell adhesion and proliferation increased on the 2D poly(3-hydroxybutyrate-co-3-hydroxyhexanoate) (PHBHHx) films and 3D porous sponges when coated with SF.

These results suggested that silk fibrion modification on the polymer surface also plays a major role in the biocompatibility and cell behavior.

Apparently, SaOS-2 cells seeded on the nitrogen plasma treated and SF modified mats ($PS/N_2$) show the highest cell viability during culture days in accordance with the literature, indicating that this nanofiber mat is suitable for the SaOS-2 cells adhesion and proliferation.

### *5.4.3 Morphologies of SaOS-2 cells Growing on the Studied Fiber Mats*

The morphologies of SaOS-2 cells seeded on P, PS, $P/O_2$, $P/N_2$, $PS/O_2$ and $PS/N_2$ mats after 7 days of culture are shown in Figure 5.22. The cells exhibited a spheroidal shape and firmly attached to the nanofibers for all the mats. Filopodia that reached into the interspaces between the nanofibers was clearly observed around the SaOS-2 cells. Similar observations were reported by Tuzlakoglu et al. (2005) where SaOS-2 cells were seeded onto starch/polycaprolactone scaffolds and by Tong, Wang, & Lu (2012) where the same cell line were seeded on to PHBV-based fibrous scaffolds.

Figure 5.22 clearly illustrates the penetration of cells into the inner layers of the nanofiber mats after 7 days cell culture. Especially, in Figures 5.22.c and f. numerous filopodia extending from SaOS-2 cells were observed.

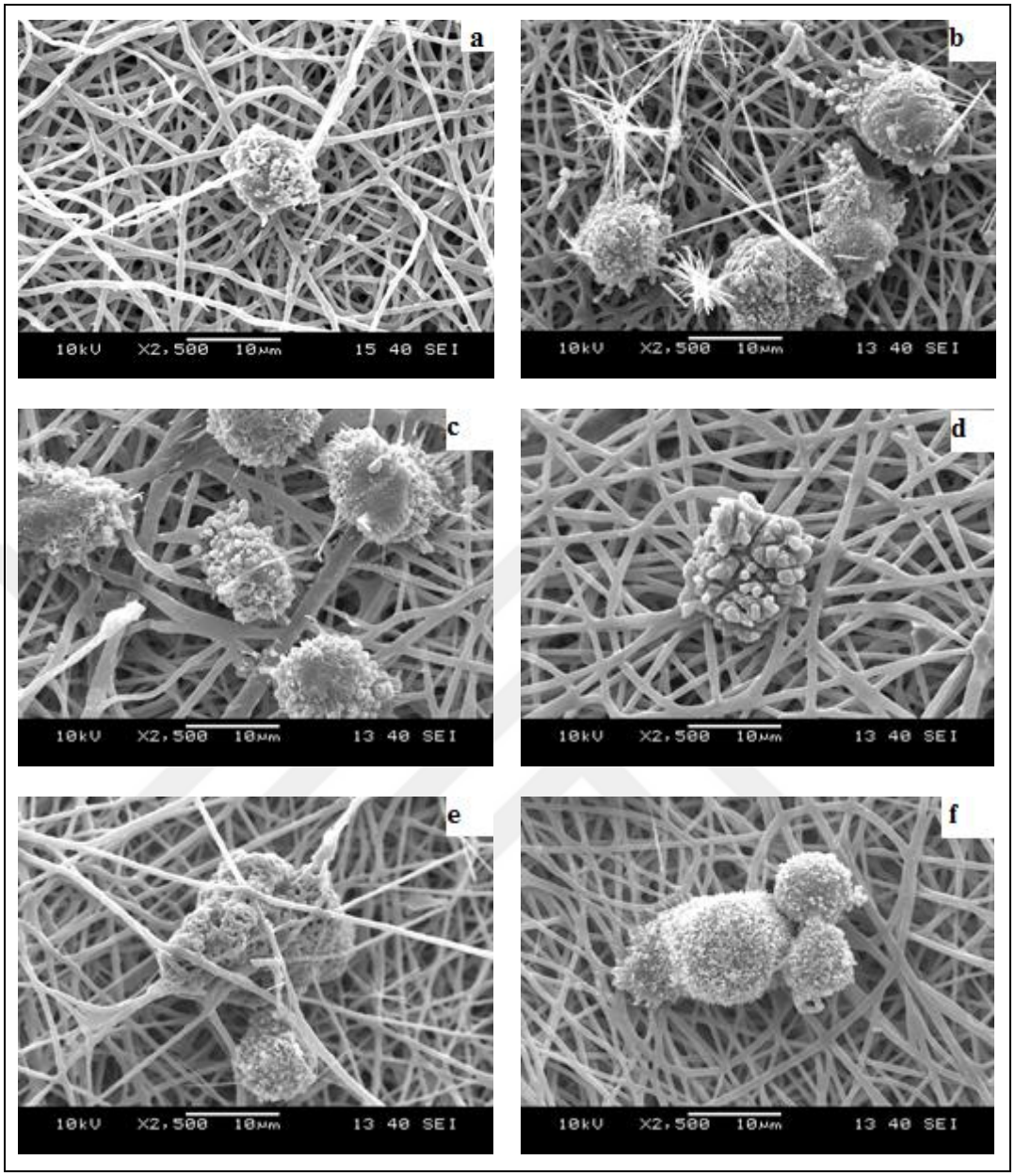


Figure 5.22 SEM images of SAOS-2 cells on various PHBV nanofiber mats (7 day) a. Untreated, b. PS, c. $P/O_2$, d. $PS/O_2$, e. $P/N_2$, f. $PS/N_2$.

### *5.4.4 Cytotoxicity Test of the Fiber Mats*

The visual examination showed no cytotoxic effect of the tested PHBV nanofiber mats on SaOS-2 cells and L929 cells (Figure 5.23-24). The cells were able to penetrate cavities between fibres and no significant difference in their behaviour was observed between the test sample and control, despite the difference on the surface of materials.

The Figure 5.23 shows the images of L929 cells cultivated for 72 hours on PHBV nanofiber mats. The PS, $PS/O_2$ and $PS/N_2$ nanofiber mat (Figure 5.23.c, e and g, respectively) showed a good biocompatibility, in other words no cytotoxicity, when compared with the control cell culture (Figure 5.23.a). However, decreased viability of L929 cells was observed on P, $P/O_2$ and $P/N_2$ nanofiber mats when compared to the control group, due to absence of SF (Figure 5.23.b, d and f, respectively).

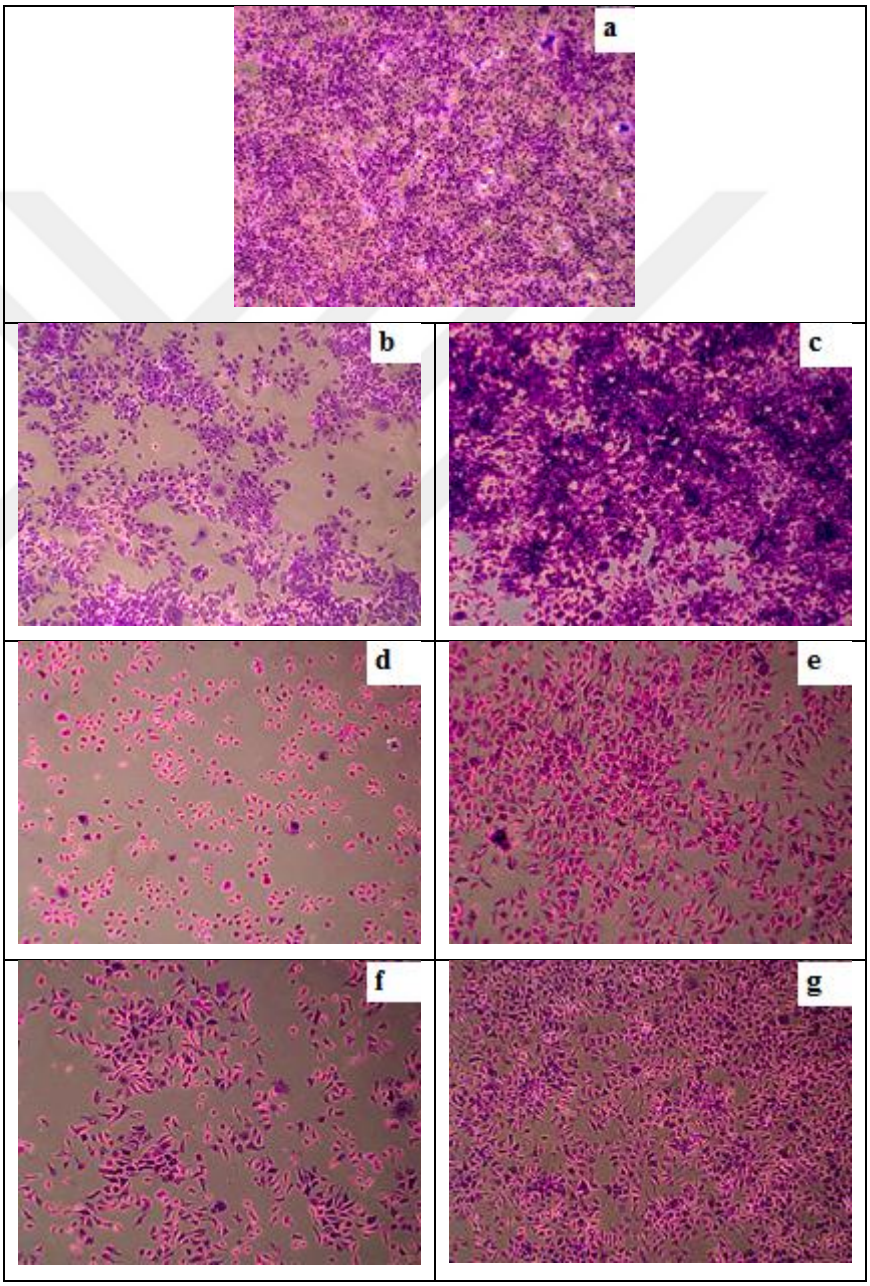


Figure 5.23 Reverse phase microscope images of L929 cells after crystal-violet staining (10X) a. Control, b. P., c. PS, d. $P/O_2$, e. $PS/O_2$, f.$P/N_2$, g. $PS/N_2$.

Cultivation of SaOS-2 cells on the PHBV nanofiber mats are given in Figure 5.24. The PHBV nanofiber mats did not have any cytotoxic effect on SaOS-2 cells. However, cell viability onto $P/O_2$ and $PS/O_2$ nanofiber mats was less than both the control group and the nitrogen plasma treated mats due to the negatively charged oxygen-containing groups on the mat surface.The results of the cytotoxicty test based on SaOS-2 cells are coherent with the results of MTT assay.

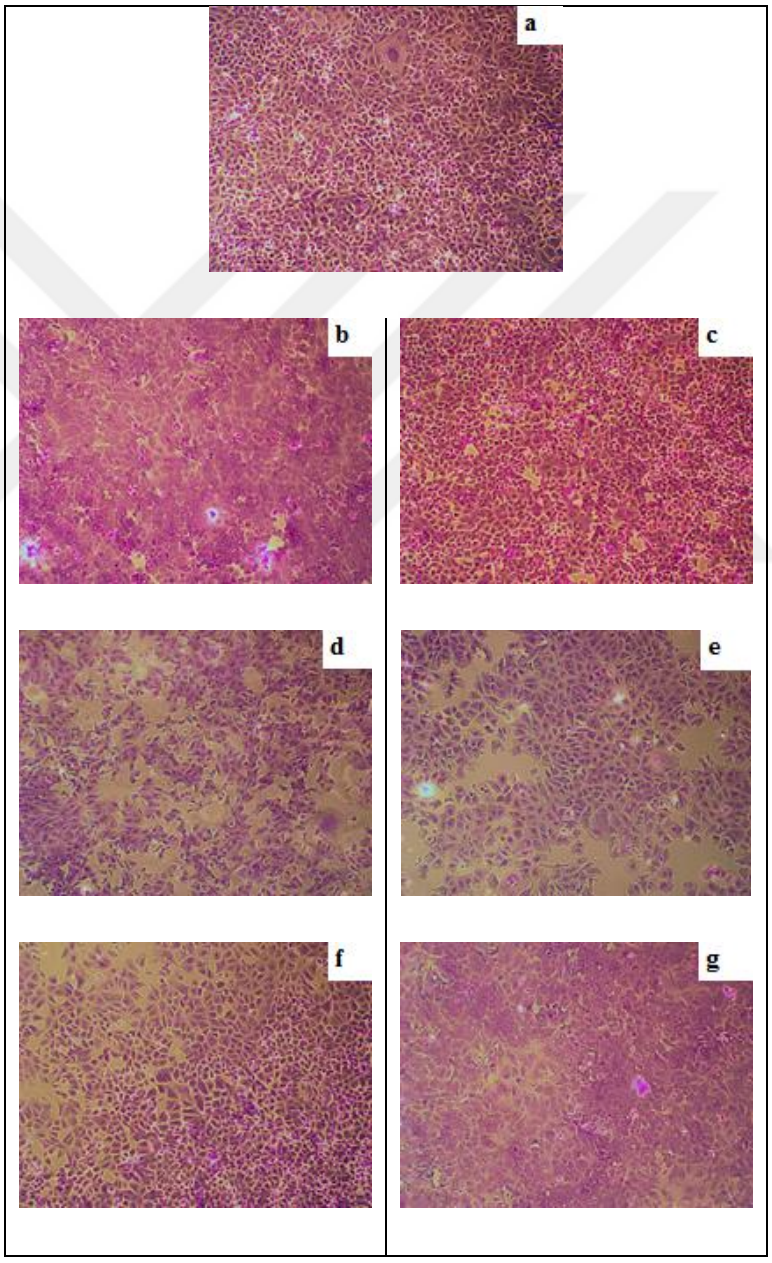


Figure 5.24 Reverse phase microscope images of SAOS-2 cells after crystal-violet staining (10X) a. Control, b. P., c. PS, d. $P/O_2$, e. $PS/O_2$, f.$P/N_2$, g. $PS/N_2$.

# CHAPTER SIX
# CONCLUSION

PHBV nanofiber mats with the average fiber diameter of 637±95 nm have been successfully produced via electrospinning technique to be used in tissue engineering applications. The optimum electrospinning parameters were achieved with the 3 % (w/v) of PHBV and 0.2% (w/v) BTEAC solution using the flow rate of 1 ml/h, at a voltage of 20 kV and at a distance of 15 cm.

PHBV nanofiber mats obtained from optimized electrospinning parameters were treated with radio-frequency (RF) plasma in the presence of either oxygen or nitrogen gases. The plasma power was 25 W and exposure time was 2, 5, or 10 min. 10 minutes of exposure time was selected as an optimal time in our experiment as we obtained the highest hydrophicity with no morphology change. The nitrogen gas plasma seems to be more effective to enhance the surface hydrophilicity of the PHBV nanofiber mats compared to $O_2$ plasma. However, over time hydrophobic recovery was faster on $N_2$ plasma modified surfaces.

Sustainability of surface hydrophilicity of plasma treated polymeric mats is the main problem for the fabrication of tissue scaffold due to hydrophobic recovery. This hydrophobic recovery problem was tried to be solved by SF modification which inhibited the reorientation of polar groups. The contact angle of PS/$N_2$ nanofiber mats was stabilized to 74$^o$ after SF modification. However, hydrophobic recovery was still present on PS/$O_2$ nanofiber mats which was probably due to the repulsion between negatively charged SF and oxygen plasma treated mat surface.

SF modification as well as oxygen plasma promoted the nucleation of spherical apatite-like minerals due to the creation of negatively charge surfaces. Apatite-like minerals were distributed homogenously on the entire PS mat and especially on PS/$O_2$ mat surface. However, neither spherical apatite-mineral formation nor surface coverage were observed on PS/$N_2$, P, P/$N_2$ and P/$O_2$ mats.

In vitro biological studies have clearly demonstrated that all the mats investigated supported SaOS-2 cells viability and proliferation. According to the results, proliferation of SaOS-2 cells was more pronounced on the PS/$N_2$ nanofiber mat compared to PS/$O_2$ mat as SaOS-2 cells like to proliferate on positively charged surfaces. The SaOS-2 cells exhibited a spheroidal shape with filopodia that reached into the interspaces between the nanofibers for all the mats. Besides, all PHBV nanofiber mats did not show any noticeable cytotoxicity effect compared to polystyrene control group.

Even though calcification was more enhanced on the PS/$O_2$ mat cell behavior was not similarly enhanced. Consequently, the produced PS/$N_2$ nanofiber mat would be a promising candidate for bone tissue engineering applications.

## REFERENCES


Bartolo, L. D., Rende, M., Morelli, S., Salerno, S., A, P., Gordano, A., & Vito, A. D., et al. (2008). Influence of membrane surface properties on the growth of neuronal cells isolated form hippocampus. *Journal of Membrane Science, 325*, 139-149.

BaoLin, G., & Ma, P. X. (2014). Synthetic biodegradable functional polymers for tissue engineering: A brief review. S*cience China Press and Springer-Verlag Berlin Heidelberg,* 57 (4), 490–500.

Bhardwaj, N., & Kundu, S. C. (2010). Electrospinning: a fascinating fiber fabrication technique. *Biotechnology Advances*, 28, 325–347.

Burg, K., Porter, S., & Kellam, J. F. (2000). Biomaterial developments for bone tissue engineering. *Biomaterials,* 21, 2347-2359.

Butt, H. J., Karlheinz, G., & Micheal, K. (2006). Physics and chemisty of interface. *Wiley-VCH,* 76-82.

Casper, C. L., Stephens, J. S., Tassi, N. G., Chase, D. B., & Rabolt, J. F. (2004). Controlling surface morphology of electrospun polystryne fiber: Effect of humadity and molecular weight in the electrospinning process. *Macromolecules*, 37, 573-578.

Chan, B. P., & Leong, K. W. (2008). Scaffolding in tissue engineering: General approaches and tissue-specific considerations. *European Spine J*ournal, 17 (l4), 467–S479.

Chang, H. & Wang, Y. (2011). C*ell responses to surface and architecture of tissue engineering scaffolds.* D. Eberli,(Ed.), Regenerative medicine and tissue engineering - cells and biomaterials in (569-588). USA: InTech.

Chung, T. W., Liu, D. Z., Wang, S. Y., & Wang, S.S. (2003). Enhancement of the growth of human endothelial cells by surface roughness at nanometer scale. *Biomaterials*, 24, 4655-4661.

Dadsetan, M., Pumberger, M., Casper, M. E., Shogren, K., Giuliani, M., Ruesink, T., et al. (2011). The effects of fixed electrical charge on chondrocyte behavior. *Acta Biomaterialia*, 7 (5), 2080–2090.

Dayong, Y., Yang, W., DongZhou, Z.,YingY, L., & XingYu, J. (2009). Control of the morphology of micro/nanostructures of polycarbonate via elctrospinning. *Chinese Science Bulleti,* 54 (17), 2911-2917.

Deroanne, C. F., Lapiere, C. M., & Nusgens, B. V. (2001). In vitro tubulogenesis of endothelial cells by relaxation of the coupling extracellular matrix–cytoskeleton. *Cardiovasc Research*, 49, 647–58.

Deitzel, J. M., Kleinmeyer, J., Harris, D., & Tan, N. C. B. (2001). The effect of processing variables on the morphology of electrospun nanofibers and textiles. *Polymer*, 42 (1), 261e72.

Dhandayuthapani, B., Yoshida, Y., Maekawa, T., & Kumar, D. S. (2011). Polymeric scaffolds in tissue engineering application: A review. *International Journal of Polymer Science*, 2011, 19.

Engler, A. J., Sen, S., Sweeney, H. L., & Discher, D. E. (2006). Matrix elasticity directs stem cell lineage specification. *Cell,* 126, 677-689.

Espesito, A. R., Kamikawa, C. M., Lucchesi, C., Ferreira, B. M. P., & Duek, E. A. R. (2013). Benefits of oxygen and nitrogen plasma treatment in verocell affinity to poly (lactide-co-glycolide acid). *Materials Research*, 64, 695-702.

Fong, H., & Reneker, D. H. (1999). Elastomeric nanofibers of styrene-butadiene-styrene tri block co polymer. *International Journal of Polym Science: Part B Polymer Physics*, 37 (24), 3488–93.

Giesche, H. (2006). Mercury porosimetry : A general overview. *Partical & Partical System Characterization,* 23, 1-11.

Goddard, J. M., & Hotchkiss, J. H. (2007). Polymer surface modification for the attachment of bioactive compounds. *Progres in Polymer Sciences*, 32, 698–725.

Gogolewski, S., Mainil-Varlet, P., & Dillon, J. G. (1996). Sterility, mechanical properties, surface treatment of melt-extruded sheets of poly (L-lactic acid). *Polymer Enginering Sciences*, 42, 299-306.

Goh, Y., Shakir, I., & Hussain, R. (2013). Electrospun fibers for tissue engineering, drug delivery and wound dressing. *Journal of Materilas Science*, 48 (8), 3027-3054.

Gunatillake, P. A. & Adhikari, R. (2003). Biodegradable synthetic polymers for tissue engineering. *European Cell and Materials*, 5, 1-16.

Huang, Z., Zhang, Y., Kotaki, M., & Ramakrishna, S. (2003). A review on polymer nanofibers by electrospinning and their applications in nanocomposites. *Composites Science and Technology*, 63, 2223–2253.

Hulbert, S. F., Young, F. A., Mathews, R. S., Klawitter, J. J., Talbert, C. D., Stelling, F. H. (1970). Potential of ceramic materials as permanently implantable skeletal prostheses. *Journal of Biomedical Material Research*, 4 (3), 433–56.

Ishikawa, J., Tsuji, H., Sato, H., & Gotoh, Y. (2007). Ion implantation of negative ions for cell growth manipulation and nervous system repair. *Surface and Coatings Technology, 201*, 8083-8090.

Karageorgious, V. & Kaplan, D. (2005). Porosity of 3D biomaterial scaffolds and osteogenesis. *Biomaterials, 26*, 5474–5491.

Kenawy, E. R., Bowlin, G. L., Mansfield, K., Layman, J., Simpson, D. G., Sanders, E. H., et al. (2002). Release of tetracycline hydrochloride from electrospun poly(ethylene-co-vinylacetate), poly(lactic acid), and a blend. *Journal of Controlled Release*, 81, 57–64.

Khadka, D. B., & Haynie, D. T. (2012). Protein- and peptide-based electrospun nanofibers in medical biomaterials. *Nanomedicine: Nanotechnology, Biology, and Medicine*, 8, 1242–1262.

Khorasani, M. T., & Irani, H. M. (2008). Plasma surface modification of poly (L-lactic acid) and poly (lactic-co-glycolic acid )films for improvement of nerve cell adhesion. *Radiation Physics and Chemistry*, 77, 280-287.

Kim, S., English., A., & Kihm, K. D. (2009). Surface elasticity and charge concentrationdependent endothelial cell attachment to copolymer polyelectrolyte hydrogel. *Acta Biomaterialia, 5*, 144-151.

Kokuba, T., & Takadama, H. (2006). How useful is SBF in predicting in vivo bone bioactivity?. *Biomaterials,* 27, 2907-2915.

Ko, Y. M., Choi, D. Y., Jung, S. C., & Kim, B. H. (2015). Characteristics of plasma treated electrospun polycaprolactone (PCL) nanofiber scaffold for bone tissue engineering. *Journal of Nanoscience and Nanotechnology*, 15, 192–195.

Kramschuster, A., & Turng, L. (2013). *Fabrication of tissue engineering scaffolds*. Ebnesajjad,S. (Ed.). Handbook of biopolymer and biodegrable plastics: Properties, processing and applications. (462), USA :Elsevier.

Kundu, B. (2013). Silk fibroin biomaterials for tissue regenerations. *Advanced Drug Delivery Reviews*, 65 (2013), 457–470.

Kumar, D., Gittings, J. P., Turner, I. G., Bowen, C. R., Hidolgo, A. B., & Cartmell, S. H. (2010). Polarization of hydroxyapatite: Influence on osteoblast cell proliferation. *Acta Biomaterialia*, 6, 1549–1554.

Kumar, M. N. V. R. (2000). A review of chitin and chitosan applications. *Reactive & Functional Polymers*, 46, 1–27.

Jang, H., Castano, O., & Kim, H. (2009). Electrospun materials as potential platforms for bone tissue engineering. *Advanced Drug Delivery Reviews*, 61, 1065–1083.

Jiang, F. X., Yurke, B., Firesein, B. L., & Langrana, N. A. (2008). Neurite ougrowth on a DNA crosslinked hyrogel with tunable stiffnesses. *Annals of Biomeical Engineering, 36*, 1565-1579.

Langer, R. & Vacanti, J. P. (1993). Tissue engineering. *Science,* 260 (5110), 920-926.

Lee, Y., & Arinzeh, T. L. (2011). Electrospun nanofibrous materials for neural tissue engineering. *Polymers, 3*, 413-426.

Lee, J. H., Jung, H. W., Kang, I. K., & Lee, H. B. (1994). Cell behaviour on polymer surfaces with different functional groups. *Biomaterials, 15*, 705-711.

Lee, S. J., Choi, J. S., Park, K. S., Khang, G., Lee, Y. M., & Lee, H. B. (2004). Response of MG63 osteoblast-like cells onto polycarbonate membrane surfaces with different micropore sizes. *Biomaterials, 25*, 4699-4707.

Liu, X., & Ma, P. X. (2004). Polymeric scaffolds for bone tissue engineering. *Annals of Biomedical Engineering*, 32 (3), 477–486.

Liu, H., Ding, X., Zhou, G. (2013). Electrospinning of nanofibers for tissue engineering applications. *Hindawi Publishing Corporation Journal of Nanomaterials*, 11.

Ma, P. X., & Zhang, R. (1999). Synthetic nano-scale fibroius extracellular matrix. *Journal of Biomedical Material Research,,* 46 (1), 60-72.

Ma, P. X., & Choi. J. W. (2001). Biodegradable polymer scaffolds with well-defined interconnected spherical pore network. *Tissue Engineering,* 7, 23–33.

Ma, Z., Mao, Z. & Gao, C. (2007). Surface modification and property analysis of biomedical polymers used for tissue engineering. *Colloids and Surfaces B: Biointerfaces*, 60, 137–157.

Makohliso, S. A., Valentini, R. F., & Aebischer, P. (1993). Magnitude and polarity of a fluoroethylene propylene electret substrate charge influences neurite outgrowth in vitro. *Journal of Biomedical Materials Research, 27*, 1075-1085.

Martins, A., Reis. R. L., & Neves N. M. (2008). Electrospinning: Processing technique for tissue engineering scaffolding. *International Materials Reviews*, 53 (5), 257-274.

Martins, A., Pinho, E. D., Faria, S., Pashkuleva, I., Marques, A. P., Reis, R. L., & Neves, N. M. (2009). Surface modification of electrospun polycaprolactone nanofiber meshes by plasma treatment to enhance biological performance. *Small,* 5 (10), 1195–1206.

Meechaisue, C., Dubin, R., Supaphol, P., Hoven, V. P., & Kohn, J. (2006). Electrospun mat of tyrosine-derived polycarbonate fibers for potential use as tissue scaffolding material. *Journal of Biomaterial Science Polymer Edition* , 17 (9), 1039e56.

Megelski S., Stephens, J. S., Chase D. B., & Rabolt, J. F., (2002). Micro- and nanostructured surface morphology on electrospun polymer fibers. *Macromolecules,* 35 (22), 8456e66.

Mikos, A. G., & Temenoff, J. S. (2000). Formation of highly porous biodegradable scaffolds for tissue engineering. *Electronic Journal of Biotechnology*, 3 (2), 0717-3458.

Mitra, J., Tripathi, G., Saharma, A., & Basu, B. (2013). Scaffolds for bone tissue engineering: Role of surface patterning on osteoblast response. *Royal Society of Chemistry Advances*, 3, 11073.

Mit-uppatham, C., Nithitanakul, M., & Supaphol, P. (2004). Ultrafine electrospun polyamide-6 fibers: Effect of solution conditions on morphology and average fiber diameter. *Macromolecular Chemistry and Physics*, 205, 2327–38.

Murphy, C. M., Haugh, M. G., & O'Brien, F. J., (2010). The effect of mean pore size on cell attachment, proliferation and migration in collagen–glycosaminoglycan scaffolds for bone tissue engineering. *Biomaterials*, 31, 61–466.

Nair, L. S. & Laurencin, C. T. (2007). Biodegrable polymers as Biomaterials. *Progress in Polymer Science,* 32, 762-798.

O'Brien, F. J., Harley, B. A., Yannas, I. V., & Gibson, J. L. (2005). The effect of pore size on cell adhesion in collagen-GAG scaffolds. *Biomaterials,* 26, 433–441.

O'Brien, F. J. (2011). Biomaterials & scaffolds for tissue engineering. *Materials Today,* 14 (3), 88-95.

Pan, L. F., Chen, X., & Chen, G. H. (2006). Biocompatibility of poly (3-hydroxybutyrate-co-3-hydroxyhexanoate) modified by silk fibroin. *Journal of Material Science: Material Medical*, 17, 749–758.

Panchence, J. M., Bohrer, M. P. & Kohn, J. (2007). *Biodegrable polymers.* Lanza, R., Langer, R. & Vacanti, J. P,(Ed). (2007). Principle of tissue engineering (3rd ed.). USA: Elsevier.

Park, H., Lee, K. Y., Park, K. E., Park, W. H., Lee, S. J. (2007). Plasma-treated poly(lactic-co-glycolic acid) nanofibers for tissue engineering. *Macromolecular Research*, 15 ( 3), 238-243.

Patel, N. R., & Gohil, P. P. (2012). A review on biomaterials: Scope, applications& human anatomy significance. *International Journal of Emerging Technology and Advanced Engineering*, 2 (4), 2250-2459.

Pattanayak, D. K. , Rao, B. T., & Mohan, T. R. R. (2011). Calcium phosphate bioceramics and bioceramic composites. *Journal of Sol-Gel Sciences Technology*, 59, 432–447.

Persano, L., Camposeo, A., Tekmen, C., & Pisignano, D. (2013). Industrial upscaling of electrospinning and applications of polymer nanofibers: A review. *Macromolecular Material Engineering*, 298, 504–520.

Pharm, Q. P., Sharma, U., & Mikos, A. G. (2006). Electospinning of polymeric nanofibers for tissue engineering applications: A review. *Tissue Engineering*, 12 (5), 1197-1211.

Ponsonnet, L. Reybier, K. , Jaffrezic, N., Comte, V., Lagneau, C., Lissac, M., & Martelet, C. (2003). Relationship between surface properties (roughness, wettability) of titanium and titanium alloys and cell behaviour. *Materials Science and Engineering*, 23, 551–560.

Ramarkrishna, S., Fujihara, K.,Teo, W., Lim, T., & Ma, Z. (2005). An introduction to electrospinning and nanofibers. *Singapore: World Scientific, 3.*

Rho, K. S., Jeong, L., Lee, G., Seo, B. M., Park, Y. J., Hong, S. D., et al. (2006). Electrospinning of collagen nanofibers: Effects on the behavior of normal human keratinocytes and early-stage wound healing. *Biomaterials,* 27, 1452-61.

Rupp, F. ,Gittens, R. A., Scheideler, L., Mamur, A., Boyan, B. D., Schwartz, Z., & Geis-Gerstorfer, J. (2014) . A review on the wettability of dental implant surfaces I: Theoretical and experimental aspects. *Acta Biomaterialia*, 10, 2894–2906.

Sabir, M. I. , Xu, X., & Li, L. (2009). A review on biodegradable polymeric materials for bone tissue engineering applications. *Journal of Material Sciences*, 44, 5713–5724.

Schmidt, D. R., Waldeck, H., & Kao, W. J. (2009). *Protein adsorption to biomaterials.* D A. Puleo and R. Bizios (Eds.), Biological interactions on materials surfaces (2nd ed.) (1-18). New York: Springer- Verlag.

Schneider, G. B., English, A., Abraham, M., Zaharias, R., Stanford, C., & Keller, J. (2004). The effect of hydrogel charge density on cell attachment. *Biomaterials.* 25, 3023–3028.

Sill, T. J, & Recum, H. (2008). Electrospinning: Applications in drug delivery and tissue engineering. *Biomaterials*, 29, 1989-2006.

Silver, F. H., & Pins, G. (1992). Cell growth on collagen: A review of tissue engineering using scaffolds containing extracellular matrix. *Journal Long-Term Effects of Medical Implants,* 2, 67–80.

Singh, M., Kasper, F. K. and Mikos, A. G. (2012). *Tissue engineering scaffolds*. B. R. Ratner,(Ed). Biomaterials science: An introduction to materials in medicine (1573), USA: Academic Press.

Siraparapu, Y. D. , Bassa, S., & Sanasi, P. D. (2013). A review on recent applications of biomaterials. *International Journal of Science and Research*, 2319-7064.

Smith, L. A. , Liu. X., & Ma, P. X. (2008). Tissue engineering with nano-fibrous scaffolds. *Soft Matter,* 4, 2144–2149.

Subia, B. , Kundu, J., & Kundu, S. C. (2010). *Biomaterial scaffold fabrication techniques for potential tissue engineering applications.* D. Eberli, (Ed). Regenerative medicine and tissue engineering - cells and biomaterials in (540-568) Publisher: InTech.

Sultana, N. , & Wang, M. (2008). Fabrication of HA/PHBV composite scaffolds through the emulsion freezing/freze-drying process and characterisation of the scaffolds. *Journal of Materials Science: Materials in Medicine,* 19, 2555-2561.

Tanner, K. E. (2010). Bioactive composites for bone tissue Engineering. *Journal of Engineering in Medicine*, 224.

Tong, H. W, & Wang, M. (2011). Electrospinning of poly (hydroxybutyrateco-hydroxyvalerate) fibrous scaffolds for tissue engineering applications: Effects of electrospinning parameters and solution properties. *Journal of Macromolecular Science, Part B: Physics,* 50 (8),1535-1558.

Tong, H. W, Wang, M., & Lu, W. W. (2011). Electrospinning and evaluation of PHBV-based tissue engineering scaffolds with different fibre diameters, surface topography and compositions. *Journal of Biomaterials Science,* 23, 779–806.

Tuzlakoglu, K., Bolgen, N., Salgado, A. J., Gomes, M. E., Piskin, E., & Reis, R. L. (2005). Nano- and micro- fiber combined scaffolds: A new architecture for bone tissue engineering. *Journal of Material Science Material Medicine,* 16, 1099 .

Valence, S., Tille, J., & Gurny, R., (2013). Plasma treatment for improving cell biocompatibility of a biodegradable polymer scaffold for vascular graft

applications. *European Journal of Pharmaceutics and Biopharmaceutics,* 85, 78–86.

Vert, M. (2007). Polymeric biomaterial: Strategies of the past vs strategies of the future. *Progress Polymer Science,* 32, 755-761.

Vert, M., Doi, Y., Hellwich, K., Hess, M., Hodge, P., Kubisa, P., Rınaudo, M., & Schue, F. (2012). In the terminology for biorelated polymers and applications. *IUPAC Recommendations Pure and Applied Chemical,* 84, *37-410.*

Yang. J, Shi, G., Bei, J., Wang, S., Cao, Y., Shang, Q., Yang, G., & Wang, W. (2002). Fabrication and surface modification of macroporous poly(L-lactic acid) and poly(L-lactic co-glycolic acid) (70/30) cell scaffolds for human skin fibroblasts cell culture. *Journal of Biomedical Materials Research,* 62, 438-446.

Zhang, C. X., Yuan, X. Y., Wu, L. L., Han, Y., Sheng, J. (2005). Study on morphology of electrospun poly (vinyl alcohol) mats. *European Polymer Journal,* 41 (3), 423e32.

Zhou, P., Mei, N., Pan, L. F, Chen, G., Wu, C. G., Chen, X., Shao, Z. Z., & Chen, G. Q. (2006). Biocompatibility of poly (3-hydroxybutyrate-co-3-hydroxyhexanoate) modified by silk fibroin. *Journal of Material Science: Material Medicine*, 17, 749–758.

Zhou, P., Sun, M., Pan, L. F., Liu, S., & Yang, H. X. (2009). Enhanced cell afinity of silk fibroin modified PHBHHx material. *Journal of Material Science: Material Medicine*, 20, 1743-1751.

Zhu, P., Masuda, Y., Yonezawa, T., Koumoto, K. (2003). Investigation of apatite deposition onto charged surfaces on aqueous solutions using a quartz-crystal microbalance. *Journal of American Ceramical Society,* 86 (5), 782–90.

Wang, Y. X. (2003). Effects of the chemical structure and the surface properties of polymeric biomaterials on their biocompatibility. *Pharmaceutical Research,* 21 (8), 0724-8741.

Wang, Y. X. , Robertson, J. L. Spillman, W. B. & Claus, R. O. (2004). Effects of the chemical structure and the surface properties of polymeric biomaterials on their biocompatibility. *Pharmaceutical Research*, 21 (8).

Wang, X., Hu, X., Daley, A., Rabotyagova, O., Cebe, P., & Kaplan, D. L. (2007). Nanolayer biomaterial coatings of silk fibroin for controlled release. *Journal of Control Release*, 121 (3), 190–199.

Wei, J., Igarashi, T., Okumori, N., Maetani, T., Liu, B. S., & Yoshinari, M. (2009). Influence of surface wettability on competitive protein adsorption and initial attachment of osteoblasts. *Biomedical Materials,* 4, 045002.

Wu, X., Oleschuk, R. D., & Cann, N. M. (2012). Characterization of microstructured fibre emitters: In pursuit of improved nano electrospray ionization performance. *Analyst,* 137, 4150-4161.

Xie, J., Li, X., & Xia, Y. (2008). Putting electrospun nanofibers to work for biomedical research. *Macromolecular Rapid Commun,* 29 (22), 1775–1792.

Xu, L. C., & Siedlecki, C. A. (2007). Effects of surface wettability and contact time on protein adhesion to biomaterial surfaces. *Biomaterials*, 28, 3273–3283.